

APR 12 1943

6900
308
~~Copy~~
~~copy~~

~~LANGLEY SUB LIBRARY~~

TECHNICAL MEMORANDUMS
NATIONAL ADVISORY COMMITTEE FOR AERONAUTICS

No. 1042

THEORETICAL DETERMINATION OF AXIAL FAN PERFORMANCE

By E. Struve

Central Aero-Hydrodynamical Institute

FILE COPY

*To be returned to
the files of the Langley
Memorial Aeronautical
Laboratory.*

NACA LIBRARY
LANGLEY MEMORIAL AERONAUTICAL
LABORATORY
Langley Field, Va.

Washington
April 1943



NATIONAL ADVISORY COMMITTEE FOR AERONAUTICS

TECHNICAL MEMORANDUM NO. 1042

THEORETICAL DETERMINATION OF AXIAL FAN PERFORMANCE*

By E. Struve

The report presents a method for the computation of axial fan characteristics. The method is based on the assumption that the law of constancy of the circulation along the blade holds, approximately, for all fan conditions for which the blade elements operate at normal angles of attack (up to the stalling angles). Pressure head coefficient K_a and power coefficient K_u for the force components in the axial and tangential directions, respectively, and analogous to the lift and drag coefficients C_y and C_x are conveniently introduced. Comparison of the expressions

$$H = \eta_{pr} \rho c_u \left(u - \frac{c_u}{2} \right)$$

$$H = K_u \rho w_m^2 \frac{b_i}{2\pi r}$$

with the expression

$$\theta = \alpha + \beta$$

enables the determination of all magnitudes characterizing the blade element performance and the performance of the fan as a whole, the value of c_u being given.

The report can be divided into five parts:

1. Exposition of the blade element theory based on the general laws of mechanics and on the fundamental coefficients of experimental aerodynamics, respectively.
2. Discussion of the physical basis of the phenomena in fan operation and generalization to different operating conditions.

*Report No. 295, of the Central Aero-Hydrodynamical Institute, Moscow, 1937.

3. Explanation of the new modification of axial fan computation, whereby use is made of the pressure and power coefficients.

4. Method of determination of axial fan performance.

5. Comparison of theoretical with experimental results and discussion of several conclusions drawn therefrom.

Comparison with experiment shows that the method presented permits construction of that portion of the axial fan characteristic lying within the range of maximum efficiency with an accuracy sufficient for practical purposes. There is brought out the need for further detailed study of an airfoil situated in a flow having a rotational component and of the mutual interference of the blades of a cascade in order to obtain further accuracy in the method described. In this connection a method is outlined for obtaining the aerodynamic characteristics of the airfoil from the fan characteristics. An approximate method for plotting the fan characteristics, that does not involve much computation work and may be used for tentative computation, is also presented.

I. BLADE ELEMENT THEORY OF AN AXIAL FAN

1. General Considerations

The blade element theory is based on the assumption that each element works independently of its neighboring elements with the reservation, however, that this independence is possible, provided that certain conditions are observed. We shall see below, in considering the physical basis of axial fan operation, that the work of the individual blade elements is associated with general laws, the most important of which is that of the constancy of the circulation for all elements. For this reason, in speaking here of the independent action of the individual elements, we understand the following. The aerodynamic forces arising at a given element are entirely determined by the direction and magnitude of the flow velocity at the element, these forces being assumed identical with the forces arising at a wing element (with the same profile), having an infinite span and situated in a plane parallel flow. On this assumption is based the possibility in the fan computation of making use of the aerodynamic airfoil characteristics obtained in wind tunnel tests.

The above-mentioned possibility, of considering the blade elements as working independently of each other enables us to

determine the discharge Q_{e1} , pressure head developed H_{e1} and required power N_{e1} of each element.

In analyzing the work of each blade element we shall make use of the generally familiar method of considering a cascade of blades. The mean cylindrical surface defining a blade element* is developed into a plane, the flow pattern remaining unchanged. The sections of the fan blades, which actually lie on a cylindrical surface, will then lie successively in a plane.

Figure 2 shows the construction of a blade cascade for various radii and clearly brings out the increase in blade thickness and blade angle with decreasing distance from the hub, as is typical of the characteristic of the CAHI type fan. The velocity vector diagrams are also given, the letter w denoting the velocity relative to the given blade section, u the peripheral velocity, and c the absolute velocity.

Figure 3 shows an example of the flow through a blade cascade. We may note the following characteristics:

1. In passing through the cascade the lines of flow are deformed and become straight again only at a certain distance behind the cascade.
2. Ahead of the cascade the lines of flow are not curved since there are no forces which could bring about their curvature. In other words the direction of the absolute velocity at the inlet to the blade cascade coincides with the axial direction so that $c = c_a$.
3. By the action of the blade cascade the flow behind the latter deviates from the direction it had at the entrance. As a result the direction of the absolute velocity behind the cascade cannot coincide with the axial direction and a rotational component of the absolute velocity appears, the so-called velocity of twist c_u . We may also note that the deviation of the flow behind the cascade results also in a decrease in the magnitude of the relative flow velocity.

*A blade element is determined by two bounding cylindrical surfaces as shown in fig. 1. If the width b of the element is known, however, then the element is entirely determined by any cylindrical surface intersecting the element. For this surface we shall choose the cylindrical surface dividing the area swept by the element into two equal parts.

Having noted the flow characteristics through the blade cascade, we now proceed to the determination of quantitative relations for the blade element. These relations may be found by two methods:

1. By the general theory of mechanics;
2. By the basic experimental aerodynamic coefficients C_y and C_x characterizing the given airfoil section.

2. Computation of Blade Element from

General Mechanical Theory

The blade element of a fan is computed by considering the relative flow and applying the general theorems of mechanics, in particular the equation of Bernoulli, all of which are assumed as proven.

In considering the question of the origin of aerodynamic forces on the blade cascade, the answer will be found by recalling the above-enumerated properties of the flow through the cascade. The aerodynamic forces on the blades arise as a result of the change in momentum of the flow through the cascade (relative velocity decreases) simultaneously with the change in pressure (a drop in the relative velocity is followed, according to the Bernoulli equation, by an increase in pressure). We may note that if in an analogous manner we consider the absolute velocity we would observe that the moment imparted to the element produces a change in the flow momentum and simultaneously a rise in the pressure.

Applying the momentum equation* and the equation of Bernoulli we may establish the quantitative relations holding for each blade element. We make only the following reservation: namely, that the friction is neglected in deriving these relations. The effect of friction is relatively small and we shall take account of it by introducing special corrections. (These relations are derived from Prandtl.)

In the flow region about the blades let us consider the zone of action of one blade (fig. 4). The boundaries of this

*The law which we have in mind states: the change in momentum of the mass flowing through per second is equal to the resultant of all applied forces.

zone will serve as control surface for the application of the above-mentioned theorems of mechanics. The boundaries evidently can be taken as lines of flow and straight lines parallel to the direction of the peripheral velocity; these lines will be taken far enough removed from the cascade that the lines of flow may be considered parallel. There is no obvious flow across the zone boundaries constituted by the lines of flow, as the pressures at the corresponding points of these boundaries are equal, so that these boundaries may be excluded from consideration.

It thus remains to consider the change in momentum per second of the mass flowing across the boundaries of the control zone parallel to the direction of motion of the cascade. Since we are interested in the projections of the aerodynamic forces along the tangential and axial directions, respectively, we shall consider the change in momentum in these directions. In the axial direction there is obviously no change in momentum in passing through the cascade, since the axial velocity of the air through the cascade does not vary, because of the constant discharge through the cascade. There thus remains to consider the change in momentum in the tangential direction.

The momentum at the entrance is equal to the product of the velocity u by ρQ_{sec} where Q_{sec} is the volume of air flowing through per second. Substituting for Q_{sec} the product of the axial velocity by the cross-sectional area perpendicular to the axial direction, we obtain for the momentum, at the entrance, the expression

$$uc_a \rho \frac{2\pi r}{i} dr \quad (1)$$

where u is the peripheral (or tangential) velocity, c_a the axial velocity, ρ the density of air, $2\pi r/i$ the distance between the blades of the cascade, since r is the radius of the cross section considered, and i the number of blades; dr is the width of the blade element and hence the thickness of the flowing layer of the medium. At the exit of the cascade it is necessary, in the expression for the momentum, to substitute the difference between the peripheral velocity and the component of the absolute velocity c along this direction, that is, the velocity of flow rotation c_u . Hence the momentum at the exit is equal to the product

$$(u - c_u) c_a \rho \frac{2\pi r}{i} dr \quad (2)$$

The increase in the momentum in the direction considered is equal to the force denoted in figure 5 by X. For the latter we thus obtain the expression

$$X = u c_a \rho \frac{2\pi r}{i} dr - (u - c_u) c_a \rho \frac{2\pi r}{i} dr$$

which simplifies to

$$X = \frac{2\pi r c_u}{i} \rho c_a dr \quad (3)$$

The quantity $2\pi r c_u / i$ is the circulation* Γ_i about one blade of the cascade. This can readily be seen if the circulation is taken around the contour formed by the boundaries of the control zone. The parts of the contour which are constituted by the lines of flow may be excluded from consideration since the velocities at corresponding points are equal and the circulation about these lines are equal in magnitude and opposite in direction. The circulation along the remaining parallel lines will be equal to

$$\Gamma_i = u \frac{2\pi r}{i} - (u - c_u) \frac{2\pi r}{i} = \frac{2\pi r c_u}{i} \quad (4)$$

The above equation brings out the physical meaning of circulation; namely, that it is a measure of the rotation of the flow behind a blade element.

Making use of the concept of circulation the formula for the force X may be written as

$$X = \rho \Gamma_i c_a dr \quad (5)$$

We shall now proceed to the determination of the other component of the resultant force at the blade; namely, the force Y directed along the axis. As we have seen, the momentum ahead of and behind the cascade remains constant

*The circulation is the limit of the sum of elements $v d\ell$ where $d\ell$ is the length of an element along which the velocity v may be considered constant.

in the axial direction. The force Y is therefore given by the difference in pressures ahead of and behind the cascade. Applying the equation of Bernoulli the following equation may be written for the total pressures at the corresponding points:

$$p_1 + \rho \frac{w_1^2}{2} = p_2 + \rho \frac{w_2^2}{2} \quad (6)$$

The difference in pressures ahead of and behind the cascade gives the pressure head produced by an element.

$$H_{e1} = \frac{\rho}{2} (w_1^2 - w_2^2) \quad (7)$$

Substituting for w_1^2 and w_2^2 in the above formula, their values from the velocity diagrams at the inlet and outlet, we obtain

$$H_{e1} = \frac{\rho}{2} [u^2 + c_a^2 - (u - c_u)^2 - c_a^2]$$

or

$$H_{e1} = \rho c_u (u - c_u/2) \quad (8)$$

From the pressure head H_{e1} the force Y can readily be found by multiplying by the area $2\pi r dr/i$ over which the pressure acts. We thus obtain

$$Y = \rho \frac{2 \pi r dr}{i} c_u \left(u - \frac{c_u}{2} \right) \quad (9)$$

or, substituting the expression for the circulation,

$$Y = \rho \Gamma_i \left(u - \frac{c_u}{2} \right) dr \quad (10)$$

Formulas (5) and (10), which give the relation between the velocity components of the flow and the aerodynamic force

components, permit us to establish also the quantitative relation between the resultant velocity w_r , the resultant force P , and also the direction of the latter. In formulas (5) and (10) there enter the axial velocity c_a and the tangential component $u = c_u/2$. It is, therefore, natural to consider, as is shown in figure 6, the rectangle formed by these velocities and the rectangle of the forces X and Y , superposing for convenience the application point of the forces on the point from which the velocity components are drawn. These rectangles are similar since the proportionality of the sides follow from formulas (5) and (10), the corresponding sides being X and C_a and $u = c_u/2$. From the similarity of the rectangles it may be shown that the diagonals are mutually perpendicular and have the same coefficient of proportionality so that

$$P = \rho \Gamma_i w_m dr \quad (11)$$

The velocity w_r characterises the direction of the approach of the flow toward the blades of the cascade. The angle formed by this velocity with the direction of the peripheral velocity is, therefore, denoted as the effective pitch angle β . Since the force P is perpendicular to the direction of the flow, we may denote it as the lift force. The relation (11) may now be formulated as follows: The lift force at a blade of the cascade is perpendicular to the relative velocity w_r and is numerically equal to the product of the air density ρ , the circulation Γ_i about the blade, the relative velocity w_r , and the width dr of the blade element. The well-known Joukowski theorem on the airfoil lift has been applied here.

We shall complete our review of the performance of the blade element by determining the power that is necessary to impart to the element in order to obtain from it the required pressure head for a given volume of air delivered. The power, as is known, is obtained by taking the product of the acting force by the velocity of displacement of the point of application of the force. In our case, evidently, it is necessary to take the product of the force of magnitude X which defines the resistance to the motion of the blade element by the velocity of motion of the element $u = r\omega$. Denoting the required power by N_{e1} and making use of expression (3), we obtain

$$N_{el} = \frac{2\pi r c_u}{i} \rho c_a dr u \quad (12)$$

where the magnitude $2\pi r dr/i$ represents, as is clearly seen from figure 4, the cross-sectional area of the flow, limited by the action zone of one blade of the cascade; $2\pi r dr$ being the area of a ring of width dr (fig. 1) through which the flow at the given section passes and $2\pi r dr/i$ the portion of the ring area corresponding to one blade. Hence the product of this portion of the ring area by the axial velocity gives the volume of air flowing through per second

$$Q_i = \frac{2\pi r dr}{i} c_a \quad (13)$$

Substituting the value of Q_i in expression (12) the latter may be written in the following final form

$$N_{el} = \rho Q_i c_u u \quad (14)$$

The same formula might have been arrived at in another manner, by making use of the theorem on the moment of momentum and determining the power as the product of this moment by the angular velocity ω :

$$N_{el} = M_{el} \omega \quad (15)$$

To compute the moment M_{el} , we form an expression for the increase in momentum in the tangential direction. This increase will be equal to the product to the mass ρQ_i by the velocity of twist c_u ; hence

$$M_{el} = \rho Q_i c_u r \quad (16)$$

and

$$N_{el} = \rho Q_i c_u r \omega = \rho Q_i c_u u$$

that is, the same as expression (14).

Finally the power developed by a blade element may be determined as the product of the maximum theoretical pressure head H_{th} by the discharge per second Q_i

$$N_{el} = H_{th} Q_i \quad (17)$$

Comparing the above with expression (14), we obtain

$$H_{th} = \rho c_u u \quad (18)$$

We may note that this expression for the maximum theoretical pressure head also arrived at by application of the Euler theorem which, as is known, is of general application.

We have seen, however, that the pressure produced by a blade element is

$$H_{el} = \rho c_u \left(u - \frac{c_u}{2} \right) \quad (8)$$

thus it is evident that the pressure produced by an element of the fan blade is less than the maximum possible theoretical pressure. The question naturally arises as to what causes this loss in pressure and whether the loss is recoverable. The answer to this question lies at the very basis of the phenomenon. The imparting of power from the fan to the air and, as a consequence, the production of pressure is impossible, as we have seen, without the introduction of a twist component of the absolute velocity at the exit of the blade cascade, which component we denoted by c_u . The magnitude of the pressure head loss ΔH_t is obtained from the difference

$$\Delta H_{rot} = H_{th} - H = \rho c_u u - \rho c_u \left(u - \frac{c_u}{2} \right)$$

and is equal to

$$\Delta H_{rot} = \rho \frac{c_u^2}{2} \quad (19)$$

Equation (19) brings out the physical meaning of the loss under consideration and shows that this loss is recoverable. The process of producing a pressure difference in the blade cascade is accompanied by the formation of a potential pressure source in the form of a dynamic pressure head $\rho c_u^2/2$ corresponding to the twist component. By arranging blades of special construction (guide vanes), behind the cascade, it is possible, in general, to reconvert the dynamic head of the rotational component into a useful head. In the case of absence of such vanes not all the power imparted to the fan is converted into useful power. There then arises the need for introducing the efficiency of the twist η_t . The expression for the twist efficiency may be obtained as follows. In the presence of twist the pressure produced by an element of the blade, as we have found before, is equal to

$$H = \rho c_u \left(u - \frac{c_u}{2} \right) \quad (8)$$

The maximum theoretically possible pressure is equal to

$$H_{th} = \rho c_u u \quad (18)$$

The efficiency is naturally equal to the ratio between the two

$$\eta_t = \frac{\rho c_u \left(u - \frac{c_u}{2} \right)}{\rho c_u u}$$

which reduces to

$$\eta_t = \frac{u - \frac{c_u}{2}}{u} \quad (20)$$

which enters into the general formula for the efficiency of a blade element.

With this we may conclude the review of the relations which we have derived from general mechanical theory for the

computation of a blade element. We may remark again that all of these relations have been derived with the effect of friction neglected. We shall return to the question of the effect of friction in paragraph 4.

3. Computation of the Fan Blade Element with the Aid of the Coefficients of Experimental Aerodynamics

In moving through a viscous liquid the blade experiences a drag as well as a lift force. Thus, as shown in figure 7, the resultant of the aerodynamic forces deviates somewhat from the direction perpendicular to that of the velocity of approach. Experimental aerodynamics provides, as is known, methods for experimentally determining the forces arising at the wing, the resultant force R not being directly, but indirectly, determined by its lift and drag components, P and L , respectively.

In order to be able to compare the aerodynamic forces for wings of various shapes and dimensions, experimental aerodynamics makes use of nondimensional coefficients; namely, the lift and drag coefficients C_y and C_x . We may note here that these coefficients are differently denoted in the literature of the different sources. To avoid confusion we shall denote the coefficients defined by the new method by C_{xnew} and C_{ynew} , respectively. The formulas for passing from one notation to the other are

$$C_y = \frac{C_{ynew}}{200} \quad (21)$$

$$C_x = \frac{C_{xnew}}{200} \quad (22)$$

By means of the coefficients C_x and C_y the force components arising at the wing in the direction of approach and at right angles to it can be computed. The drag and lift forces are, respectively

$$L = C_x \rho_w^2 b l \quad (23)$$

$$P = C_y \rho_w^2 b l \quad (24)$$

where l is the span and b the chord of the wing.

We see, however, that for the purpose of computing the axial fan it is not these two components but rather the components in the tangential and axial directions that are of interest. It is natural to define nondimensional coefficients analogous to the lift and drag coefficients by means of which the components of the force along these directions for a given profile for any dimension and at any angle of attack can be found. We have denoted the coefficient by which the axial component is obtained as the pressure head coefficient K_a , and the coefficient by which the rotational component is obtained as the power coefficient K_u . Since the coefficients C_y , C_x , K_a and K_u are proportional to the corresponding forces P , L , R_H and R_N we may find the relations between these coefficients by considering the projections of the forces in the axial and tangential directions and denoting the corresponding coefficients by the subscripts a and u , respectively. Considering figure 8 and remembering that the projection of the resultant is equal to the algebraic sum of the projections of the components and dropping the magnitude $\rho_w^2 b l$ entering as a common factor in all expressions, we may write at once

$$K_a = C_{y_a} - C_{x_a}$$

Remembering that $\angle BOC$ and $\angle DOE$ are equal to the angle β we obtain

$$C_{y_a} = C_y \cos \beta$$

$$C_{x_a} = C_x \sin \beta$$

and hence the pressure head coefficient

$$K_a = C_y \cos \beta - C_x \sin \beta \quad (25)$$

By analogous considerations we determine the power coefficient K_u . Using the subscript u to denote the projection in the tangential direction we find

$$K_u = C_{y_u} + C_{x_u}$$

or

$$K_u = C_y \sin \beta + C_x \cos \beta \quad (26)$$

The values of K_a and K_u evidently depend on two factors; namely, the angle of attack and the effective pitch angle. Since we have seen that the effective pitch angle for an axial fan varies very much with the radius of the element considered it is of advantage, before proceeding to the computation, to construct graphs of the pressure and power coefficients for the required range of angles. Such graphs are given in appendix I for the three basic profile sections used in the construction of the axial fans of the CAHI type. These profiles are the following:

1. A series of English propeller profiles of various thickness suited for cast metal construction or for hollow blades fastened or welded of two halves with inside reinforcing rod
2. Metal curved blades suitable for sheet metal construction:
3. Symmetrical profile suitable for reversible fans

In order not to encumber the text unduly we present a sample graph of the K_a and K_u coefficients for the English propeller profile section of relative thickness $\bar{\delta}$, that is, ratio of maximum thickness to profile chord equal to 0.1. The K_a and K_u curves given in figures 9 and 10 represent a family of curves analogous to the lift curves. The curves are plotted against the angle of attack α with the pitch angle β as parameter.

In analogy with the efficiency of an airfoil C_y/C_x , the ratio K_a/K_u may be denoted as the efficiency of a fan blade element. It should be noted, however, that the fan

blade efficiency does not completely characterize the economy of the fan and enters, as we shall see below, as one of the factors of the so-called profile efficiency of the fan. The ratio K_a/K_u is a measure rather of the pressure developable by a fan blade. Figure 11 gives a family of curves $U = K_a/K_u$ of a blade element as a function of the angle of attack for the same English propeller profile section with relative thickness $\delta = 0.1$.

With the aid of the coefficients K_a and K_u the pressure and power of a blade element of the fan are readily determined. The thrust of a blade element or the reaction force equal in magnitude and opposite in direction is expressed by the product $K_a \rho w_m^2 b dr$, where b is the chord of the blade element, dr its width. Dividing this product by the area of the ring over which the element acts, equal to $2\pi r dr$, we obtain the pressure produced by the element

$$H_{el} = \frac{K_a \rho w_m^2 b}{2 \pi r} \quad (27)$$

Similarly the force resisting the rotation of the element is given by the product

$$K_u \rho w_m^2 b dr$$

and the corresponding rotational moment by

$$K_u \rho w_m^2 b r dr$$

Hence the power, which it is necessary to supply to rotate the element, is equal to

$$N_{el} = K_u \rho w_m^2 r \omega dr$$

where ω denotes the angular velocity of the element. Remembering that $r\omega$ is equal to u - the peripheral

velocity of the element - the formula for obtaining the power of the blade element may be written as follows:

$$N_{el} = K_u \rho w_m^2 u b dr \quad (28)$$

To the pressure and power formulas there should be added the formula for the discharge for each blade element. From the velocity polygon (fig. 2) it is clear that the axial velocity is

$$c_a = \left(u - \frac{cu}{2} \right) \tan \beta \quad (29)$$

and hence the discharge

$$Q_{el} = 2 \pi r c_a dr = 2 \pi r \left(u - \frac{cu}{2} \right) \tan \beta dr \quad (30)$$

The introduction of the pressure and power coefficients K_a and K_u very much simplifies the analysis of the theoretical fan efficiency. To obtain this efficiency, we make use of the well-known general formula for the fan efficiency

$$\eta = \frac{QH}{N} \quad (31)$$

where Q is expressed in cubic meters per second, H in millimeters of water or kilogram per square meter, N in kilogram-meters per second. Substituting in the above formula the values of the discharge, pressure, and power for the blade element from relations (27), (28), and (30), we obtain

$$\eta_{el} = \frac{2 \pi r \left(u - \frac{cu}{2} \right) \tan \beta dr K_a \rho w_m^2 \frac{b}{2 \pi r}}{K_u \rho w_m^2 u b dr}$$

and simplifying

$$\eta_{el} = \frac{K_a}{K_u} \tan \beta \frac{u - \frac{c_u}{2}}{u} \quad (32)$$

where the ratio $(u - c_u/2)/u$ denotes, as we have seen, the flow twist efficiency. The expression

$$\frac{K_a}{K_u} \tan \beta = \eta_{pr} \quad (33)$$

maybe denoted as the profile efficiency of the fan blade element.

We conclude our consideration of the computation formulas for the fan blade element that were obtained with the aid of the fundamental experimental coefficients and proceed to compare these formulas with those obtained on the basis of the general theorems of mechanics.

4. Comparison of Computation Formulas

for the Blade Element

As already pointed out the fundamental difference between the formulas obtained from the general theorems of mechanics and those derived on the basis of experimental coefficients consists in the fact that in the former, the factor of friction is not taken into account. The presence of friction gives rise to additional rotation of the flow behind the blade element. The question arises whether it is possible to take the effect of friction into account by simply substituting a larger value for c_u in the formulas derived on the basis of the general theorems of mechanics. We shall answer this question in detail for each of the magnitudes considered; namely, the power, air discharge and pressure.

By the very method of derivation of the formula for the power it is clear that such a substitution is entirely justified. The expression for the power was obtained from the momentum imparted per second to the rotating flow. It

is obvious that in this expression for the momentum it is necessary to substitute a greater value of the rotational velocity c_u which occurs with the presence of friction. Thus the formula

$$N_{e1} = \rho Q_i c_u u \quad (14)$$

may also be applied in the case of friction.

It is obvious that the formula for the volume flow

$$Q_{e1} = \left(u - \frac{c_u}{2} \right) \tan \beta F_{ring} \quad (34)$$

remains true also for the case of friction since the flow direction is determined by the actual value of c_u . The case is otherwise with the pressure head. As in the ideal case and also in the presence of friction the pressure remains proportional to the product

$$\rho c_u \left(u - \frac{c_u}{2} \right)$$

In the presence of friction, it is of course, incorrect to put

$$H_{e1} = \rho c_u \left(u - \frac{c_u}{2} \right)$$

since the friction evidently leads to a loss in pressure head. On account of the above proportionality we may set

$$H_{e1} = K_{fr} \rho c_u \left(u - \frac{c_u}{2} \right) \quad (35)$$

It is not difficult to see that the factor K_{fr} defines the profile efficiency of the blade element

$$K_{fr} = \eta_{pr} \quad (36)$$

If in the ideal frictionless fluid the same rotational velocity c_u at a given angle of attack were produced, as in the case of friction, then for the same discharge the pressure produced by the fan would be

$$H = \rho c_u \left(u - \frac{c_u}{2} \right)$$

Since the values of the discharge and power would be equal to the values obtained in the case of friction the profile efficiency of the fan would be given by the ratio of pressures; that is,

$$\eta_{pr} = \frac{K_{fr} \rho c_u \left(u - \frac{c_u}{2} \right)}{\rho c_u \left(u - \frac{c_u}{2} \right)} \quad (37)$$

It is thus clear that $K_{fr} = \eta_{pr}$. The formula for the computation of the pressure may then be written as follows:

$$H = \eta_{pr} \rho c_u \left(u - \frac{c_u}{2} \right) \quad (38)$$

A somewhat different method for arriving at the correction for the effect of friction is that given by K. Ushakov (reference 1.) His method is essentially the following. Assume at our disposal an ideal smooth profile geometrically identical with the given real profile and let the former develop the same lift which the real element would develop. The pressure head H_{id} developed by the ideal profile will be somewhat greater than H developed by the real airfoil on account of the presence of friction. Denoting the correction coefficient by K_{pr} we may write

$$H_{id} = HK_{pr} \quad (39)$$

The magnitude of the rotational component c_{uid} corresponding to the ideal case (and hence also the value of the circulation Γ_{id}) may be found from the relation

$$H_{id} = \rho c_{uid} \left(u - \frac{c_{u id}}{2} \right) \quad (40)$$

With the circulation Γ_{id} known, the width b of the element for the real profile section can be readily computed. Comparing the expression for the lift for the ideal and real profiles we shall have

$$P = \rho \Gamma_{id} w_m dr \quad (41)$$

$$P = C_y \rho w_m^2 b dr \quad (42)$$

Equating the right sides of the two equations we obtain

$$\Gamma_{id} = C_y b w_m \quad (43)$$

whence

$$b = \frac{\Gamma_{id}}{C_y w_m} \quad (44)$$

It is of interest to compare the two methods of introducing the corrections for the computation of the effect of friction and to show that both lead to identical results. We shall make this comparison by analyzing the force diagram for a blade element (fig. 12). For simplicity we shall denote the forces by the coefficients corresponding to them since, as we have already shown, the ratios of the forces are proportional to the ratios of the coefficients.

According to the first method, that is, assuming that in the ideal case the same rotational component c_u is produced as in the case of friction, we must assume that in the ideal case the projection of C_{yid} in the tangential direction is

$$K_{uid} = K_u \quad (45)$$

This condition can be satisfied only for the case that the segment $AB = C_y id$. The segment $AB = K_{id}$ will then evidently correspond to the pressure which would be obtained in the ideal case. The actual pressure, however, is that determined by the coefficient K_a . Hence the ratio $K_a/K_{a id}$ determines the profile efficiency of the fan blade element.

$$\frac{K_a}{K_{a id}} = \eta_{pr} \quad (46)$$

But $K_{a id} = K_u \cot \beta$ (fig. 12), hence

$$\eta_{pr} = \frac{K_p}{K_u \cot \beta}$$

or

$$\eta_{pr} = \frac{K_a}{K_u} \tan \beta \quad (33)$$

Thus we have directly arrived at the same expression for the profile efficiency of a blade element as would have been obtained starting from the general formula for the efficiency of the blade element.

According to the second method based on the fact that the effect of the friction is to give rise to the vector C_x the efficiency of the blade element is impaired both on account of the loss in pressure and chiefly on account of the increase in power. From this point of view the ideally possible pressure is given by the magnitude of the segment MN equal to $C_y \cos \beta$ and the required power for the case of absence of friction by the segment $ON = C_y \sin \beta$, the profile efficiency then being equal to one. With friction present the pressure is determined by the magnitude K_a and the power by K_u . Hence, due to the drop in pressure, the effi-

ciency varies in the ratio $K_x/C_y \cos \beta$,* and due to the increase in power in the ratio $C_y \sin \beta/K_u$. Thus the profile efficiency, which in the absence of friction is equal to unity, will in the presence of friction be equal to

$$\eta_{pr} = 1 \frac{K_a}{C_y \cos \beta} \frac{C_y \sin \beta}{K_u} \quad (47)$$

or

$$\eta_{pr} = \frac{K_a}{K_u} \tan \beta \quad (33)$$

so that we see that the second method leads to the same result as the first.

We may note, from a consideration of the forces arising at the blade element, that a coefficient K_{c_u} can be computed which permits passing from the ideal rotational component $C_{u id}$ to the real component c_u that takes friction into account. The values of c_u are proportional to the powers and the latter are proportional to the projections of the corresponding lift coefficients in the peripheral direction. With this in mind it is clear that

$$\frac{c_u}{C_{u id}} = \frac{K_u}{C_y \sin \beta} = K_{c_u} \quad (49)$$

*It is not difficult to see that the reciprocal of this ratio is the correction coefficient K_{pr} . Thus

$$K_{pr} = \frac{1}{\frac{K}{C_y \cos \beta}} = \frac{1}{1 - \mu \tan \beta} \quad (48)$$

where

$$\mu = \frac{C_x}{C_y}$$

For good profile sections the value of K_{pr} differs very little from unity.

Substituting for K_u its value in terms of C_y and C_x , we have

$$K_{cu} = \frac{C_y \sin \beta + C_x \cos \beta}{C_y \sin \beta}$$

whence, denoting by μ the reciprocal of the wing efficiency, we obtain

$$K_{cu} = 1 + \frac{\mu}{\tan \beta} \quad (50)$$

With the above, we conclude our considerations that take account of the effect of friction on the performance of the blade element of an axial fan and proceed to consider the physical basis of the fan performance as a whole.

II. PHYSICAL BASIS OF FAN PERFORMANCE

1. General Observations

Our object, in the present section, is to build up a model which will provide us with a clear understanding of the physical nature of the phenomena that occur during the fan operation, neglecting for simplicity certain of their details. The model will be obtained from a consideration of the flow pattern at the fan inlet. We shall first, however, make a few general observations.

The first of these is in connection with the history of the problem. An axial fan of an improved type was first constructed under the supervision of N. Joukovsky as far back as 1913. This fan was designed by the vortex theory developed by Joukovsky. Since that time the design of axial fans of the CAHI type has not undergone any essential modifications until recently when certain corrections were introduced in the physical considerations by K. Ushakov (CAHI). We shall follow the latter in our discussion.

The second observation, is in connection with the fan inlet conditions. One of the fundamental characteristics

of axial fan operation is that the lines of flow are parallel to the fan axis at the inlet. When the fan operates in a cylindrical casing the above condition is observed only for smooth entrance - with the aid of a collector at the fan inlet. The following discussion refers only to fans for which good inlet conditions are assured. All the tested fans were correspondingly provided with collectors.

A very strong effect on the performance of the axial fan is exerted by the clearance between the wheel and casing. The presence of a clearance leads to a considerable drop in the pressure produced by a fan. In view of the fact, however, that up to the present no satisfactory axial fan theory has been developed that takes clearance into account the conclusions of the present paper will, strictly speaking, apply to fans with negligibly small clearances. Through the introduction, however, of a corresponding empirical coefficient it will be possible to take into account the loss in pressure and practically apply the results of the present paper to the computation of the fan characteristics with the clearance between the wheel and casing taken into account.

2. Flow Pattern at Inlet to Fan

In considering the flow pattern at the inlet and later at the outlet of the fan we shall be interested in the velocity and pressure distributions. From a consideration of the flow picture at the inlet to the fan (fig. 2) we find that where the flow is not disturbed by the blades of the cascade the lines of flow are parallel. The velocity vectors at a certain distance ahead of the fan are parallel to the fan axis since there are no forces that could bring about a curvature of the lines of flow ahead of the fan. The presence of the blade cascade, as is shown in figure 3, disturbs the parallelism of the lines of flow only at a very small distance ahead of the cascade. We may thus state the first physical characteristic of the axial fan performance; namely, that the flow ahead of the fan has no rotation.

On figure 2 are drawn, for all cross-sections under considerations, the velocity parallelograms at the entrance to the blade cascade. At all these parallelograms, owing to the fact that the flow ahead of the fan has no curvature, the axial components c_a of the relative entrance velocities are the same for all sections. The relative velocities w

themselves for all blade elements are different, however, since the components of these velocities in the tangential direction vary. It is clear from figure 2 that the relative velocity increases as the blade periphery is approached because of the increase in the rotational component. This fact constitutes the second characteristic of the performance of an axial fan. Since the flow ahead of the fan is not curved, the static pressure remains constant for all sections, which fact constitutes a third characteristic of axial fan performance.

3. Flow Pattern at Fan Outlet

From the consideration of the performance of each blade element of the axial fan we have seen that the transfer of power from the blade element to the air is not possible without imparting a rotational component to the air behind the element. The rotational component c_u for each blade element is directed along the direction of motion of the cascade and hence is a vector tangent to the cylindrical surface formed by a given element and simultaneously a tangent in the plane perpendicular to the fan axis. It is thus clear that the flow particles behind the fan possess in addition to a forward velocity c_a a rotational velocity c_u about the prolonged axis of the fan. Due to inertia this rotational component tends to be maintained indefinitely and vanishes in a real fluid only because of the presence of friction, a fact which constitutes a fourth characteristic of axial fan operation.

Again, in considering the operation of a blade element, we have seen that the same blade section used for the construction of the blade element may produce a different rotational component of the flow depending on the blade angle at which it is set. Since each blade element produces its own component c_u it is necessary to consider whether the velocity distribution c_u for the various blade elements may be arbitrary for the performance of the fan as a whole, especially if it is desired that the flow enter the fan along cylindrical surfaces coaxial with the fan.* Under what conditions this restriction in the twisted flow is observed will become clear from a consideration of the forces that arise.

*We should note that only for this restriction are the formulas derived in the previous section for the blade element computation applicable.

In a flow with rotation, centrifugal forces arise under the action of which a cross flow may occur from one concentric layer to another (we assume layers of equal flow discharge). This cross flow under the action of centrifugal forces can occur only for a definite relation of the pressures at the layers considered such that the centrifugal forces will be balanced by the differences in pressure. Since in a fluid flow the pressures and velocities are connected with each other (through the Bernoulli equation) the pressure ratios at which there will be no cross flow will correspond to a definite radial distribution of the rotational component. It is found that in this case the velocities c_u are inversely proportional to the radius; that is, that

$$r c_u = \text{constant} \quad (51)$$

Since this law is of cardinal importance for understanding axial fan operation we shall give a brief derivation of this relation here, restricting ourselves because of the lack of space, to the frictionless ideal fluid. We consider two neighboring sufficiently narrow concentric fluid layers rotating according to the law $r c_u = \text{constant}$ (fig. 13). The pressure in the outer layer should be greater than that in the inner since it is the excess pressure in the former that produces the centripetal forces that make the fluid move along a curved trajectory. The centripetal force may be computed as the product of the mass of the layer by the centripetal acceleration. The volume of the outer layer is given by the product

$$2 \pi r dr \delta$$

where δ is the thickness of the rotating layer above the plane of the sketch (fig. 13). The mass of the layer is

$$dm = \rho \delta 2 \pi r dr \quad (52)$$

If the rotational velocity is c_u the centripetal acceleration is

$$\chi = \frac{c_u^2}{r} \quad (53)$$

The centripetal force is, therefore

$$P = 2 \pi \rho r c_u^2 dr \quad (54)$$

The pressure difference dp between the layers is found by dividing the centripetal force by the contact area of the layers. Since the latter area is equal to $2\pi r l$, we obtain

$$dp = \rho \frac{c_u^2}{r} dr \quad (55)$$

The pressure difference may also be obtained by applying the Bernoulli equation to the curved flow in the layers under consideration. In doing so we make the following very important assumption; namely, that the constant entering the Bernoulli equation is the same for all concentric layers.* From the following considerations it will appear clear that for this assumption, equilibrium in the rotating fluid is maintained; that is, there is no cross flow from one layer to the next.

The static pressure, or simply, the pressure in the outer layer should, as we have seen, be greater than the pressure in the inner layer. Hence, in view of the constancy of the constant in the Bernoulli equation, the velocity in the outer layer should be less than that in the inner. The velocity increment dc_u should thus be taken negatively. This explains the apparently paradoxical fact that in the following expressions for the pressure difference dp between the layers a minus sign stands before the right hand side of the equation.

Denoting the velocity in the outer layer by c_u we should, according to the generally accepted rule, denote the velocity in the inner layer by $c_u - dc_u$.** From the

*This assumption is actually valid for a fan with pressure $H_{th} = \rho u c_u$ constant along the radius.

**Again we emphasize that an error in the sign before dc_u in this expression leads to an entirely incorrect result. The minus sign is taken before dc_u because we pass to a layer of smaller radius.

equation

$$p_{\text{outer}} + \rho \frac{c_u^2}{2} = p_{\text{inner}} + \rho \frac{(c_u - dc_u)^2}{2} \quad (56)$$

we obtain, for the pressure difference dp after removing the parenthesis and combining similar terms, the following relation (neglecting $|dc_u|^2$).

$$dp = p_{\text{outer}} - p_{\text{inner}} = -\rho c_u dc_u \quad (57)$$

Equating the above expression to the one earlier obtained for the pressure difference, we find

$$\rho \frac{c_u^2}{r} dr = -\rho c_u dc_u \quad (58)$$

Dividing by ρc_u and separating the variables

$$\frac{c_u}{dc_u} = -\frac{r}{dr} \quad (59)$$

Integrating, we have

$$\ln c_u = -\ln r + \text{constant}$$

or

$$\ln c_u + \ln r = \text{constant} \quad (60)$$

The sum of the logarithms on the left hand side of the equation is equal to the logarithm of the product

$$\ln (rc_u) = \text{constant} \quad (61)$$

or

$$rc_u = \text{constant} \quad (62)$$

Thus we have proven the required relation for a fluid without friction. Since, however, the effect of the internal friction for the fluid under consideration;—namely, air, is small;—it may be assumed that the rotational velocity distribution along the radius for air does not deviate much from the law $rc_u = \text{constant}$. There is merely a small change in the constant. In fact we have already seen in considering the effect of friction on the performance of a blade element that the rotation of the flow increases in the presence of friction. Denoting this increased rotational velocity, due to friction by c_u , and the rotational velocity under otherwise equal conditions, without friction by c_{uid} , then evidently $rc_u > rc_{uid}$.

Thus we have shown that in the rotating liquid there is no flow along the radius if the Bernoulli constants for the various layers are the same. We may note that the same restriction remains if all the particles simultaneously possess a forward motion with the same velocity. In this case the Bernoulli equation becomes

$$p_1 + \rho \frac{c_1^2}{2} = p_2 + \rho \frac{c_2^2}{2} \quad (63)$$

where c_1 and c_2 are the resultant velocities. Since, however,

$$\rho \frac{c_1^2}{2} = \rho \frac{c_a^2}{2} + \rho \frac{c_{u1}^2}{2}$$

and

$$\rho \frac{c_2^2}{2} = \rho \frac{c_a^2}{2} + \rho \frac{c_{u2}^2}{2}$$

equation (63) may be rewritten

$$p_1 + \rho \frac{c_a^2}{2} + \frac{\rho c_{u1}^2}{2} = p_2 + \rho \frac{c_a^2}{2} + \rho \frac{c_{u2}^2}{2} \quad (64)$$

Dividing through by $\rho c_a^2/2$ we arrive at the same condition which we assumed in deriving the law $rc_u = \text{constant}$.

It is clear, from this, that if we wish the flow through the fan to pass along cylindrical surfaces coaxial with the fan, we should give the blade elements a setting such that the rotational components produced by the elements obey the law $rc_u = \text{constant}$. Since the choice of the blade angles of the elements is at our disposal we may consider that this choice has, in general, been made.

We have seen that the presence of a rotational component behind each blade element is characterized by the presence of circulation about the given element.

$$\Gamma_i = \frac{2 \pi r c_u}{1} \quad (4)$$

Thus, the condition requiring that the blade element be chosen such that the rotational velocities obey the law $rc_u = \text{constant}$ is equivalent to the constancy of the circulation along the blade. Since the magnitude of the circulation may be taken as a measure of the twist of the flow we shall determine the circulation. Since the latter about any contour around the axis of rotation is the same, we may choose the most suitable one, which is a circle of radius r . Evidently

$$\Gamma = 2 \pi r c_u$$

A fact to be observed is that the circulation in the rotational flow behind the fan is equal to the circulation about one blade multiplied by the number of blades. It is thus possible, from the circulation about one of the blades of the axial fan, to obtain the entire circulation of the flow behind the fan. It is for this reason that we present the so-called vortex theory first developed by N. Joukovsky which has been so fruitful of results. The advantage of the following theory is that it permits a very simple treatment of axial fan operation as a whole.

4. Vortex System of Axial Fan

It is known that if the circulation along the wing, or as in our case, along the fan blade, is constant the wing or

blade may be replaced by a single resultant vortex whose circulation is equal to that about the wing or blade. The question arises as to whether the resultant vortex ends abruptly at the blade boundaries or whether it continues beyond these limits. We emphasize the importance of this question since, at first glance, it is not clear how the vortex arising at the blade can exist beyond its limits. We have seen, however, that the blades of the fan produce behind it a rotation of the flow, which in a frictionless fluid, on account of inertia, is extended infinitely behind the fan. This rotation, behind the fan, may be considered associated with the vortex, or more accurately, the vortex "braid," which is the resultant of the vortices of the individual blade elements. In fact we have seen that the circulation in the rotational flow behind the fan is equal to the sum of the circulations about the blade and this condition is observed when a number of vortices are combined into a single vortex.

In view of this the vortex system of the fan may be represented as shown in figure 14. The resultant vortices which replace the blades do not break off here at the hub but rotate by 90° and combine, behind the fan, into a single vortex which then extends infinitely far behind. It is natural to suppose that the resultant vortex does not also break off at the other end of the blade and is carried along by the flow in the form of a line vortex as illustrated in figure 15. This is actually the case if the fan operates without a casing or if there is a sufficient clearance between the fan and casing. Because of the difference in pressure ahead of and behind the fan a flow takes place across the tip of the blade due to the clearance and gives rise to the vortex line shown in figure 15. It is evident that the smaller the clearance the weaker will be the flow and in the limit, when the clearance becomes infinitely small, the vortex line springing from the blade tip vanishes. In this case the resultant vortex continues downstream supporting itself against the wall. The effect of the clearance on the operation of the axial fan is, in general, very small but as we have shown may be taken into account by the introduction of a correction coefficient to the pressure head developed by the fan. In all theoretical computations we shall consider the clearance as vanishingly small and make a correction for the clearance only when illustrating concrete computation examples. For this reason, in our vortex system for the fan, we have presented the vortices replacing the fan blade as breaking off at the casing walls.

5. Pressure Distribution in the Flow Behind the Fan

We have shown that radial flow in a rotating fluid is absent if the condition $rc_u = \text{constant}$ is observed. In deriving this relation we have seen that the pressure in the inner of two neighboring layers is less than that in the outer layer. The difference in pressure is balanced by the centrifugal forces arising in the inner layer. Generalizing this conclusion we may say that the pressure in a rotating flow behind the fan drops as the fan axis, or the vortex axis behind the fan is approached. By comparing the pressure distribution behind the fan with the distribution ahead of it, we may conclude that the pressure drop developed by each blade element of the fan decreases as the hub of the fan is approached, since the pressure over the entire cross-section ahead of the fan is constant. The fifth characteristic of the axial fan operation may be, therefore, formulated as follows. The total pressure head developed by the blade elements* is not uniformly distributed over the fan disk but gradually decreases toward the hub. We may note that the above statement does not contradict the view as regards total pressure of the fan as a whole as being the difference in pressures ahead of and behind the fan taken in the absolute flow. The flow is deflected by the fan in a region where the same pressure prevails and, therefore, the head actually produced by the fan is determined by this difference in total pressures. It is merely necessary to keep in mind that the total pressure produced by the fan as a whole is somewhat larger than the mean pressure which we would obtain by adding the pressures produced by the individual blade elements.** There must, therefore, exist an additional source of pressure. We shall show that such a source appears in the flow rotation produced by the fan, which operates like a centrifugal fan.

We have already shown that, notwithstanding the difference in pressures at the periphery and center, respectively, of the rotating stream, no radial flow occurs from the periphery to the center. There is also no radial flow in the rarefied region lying immediately behind the fan outside the rotating

*The pressure head of an element may be defined by the difference in static pressures ahead of and behind it. It may be considered as the total pressure in view of the constancy of c_a and hence also equality of the dynamic pressure at inlet and outlet.

**This mean pressure may be arrived at in the following way. Determine for each element the thrust, integrate and find the resultant of the individual thrusts, that is, the fan thrust, and finally divide this thrust by the fan disk area.

medium. The absence of such flow may be explained by the fact that in this interval an additional pressure head is developed from the latent source in the form of dynamic pressure of rotation. This will become especially clear from the curve of pressure behind the fan. This curve is constructed by laying off the radii of the blade cross-sections considered along the axis of abscissas and the corresponding pressures along the axis of ordinates. Figure 16 shows an example of such a curve obtained by computation for one of the fan operating conditions considered below. The curve shows, first of all, that the value of $H_{th} = \rho c_u u$ is considered equal for all of the fan blade elements:

$$H_{th} = \rho c_u U = \rho \omega r c_u \quad (65)$$

where ρ and ω are constant and $r c_u$ is constant, in view of the law of constancy of the circulation. In order to obtain the rated total pressure H developed by the fan blade elements we should deduct from H_{th} the dynamic pressure of the rotating flow. It will be remembered that the value of the rated pressure head H_c is determined for each blade element by the formula

$$H_{comp} = \rho c_u \left(u - \frac{c_u}{2} \right) \quad (66)$$

The pressure head H is somewhat less on account of the pressure losses due to the profile drag of the blade. We have found that H is given by

$$H = \eta_{pr} \rho c_u \left(u - \frac{c_u}{2} \right) \quad (38)$$

The value of the velocity of rotation c_u increases with decreasing distance from the blade hub; $\rho c_u^2/2$ likewise increases and hence H_r decreases. The variation in H_c is clearly seen on the pressure curve. We may note that the curve H_c is a parabola with vertex lying on the maximum blade radius equal to the fan radius, the axis of the parabola being parallel to the axis of ordinates. The pressure

H actually developed by the fan and determined by formula (38) lies somewhat below the curve H_C . In figure 16 it is represented by a dot-dash curve. The figure also gives the curve of total fan pressure shown by the dotted curve as obtained from experiment. This latter pressure is denoted by $H_{t\text{est}}$. It is evident that the difference between the test pressure and the pressure H for which the individual blade elements are computed is due to the dynamic pressure of rotation.

We now proceed to explain a fact which is fundamental for the understanding of axial fan computation. On figure 16 it is noted that the curves $H_{t\text{est}}$ and H meet at the blade tip element. In other words the pressure difference ahead of and behind the tip element is entirely produced from the pressure head H developed by this element. That this could only be the case will be clear if it is considered that the static pressure behind the tip element cannot be equal to the atmospheric pressure, or more accurately, to the pressure in the rotating medium behind the fan. From the fact that there is an increase in the static pressure produced by the tip element from the low pressure ahead of the fan to atmospheric pressure and the dynamic pressure ~~ahead of and behind the fan~~ is the same because of the constancy of the axial velocity (c_a), it follows that

$$H_{t\text{est}} = H_{\text{tip el}} \quad (67)$$

both of these pressures being, in fact, determined by the same equation

$$\left(p_a + \rho \frac{c_a^2}{2} \right) - \left(p_{st} + \rho \frac{c_a^2}{2} \right) = p_a - p_{st} \quad (68)$$

where p_a is the pressure immediately ahead of the fan. The fact that the pressure of the fan as a whole is equal to the pressure produced by the tip element constitutes the sixth characteristic of the axial fan operation.

From figure 16 it is seen that only a part of the dynamic pressure of rotation is lost; namely, that developed by the blade tip element. To avoid this loss, or more accurately, to utilize a part of the loss dynamic pressure, is possible only through the use of guide vanes.

The credit for pointing out the presence of a low pressure region behind the axial fan produced by the rotation of the flow and the impossibility of considering the fan thrust,* as equal to the product of the pressure by the fan disk area, as well as for introducing changes in the computation of the axial fan in connection with the fact that the pressure of the fan as a whole is equal to the pressure of the blade tip element belongs, apparently, to K. Ushakov (CAHI), since other authors either have not sufficiently brought out these facts or have permitted errors to enter. Among the mistaken statements is the one that all the elements of the fan blade can develop the constant total pressure H , a statement which is equivalent to the incorrect assumption of constancy of the static pressure behind the fan.

In concluding this section we may briefly summarize the characteristics of axial fan operating at the rated operation condition:

1. The flow ahead of the fan is without rotation.
2. The relative velocity of the flow through the fan increases from the center toward the periphery.
3. The static pressure ahead of the fan remains constant along the blade.
4. The flow behind the blade possesses rotation, the rotational velocity following the law $rc_u = \text{constant}$.
5. Due to the rotation of the flow behind the fan the static pressure cannot be constant but decreases toward the hub. This results also in a decrease in the pressure developed by the fan elements.
6. The general pressure produced by the fan is equal to the pressure of the blade tip element.

III. GENERALIZATION OF PHYSICAL BASIS OF AXIAL FAN OPERATION

In the present section we shall present, briefly, some basic considerations which permit us to proceed to the computation of the axial fan for operating conditions other than the one for which the fan is computed.

*By the thrust of the fan is understood the resultant of the force arising during fan operation in the direction opposite to the flow.

The fundamental simplification underlying our method of computation of the axial fan is the assumption that the law $rc_u = \text{constant}$ - approximately the law of constancy of the circulation along the blade - remains valid for all operating conditions within the interval of normal blade angles (up to $C_{y \text{ max}}$) and that this law is applicable also for smaller number of blades (removal of some of the blades). The transition from one operating blade angle to another is characterized by a change in the value of the constant in the law $rc_u = \text{constant}$, or in other words, by a change in the magnitude of the circulation about the blade, the circulation being maintained constant along the radius.

Due to the lack of time there have been, unfortunately, no means at our disposal for checking the possibility of the application of the above assumption by the direct determination of the velocities and pressures behind and ahead of the fan. An investigation of this kind of the internal process of operation of the axial fan will be undertaken in the near future. For the present we were constrained to judge the satisfaction of the method by comparing the computed characteristics obtained on the basis of the assumptions made with the fan characteristics experimentally obtained. We were able to make such a comparison for a large number of fans and thereby to draw conclusions as to the range of applicability of our method.

We have not considered it necessary, in our present work, to enter into a theoretical analysis of the magnitude of the errors we have made in applying our fundamental assumption, since it was our object to present immediate results of definite practical value and a theoretical analysis would have required large time expenditure. We shall, therefore, merely stop to clarify the physical significance of our assumption.

We have seen, in deriving the law $rc_u = \text{constant}$, that when this law is observed there is no radial flow in the rotating fluid, provided the pressure distribution in the rotating fluid is such that the equation

$$p_1 + \rho \frac{c_{u1}^2}{2} = p_2 + \rho \frac{c_{u2}^2}{2} \quad (69)$$

is satisfied.

Conversely, the assumption of the validity of the law $rc_u = \text{constant}$ is equivalent to the assumption that a pressure distribution, such as required by equation (69), is established immediately behind the fan. In other words, operating for conditions other than the computed one, the flow immediately behind the fan is of such character that there is no radial flow, all the particles moving over cylindrical surfaces coaxial with the fan.

We have assumed that the flow pattern will be incomplete, however, if we do not consider what the axial velocities c_a produced by the individual blade elements are. It is not difficult to see that for operating conditions other than those for which the computation is made the axial velocities cannot remain constant. First we may note that it is incorrect to suppose that the nonconstancy of the axial velocity along the radius in itself excludes the possibility of the operation of the law $rc_u = \text{constant}$. In fact we have seen, in deriving this law, that the axial velocities do not figure in this derivation at all. Physically, this means that regardless of whether the particles of the rotating fluid have a forward motion or not it is of importance only that at each given instant the pressure required by relation (69) be maintained at a given point.

The requirements of a redistribution of the axial velocities may be explained by the following example. Let the transition from one operating condition to another occur by a sudden sharp throttling. It is then evident that at first the axial velocities will tend, by inertia, to maintain their constant values along the radius. The direction of the approaching flow for each of the elements and the pressure itself can be determined with the aid of the pressure head coefficient K_p . It will be found that the pressure of the individual blade elements will be greater or less than the pressure which these elements must develop in order that the law $rc_u = \text{constant}$ hold behind the fan. Let us assume, for definiteness, that the pressure produced by the blade element exceeds that required by this relation. In this case the excess of pressure will give rise to an increase in the axial velocity of the flow which, in turn, will lead to an increase in the pitch angle a decrease in the angle of attack and hence also drop in the pressure. This process will continue until the relation between the pressures will become that required by the law $rc_u = \text{constant}$. From what has been said it is clear that in passing from the computed regime to another the condition of constancy of the axial velocity along the blade will be disturbed. Thus the

assumption that the law $rc_u = \text{constant}$ holds for regimes of fan operation other than the computed regime implies only that the flow takes place as before along cylindrical surfaces coaxial with the fan but with different axial velocities at the various radii. Because of the fact that the axial velocities ahead of the fan are constant along the radius the flow passes through the fan along conical surfaces. This character of the flow was neglected since we have considered that the conical surfaces along which the flow through the fan passes differ negligibly from the cylindrical surface coaxial with the fan. The author considers himself justified in publishing his method of axial fan computation based on the above physical pattern since the method gives good agreement with the experimental results and is of definite practical value.

It is of interest to elucidate the fundamental assumption regarding the maintenance of the constancy of the circulation from the point of view of the vortex theory of the fan. From this point of view the constancy of the circulation is equivalent to the assertion that the system of resultant vortices that replaces the axial fan maintains its shape for all operating conditions of the fan, there being only a change in the intensity of the vortex. As before each blade is replaced by one resultant vortex.

In conclusion we consider the question of the possibility of extending our fundamental assumption with regard to the maintenance of the law $rc_u = \text{constant}$ to the case of the rotation of the fan blades about their axes or a reduction in their number. There is, in fact, no fundamental difference in the flow phenomena when the fan operates at regimes other than the computed regime or when the fan operates with different blade angles. We may note, in confirmation of the above-mentioned assumption, that operation of the fan at a different regime or different blade angles is possible by a continuous change from the computed regime. As in the case of rotation of the blades about their axes there is no fundamental difference in the flow phenomena when the fan operates with a different number of blades.

IV. NEW MODIFICATION OF THE METHOD OF AXIAL FAN COMPUTATION

Before proceeding to the presentation of the method of computation proper we shall make some observations on the computation with the aid of the coefficients K_a and K_u .

The method of computation itself will be very briefly presented since its presentation is not the chief object of our present work and since a special paper by K. Ushakov devoted to the computation of axial fans is simultaneously being published with our paper. We shall not stop to consider the question of choice of fan, its basic parameters, determination of its diameter, peripheral velocity, and so forth.

The method presented by us is based on the same physical pattern as that mentioned in the work of K. Ushakov and our method is therefore not entitled to be considered as new but only as a modification of existing computational methods by the blade element theory or vortex theory.

The fundamental characteristic of the modification proposed by us, together with the use of the coefficient K_a and therefore with the pressure losses associated with the profile drag, is the possibility of setting a definite blade element at the most favorable blade angle corresponding to the optimum profile efficiency. In the usual computation the question of setting the blade element for the optimum operating conditions remains unclear. Strictly speaking the usual computation requires the setting of all the blade elements at the same angle of attack (under the condition of using the same profile) since the theory of the computation presupposes that all the elements have a constant μ - the reciprocal of the aerodynamic efficiency of the profile section. In other words the only clear criterion for a rational setting of the blade elements is the value of the aerodynamic efficiency, and to be consistent it is necessary, in all cases, to set the blade elements at the angle corresponding to the given maximum efficiency. This requirement, however, strongly hampers the designer since it excludes the possibility of changing the blade elements in accordance with structural considerations. In our computation, as will be clear from the discussion below, this possibility of variation is entirely feasible.

We may remark, incidentally, that the control of the rotational efficiency is not at our disposal. The value of $\rho c_u^2/2$ is uniquely determined, as we shall see, by the given value of the pressure head. It is, therefore, possible to speak only of a subsequent utilization of the dynamic pressure with the aid, for example, of guide vanes, but not of the choice of a most favorable value of $\rho c_u^2/2$.

The computation itself proceeds as follows. The value of the pressure head H in millimeterswater and the discharge Q_{hr} in cubic meters per hour are considered as given and the values of the diameter D in meters and the hub diameter d in meters and hence the ratio of the hub to fan diameter $\xi = d/D$ are considered as chosen values, as is also the number of rotations per minute n . We determine, first of all, the magnitude of the clearance (fig. 17) between the wheel and casing of the axial fan. On figure 18 is given a curve of the loss in pressure as a function of the relative clearance expressed in percent. The relative clearance is defined by the ratio of the magnitude of the clearance s to the blade length $R - r_h$ where r_h denotes the hub radius. The formula for the relative clearance is, therefore,

$$\frac{s}{R - r_{hub}} = \frac{s}{100} \quad (70)$$

Figure 18 shows the pressures for the same fan as a function of the relative clearance, the pressures being expressed in percent of the maximum pressure, which would be obtained for a vanishingly small clearance. The trend of the curve shows that the effect of the clearance is very marked, the loss in pressure already amounting to 10 percent for the practically small clearance of 1 percent. This pressure loss may be taken into account in the fan computation by computing not for the given but for an increased pressure. Thus the computed pressure is given by

$$H_{comp} = H K_{clear} \quad (71)$$

The correction coefficient K_{c1} may be defined from the curve of figure 18* on which, for convenience in using, are indicated the values of K_{c1} obtained by dividing the pressure for zero clearance by the pressure at the given relative clearance, that is,

$$K_{c1} = \frac{H_{s=0}}{H_s} \quad (72)$$

*The curve of figure 18 was obtained experimentally and represents a mean curve from a family of curves obtained in investigating the effect of clearance on the characteristics of various fans (fig. 19).

Having determined the pressure H_c for which the fan is to be computed it is possible to proceed to the determination of the rotational component c_u without which, as we have seen, it is impossible to construct the velocity triangle and hence to determine the effective pitch angle and the blade setting. We have seen, moreover, that the value of the power expended by a blade element is likewise determined from the rotational velocity. It is not difficult to see that for constant axial velocity along the blade the total power of the fan is determined from the rotational velocities at each blade element.

From the consideration of the physical basis of the fan operation it has been established that the pressure produced by the fan is that produced by the blade tip element. Conversely, if the pressure is known, the rotational velocity of the flow c_u , corresponding to this blade element, can be found. For this purpose we make use of the formula

$$H_c = \eta_{pr} \rho c_u \left(u - \frac{c_u}{2} \right) \quad (38)$$

In the above relation the values of the air density and peripheral speed are known. For normal conditions (760 mm Hg, 20° C and 50 percent humidity) for which the computation is generally made, the specific weight γ of the air is 1.2 killogram per cubic meter and hence the density

$$\rho = \frac{\gamma_{air}}{g} = \frac{1.2}{9.81} = 0.1233 \frac{\text{kg sec}^2}{\text{m}^4} \quad (73)$$

where g is the acceleration of gravity equal to 9.81 meters per second square. The peripheral speed u may be found from the formula

$$u = r \omega = r \frac{\pi n}{30} \quad (74)$$

The determination of η_{pr} for substitution in formula (38) is somewhat more involved since η_{pr} depends on the pitch angle β defined by the relation

$$\tan \beta = \frac{c_a}{u - \frac{c_u}{2}} \quad (75)$$

and hence on c_u . Since an analytic expression for η_{pr} as a function of c_u is not known, no exact analytical solution of equation (38) for c_u can be given. It is possible, however, to obtain an approximate value of η_{pr} for substitution in formula (38). We have seen (see fig. 20 and the η_{pr} curves in appendix I) that the value of η_{pr} depends very little on the blade angle and changes relatively by a small amount with the angle β . Since the latter also varies slightly with c_u (c_u is small by comparison with u and therefore with change in c_u the difference $u - c_u/2$ entering in the expression for $\tan \beta$ changes slightly) it is evident that even a relatively large change in c_u results in a very small change in η_{pr} . It is, therefore, permissible in formula (38) to substitute a value of η_{pr} determined by a value of c_u that is close to the actual value. Such a value of c_u will, for example, be the one determined by the computed pressure H_c with η_{pr} neglected, that is, according to the formula

$$H_c = \rho c_u \left(u - \frac{c_u}{2} \right)$$

obtained from formula (38) by setting $\eta_{pr} = 1$.

We now solve equation (38) for c_u putting the equation in the form

$$c_u^2 - 2 u c_u + \frac{2 H}{\rho \eta_{pr}} = 0 \quad (76)$$

Solving this quadratic equation there is obtained for c_u the expression

$$c_u = u - \sqrt{u^2 - \frac{2H}{\rho \eta_{pr}}} \quad (77)$$

where the minus sign is taken in front of the root since the rotational velocity of the flow c_u cannot exceed the peripheral velocity u .

By making use of formula (77) and taking account of what was said, with regard to the choice of η_{pr} , we have the following order of operations for the determination of c_u . We first find an approximate value c_u' for the choice η'_{pr} , assuming in formula (77) $\eta_{pr} = 1$, that is,

$$c'_u = u - \sqrt{u^2 - \frac{2H}{\rho}} \quad (78)$$

Having found c'_u we find that effective pitch angle β for the choice η_{pr} from the relation

$$\tan \beta' = \frac{c_a}{u - \frac{c_u'}{2}} \quad (79)$$

From the curve of profile efficiency we then find a value of η_{pr} near the maximum. We may note, here, that this choice of the value of η_{pr} presupposes that angle of attack at which the blade tip element should be set. Observing, however, the trend of the η_{pr} curves for usual fan profiles (fig. 20 and others in appendix 1); an exception occurs for symmetrical profiles. We find that this circumstance does not seriously hamper the designer. The angle of attack may be changed because of the width of the blade without the necessity of computing new relations determined by the rotational velocity c_u since the value of η_{pr} changes very little. Having chosen the value of η_{pr} the value of c_u for the tip element may be finally determined by formula (77).

The value of c_u thus found determines, in view of the relation $rc_u = \text{constant}$, also the rotational velocity for all remaining blade elements. Evidently the rotational velocity at radius r is

$$c_{ur} = c_{uR} \frac{R}{r} \quad (80)$$

where R is the fan radius which is the radius of the blade tip element.

With the values of c_u for all the blade elements thus determined, the values of the angle β for all elements are likewise determined. From the constancy of the axial velocity c_a for any cross-section we may determine this velocity for the given discharge Q cubic meters per second by dividing the latter by the fan disk area F

$$c_a = \frac{Q}{F} \quad (81)$$

In formula (75) defining the angle β all magnitudes are now known and it is possible to proceed to the computation of the blade elements. The problem consists in determining the blade angle θ equal, as we have seen, to

$$\theta = \alpha + \beta; \quad (82)$$

and the blade width b . From the η_{pr} curve the choice of the angle of attack offers no difficulties. It is natural to set each of the blade elements at an angle of attack corresponding to the maximum value of the profile efficiency, a deviation from this rule being considered only for structural considerations.

To determine the width b we make use of the two expressions for the pressure head developed by a blade element:

$$H = \eta_{pr} \rho c_u \left(u - \frac{c_u}{2} \right) \quad (83)$$

and

$$H = \rho K_a \left(\frac{u - \frac{c_u}{2}}{\cos \beta} \right) \frac{bi}{2 \pi r} \quad (84)$$

where i denotes the number of blades, chosen from structural considerations. Equating the right-hand sides of equations (83) and (84) we find by dividing by ρ and $(u - c_u/2)$ that

$$\eta_{pr} c_u = \frac{K_a \left(u - \frac{c_u}{2} \right) b i}{2 \pi r \cos^2 \beta}$$

Solving this equation for b we find

$$b = \frac{2 \pi r \eta_{pr} c_u \cos^2 \beta}{K_a \left(u - \frac{c_u}{2} \right) i} \quad (85)$$

This is the required formula for the determination of the blade width. We may note that the pressure head coefficient K_a , entering this formula, may be found from the corresponding curves for the pressure head coefficients since both the angles of attack and the angles β are known. In case the angle β differs from the round values of β , for which the curves were drawn, recourse is had to interpolation. This will be the case where we make use of profiles of different relative thickness if it appears that the relative thickness differs from the round values, for which the curves were drawn.

With the determination of the blade angle and blade width, the aerodynamic computation of the blade elements, and, hence, the shape of the entire blade, may be considered as completed. The description of how the blade shape is realized in practical construction is not part of our problem and the reader is referred to special literature (reference 2). Here we shall merely remark the following. In the fan working drawing the blade width and blade angle shown, are those obtained by the intersections of the blade with the vertical plane perpendicular to the axis. Evidently these values differ somewhat from the computed values corresponding to the intersection of the blade by a cylindrical surface. If the curvature of this surface is not large, however, (its radius is sufficiently large) the difference between the values of the blade angle θ and blade width b and the computed values taken from the drawing is not great. This circumstance was taken into account in order to simplify the further computations, choosing for the angles θ and

widths b used in obtaining the computed characteristics the values found from the working drawings of the blade.

To complete the aerodynamic computation of the fan, as a whole, we shall consider also the power required by the fan and determine its efficiency. In the same manner, as for the blade element, the power of the fan as a whole may be computed from the theorem on the moment of momentum. Let r_m be a certain mean blade radius* and $c_u(r_m)$ the corresponding velocity which must be assumed for the computation of the moment imparted to the moving air mass in the circumferential direction. Since the mass of air discharged per second is equal to the product of the volume by the density ρQ , the momentum is given by the product $\rho Q c_u(r_m)$ and its moment by

$$M = \rho Q c_u(r_m) r_m \quad (86)$$

The power is given by the product of the moment by the angular velocity

$$N = \rho Q c_u(r_m) r_m \omega \quad (87)$$

The above expression, for the power of the fan, is not convenient because there enter into it the undefined magnitudes of the mean radius r_m and the corresponding velocity $c_u(r_m)$. These can be eliminated through the use of the relation $r c_u = \text{constant}$ whereby the product $r_m c_u(r_m)$ can be replaced by the product of any radius of its corresponding rotational flow velocity. Since we have previously made use of the blade tip element in our calculation it is natural to use the product $c_u R$. Dropping the subscript R , and remembering that $R \omega = u$, we may write our formula for the determination of the power in the form

$$N = \rho Q c_u u \quad (88)$$

where N is in kilogram-meter per second. If the power is expressed in horsepower, as is usually the case in fan

computation, the formula becomes

$$N_{hp} = \rho \frac{Q c_u u}{75} \quad (89)$$

Finally the power of the fan may be directly computed from the power coefficient K_u by making use of the expression for the power of a blade element

$$\Delta N = K_u \rho w_m^2 b \Delta r u_r$$

By dividing the blade into a sufficient number of elements, we obtain the power as the sum of expressions of the above form multiplied by the number of blades

$$N = i \sum_{r_{hub}}^R K_u \rho w_m^2 b \Delta r u_r \quad (90)$$

In practice this formula is less suitable since it gives a sufficiently accurate result only for division of the blade into a relatively large number of elements, of the order of 8 or more. It can only be recommended as a check formula giving an independent result.

The overall efficiency of the fan is computed by the known formula

$$\eta = \frac{QH}{75 N} \quad (91)$$

where Q is expressed in cubic meters per second, H in millimeter water and N in horsepower. Since we have seen that the fan as a whole gives a pressure equal to that of the tip element it is natural, in the above formula, to substitute the pressure of the blade tip taking account, of course, of the pressure loss at the clearance. However, since we have computed the fan for a pressure that is greater by these losses we may evidently substitute the value of the actual, that is, the given pressure.

With this we may conclude the presentation of our modification of the axial fan computation. As an illustration of the method we give a sample computation sheet with the data required for carrying out the computation on pages 76 and 77. We have considered it unnecessary to overload our example with special remarks since the entire procedure is explained in detail in the present section. The reader may refer to the description of this procedure if anything in the example does not appear clear to him. In order to facilitate looking up the required place in the text we have indicated everywhere the number of the required formula and the corresponding figures. With this in mind we shall, with regard to the selected computation example make only the following remarks.

We have chosen, for our example, an axial high-pressure test fan with the following data: $Q = 13,100$ cubic meters per hour at $n = 2800$ rpm, $H = 168$ millimeter water (at relative clearance $s = 1$ percent), diameter $D = 0.6$ meter, $\xi = 0.5$, number of blades $i = 12$. Here we shall make an important observation. In the description of our computation method and in the sample fan computation no account was taken of a factor which must necessarily have an effect on the fan performance. We refer to the effect of the mutual blade interference (cascade effect). No correction coefficients, which take into account the effect of mutual blade interference have been applied in the aerodynamic axial fan computation conducted by CAHI until recently. There are two reasons for this:

1. CAHI has occupied itself with design problems of high-pressure axial fans only recently. The fans of earlier design were, in the majority of cases, characterised by low pressure and hence large blade spacing. For these fans the factor of blade interference played no important part.
2. Only in the course of our present investigation has any systematic comparison been made between the fan computation data and the test results with account taken of such factors as, for example, the effect of the clearance, the mutual blade interference and so forth. Until recently the lack of agreement of computed results with test results was corrected by a single-overall statistical correction coefficient which took the above factors into account and reduced the disagreement. In the above-mentioned work of K. Ushakov the mutual interference is taken into account with the aid of a general correction coefficient

? 1.05

K_{cas} equal to 0.05 - 0.1. With the aid of this coefficient the pressure H_c for which the fan is computed is expressed in terms of the required pressure H by the following formula:

$$H_c = H K_{cl} K_{cas} \quad (92)$$

Such a correction, however, with the aid of a constant coefficient can be made only as a first approximation. It is quite evident that the blade interference depends on a number of factors and varies with different cases. In section VI we shall present preliminary results of our attempt to estimate the effect of blade interference of the axial fan.

In figures 33 and 34 we present a sketch of the fan computed in this section and a drawing of the fan blade. The collector at the fan entrance may be noted. The results of the fan tests are given in section VI.

V. METHOD OF COMPUTATION OF AXIAL FAN

The object of a check computation of an axial fan is to determine from the geometric parameters of the fan its aerodynamic characteristics, the volume flow, pressure head and power at all operating loads of the fan. In our present paper we restrict our computation to those conditions for which all the blade elements operate under normal angles of attack up to the start of flow separation (cavitation) since as yet no satisfactory theory has been developed for the axial fan operation in this range. The range of normal angles of attack is practically the one of greatest interest since it is the range of maximum fan efficiency.

It is known that the fan pressure drops as its discharge increases.

From the relation

$$H = \eta_{pr} \rho c_u \left(u - \frac{c_u}{2} \right) \quad (93)$$

it is clear that the drop in pressure corresponds to a decrease in the rotational velocity c_u . An increase in the discharge, on the other hand, corresponds to an increase in the pitch angle β . There is thus a relation between the fan operating condition defined by the combination of values Q and H and by a certain pair of values c_u and β . It is natural, therefore, given the values c_u and β , to seek the corresponding values of the delivery and pressure: a procedure we shall use in determining the computed axial fan characteristics.

Given a fan to determine its computed characteristics. From the working drawing of the blade we determine the values of the blade angle θ , the width b , the relative profile thickness δ and the profile shape. The latter is, evidently, very important since the computation is based on the the profile aerodynamic characteristics, obtained from tests in the wind tunnel. For convenience in making the computations we plot the obtained values of θ , b and δ on a diagram. Drawing smooth curves through the points obtained we may find the required data for any blade element. Such a diagram is shown in figure 21 for one of the fans investigated by us in detail; namely, fan 4. In section VI a sketch and blade drawing of this fan are given (figs. 31 and 32).

The fundamental relations which we make use of in determining the points of the computed characteristics are found in equation (93).

$$H = K_a \rho w_m^2 \frac{b i dr}{2 \pi r dr} = K_a \rho \frac{\left(u - \frac{c_u}{2}\right)^2}{\cos^2 \beta} \frac{bi}{2\pi r} \quad (94)$$

$$\Theta = \alpha + \beta \quad (95)$$

Let us consider which magnitudes may be here assumed as known and which are required to be determined from the equations.

Omitting the known air density ρ , the number of blades i and the known values b and θ , which may be found from the auxiliary curves such as those shown in figure 21, we consider the values of the radius r and the peripheral velocity $u = r\omega$. Since our computation will be conducted

on the blade elements the radius r may be considered defined together with the corresponding element. The peripheral velocity may be considered as known since the angular velocity is also known: $\omega = \pi n/30$ where the rotational speed n in rpm is given. There remains to be determined the magnitude of the head H , the rotational flow velocity c_u , the pitch angle β , the angle of attack α , the profile efficiency η_{pr} and the pressure coefficient K_a . The two latter magnitudes may, however, be considered as known because both are functions of the angle β and the angle of attack as is seen from the corresponding diagrams. It is thus clear that in the three equations (93), (94), and (95) there are four unknown variables. Evidently if one of the variables (it is natural, for example, to choose the rotational velocity as basic) is taken as the independent variable the remaining variables will be determined since only three unknowns will then remain in the three relations. As may be readily seen, however, to give an analytical solution of these equations is impossible, first of all, because there enter the variables η_{pr} and K_a which are functions of graphically given unknowns. The choice of analytical expressions would involve us in an extremely complicated mathematical analysis. Moreover the angle β and the rotational velocity are in an indirect relationship. All these considerations made us dispense with any attempt at analytical solution and the problem was solved by the method of trial and error. We are given a pair of values c_u and β . The third of our fundamental relations (formula (95)) gives us the angle of attack and thus permits us to choose K_a from the corresponding curve. With these values determined the pressure head H can be computed by formulas (93) and (94). The pressure computed by the second formula is denoted with the subscript K_a since, generally speaking, for arbitrary values of c_u and β , the pressure computed by the second formula will not be equal to the pressure computed by the first formula. If it appears, however, that

$$H = H_{id} \quad (96)$$

it signifies that the relation between the magnitudes c_u and β is true that they satisfy our fundamental relations. The pressure H will then be the actual pressure developed by a given blade element at given c_u and β and from the angle β the volume flow through an elementary ring swept by the element under consideration can be found. Thus, the axial velocity is

$$c_a = \left(u - \frac{c_u}{2} \right) \tan \beta \quad (97)$$

and the volume

$$Q_{\text{ring}} = 2 \pi r \left(u - \frac{c_u}{2} \right) \tan \beta \, dr \quad (98)$$

With the above, we conclude our general considerations underlying our method of computation and proceed to the drawing of the computed characteristics.

We begin with the determination of the fan pressure. In discussing the physical basis of the fan operation we have established and later in the computation made use of the fact that the pressure developed by the blade tip element gives the pressure of the fan as a whole. We shall, first of all, analyze the operation of the tip element, making use of the general considerations discussed above. As a result, we shall obtain, for a given series of values of c_u a series of values of the pressure, that is, one of the coordinates of the fan characteristics and then proceed to determine the discharge.

In determining the discharge it is not sufficient to consider the operation of the single blade tip element because the axial velocities through the other elements are unknown. The assumption of the constancy of the axial velocity is, as we have seen, in section III valid only for the single computed operating condition. For other operating conditions there is a redistribution of the axial velocities and the axial velocity no longer remains constant along the blade. To determine the axial velocities for each given blade element we may proceed from the following considerations. We have assumed that the flow through the fan is such that the pressures behind the fan and hence the pressure differences developed by the blade elements are so distributed that the law $rc_u = \text{constant}$ hold true. This law may then be used to determine the value of c_u and with it the pressure head for any blade element. What follows the pitch angle β is determined by the trial and error method similar to that in analyzing the work of the tip element until the pressure computed from the found value c_u

$$H_{c_u} = \eta_{pr} \rho c_{ur} \left(u_r - \frac{c_{ur}}{2} \right) \quad (99)$$

is equal to the pressure computed from the coefficient K_a

$$H_{id} = K_a \rho \frac{\left(u - \frac{c_{ur}}{2} \right)^2}{\cos^2 \beta} \frac{b r i}{2 \pi r} \quad (100)$$

It must, of course, be remembered that the blade angle Θ and the blade width b should be taken to correspond to the given element. From the found angle β we determine

$$c_{ar} = \left(u_r - \frac{c_{ur}}{2} \right) \tan \beta_r \quad (101)$$

Finally the discharge for a given element is

$$Q_{r \text{ ring}} = c_{ar} F \quad (102)$$

where

$$F_r = 2 \pi r dr \quad (103)$$

Thus for any operating condition for which we have previously obtained the pressure, from an analysis of the performance of a blade element, we may now determine the axial velocity and with it the volume flow for any blade element. On figure 22 we show, as an example, the axial velocity distribution for various operating conditions of fan 4. Detailed computations in constructing the computed characteristics of this fan will be given below at the end of the section. Here we shall merely show how this diagram of axial velocities was constructed. The axial velocities were computed for three blade sections; namely, the tip element, the hub element, and the

element at the mean radius. Continuous curves were then drawn through the obtained values laid off as a function of the radius. If the flow volume through any of the elements is known then the total flow may be found by summation

$$Q = \sum_{r_{\text{hub}}}^R Q_{\text{ring}} \quad (104)$$

over all the elements from the hub to the fan circumference. The same result could be obtained by finding the mean axial velocity through graphical integration of the axial velocity distribution curve. The discharge would then be given by the product

$$Q = c_{a_m} F \quad (105)$$

We shall now proceed to the determination of the fan power. Since the rotation component c_u is known for all elements the power for each of the elements may also be computed from the formula

$$N_k = \rho Q_{\text{ring}} c_u u_r \quad (106)$$

where it is again pointed out that c_{u_r} and u_r - the rotational component and the peripheral velocity - must be taken at the given radius. The power expended by the fan as a whole is evidently equal to the sum of the powers of the individual elements

$$N = \sum_{r_{\text{hub}}}^R N_k = \sum_{r_{\text{hub}}}^R \rho Q_{\text{ring}} c_{u_r} u_r \quad (107)$$

In this form the formula for the power appears rather complicated. It is easily seen that it can be considerably simplified. Thus, in the sum at the right-hand side of the equation the product $c_{u_r} u_r = c_{u_r} r \omega$ where ω the angular velocity is constant as is also the air density ρ . Taking

the constants outside the summation sign we may write the expression for the power in the following form

$$N = \rho c_{ur} r \omega \sum_{r_{hub}}^R Q_{ring}$$

Remembering that $c_{ur} r = c_u R$ and $c_u R \omega = c_u u$ and also that $\sum_{r_{hub}}^R Q_{ring}$ is the total flow through the fan the result is obtained that the power expended by the fan independently of the operating conditions is given by the product

$$N = \rho Q c_u u \tag{108}$$

where c_u is the rotational component of the flow for the tip element and u the rotational velocity of the fan. We thus arrive at the conclusion, which very much simplifies the computation, that to compute the power of the fan at any operating condition it is not necessary to compute the power for each element individually.

We may note that in the expression for the fan power the power expended by the air friction at the hub does not enter. This power as experimental considerations indicate (reference 3) is given by the formula

$$N_{hub} = \beta_N \rho \omega^3 d^5 \left(1 + 3.9 \frac{b_{hub}}{d} \right) \tag{109}$$

where b_{hub} is the width of the hub and d its diameter; N is obtained in horsepower.

The coefficient β_N entering the formula is nondimensional and can be obtained from the experimental curve (fig. 23) of A. Sichev; the value of β_N being laid off as a function of the Reynolds number, defined for normal conditions by the formula

$$Re = \frac{u d}{14.46 \times 10^{-6}} \quad (109a)$$

It is also seen from the paper by Sichev that the value of the power expended at the hub remains constant for all operating conditions of the fan.

It is of great interest, finally, to check the computation by determining the power expended directly with the aid of the power coefficient K_u . The power for a given element for all blades is

$$\Delta N_{ring} = K_u \rho w_m^2 b_i \Delta r u_r \quad (110)$$

the magnitudes entering this formula being taken at the mean radius of the ring. We shall briefly consider the computational procedure. The blade is divided into a number of elements by dividing the swept area into rings of equal area (fig. 24)* and then determining the power for each element. Since the values of the pitch angle β and the relative velocity $w_m = (u - c_u/2)/\cos \beta$ for any radius are unknown we construct additional auxiliary curves for β and w_m . If these magnitudes are known the corresponding power coefficient K_u is also determined since the angles of attack for its choice are

$$\alpha_r = \Theta_r - \beta_r$$

The power of the fan is obtained as the sum of the powers of the individual elements

$$N = \sum_{hub}^R \Delta N_{ring} \quad (111)$$

taken for all the blades. We may note that, practically, it is sufficient to compute the power for eight elements, the swept area being divided into eight rings of equal area.

*In fig. 24 the diagram is given for dividing any circle into rings of equal area. The magnitudes of the ring radii are expressed as relative radii $\bar{r} = r/R$ from which the actual radii for a given fan can be readily computed.

In concluding we shall give the formulas for the efficiency. If the friction power at the hub is not taken into account the efficiency may be computed by the formula

$$\eta = \frac{Q H_s}{75 N} \quad (112)$$

In taking account of the power expended by the hub the formula becomes

$$\eta = \frac{Q H_s}{75 (N + N_{hub})} \quad (113)$$

We may note that in both formulas the head H is written with the subscript s to bring out the fact that in these formulas the pressure takes account of the presence of a clearance between the wheel and casing.

For examples of the construction of the computed fan characteristics we present, in their entirety, all computations for the two fans 4 and 5b on pages 78 to 85.. The computations are all arranged in the order which appears most logical to us and which was also adopted for the computation of the remaining seven characteristics. For convenience to the reader the formulas are numbered to correspond to the text where they are derived.

VI. COMPARATIVE ANALYSIS OF COMPUTED AND EXPERIMENTAL DATA

1. Introduction

The object of this section is to explain to what extent and within what limits our computation method applies. We shall, first of all, be interested in comparing the computed results with the test results. Incidentally, we shall also touch upon a number of questions with regard to the effect of certain fan parameters on its performance. We shall also indicate the possibility of approximate construction of the axial fan characteristics with a minimum labor of computation. Such characteristics are of importance for preliminary computations in selecting a fan for given conditions, choosing its fundamental parameters, and so forth.

The sections will, therefore, be divided into the following headings:

1. Considerations with regard to the selection of the fan for testing and their fundamental characteristic data.
2. Some special features of the test procedure.
3. General view of the agreement of the computed with test results and factors accounting for disagreement between them.
4. Method of constructing the preliminary characteristics.
5. Detailed discussion of the chief factor accounting for the difference between computed and test results; namely, the blade interference. The method of taking this factor into account depends on the possibility of obtaining the aerodynamic characteristics of the profile from the fan characteristics.

2. Selection of Fans for Investigation and Their Basic Data

Since the object of our computation is to determine the aerodynamic characteristics of a fan from its geometric dimensions we have chosen, for the purpose of comparison of the computed with test data, a number of fans that differed sufficiently in their geometric parameters, such as their diameters, ratio of hub to fan diameter, blade width, number of blades, and so forth. Moreover one of the fans tested, an axial reversible fan, in contradistinction to the sections of the other fans which were various modifications of English propeller profiles, was of symmetric profile section especially suited for the design of reversible fans.

Figures 25 to 34 give exhaustive sketches and drawings of the blades of all fans tested and with the aid of which the fans can be completely constructed. Figures 35 to 38 gives the curves of the variation of the geometric blade parameters Θ , b , and $\bar{\delta}$ as functions of the radius.*

*The curves of variation of the geometric parameters for fan 4 are given in fig. 21.

Since our object is to show the possibility of the application of the method also for the cases where the blades are rotated about their axes and for removal of a number of blades two of our fans; namely- 3 and 5- were chosen from those at the laboratory disposal that possessed rotatable and removable blades. The first of these fans was tested at the blade angles

$$(a) \Theta = 19^{\circ} 20' \text{ (initial angle)}$$

$$(b) \Theta = 16^{\circ} 50'$$

$$(c) \Theta = 14^{\circ} 05'.$$

The blade angle given is that for the blade tip element. For the other blade elements the blade angles in rotating the blades evidently vary by the same amount as the angle of the tip element. The second fan with rotatable and removable blades was tested for the number of blades

$$(a) i = 12 \text{ (rated number of blades)}$$

$$(b) i = 6$$

$$(c) i = 3.$$

For convenience we give, in addition to the blade sketches and drawings, a table of the geometric parameters and computed fan data, the rotational speed and two characteristic nondimensional magnitudes; namely, the relative circulation $\bar{\Gamma}$ defined by the ratio of the actual fan circulation $\Gamma = 2\pi R c_{uR}$ to $4\pi R u_R$:

$$\bar{\Gamma} = \frac{2 \pi R c_{uR}}{4 \pi R u_R} = \frac{c_{uR}}{2 u_R} \quad (114)$$

and the magnitude φ characterizing the degree of utilization of the rotational velocity for producing pressure and given by

$$\varphi = \frac{H}{\rho u^2} \quad (115)$$

In table I the computed and experimentally obtained values of φ are given for comparison. The computed data could

only be given for the three fans, 1, 4, and 5a. For fans 2 and 3 no preliminary computations were made.

The fans were all carefully constructed of wood. The blades of all the fans except 4 were polished. The checking of all the fans on the special laboratory apparatus for measuring fans showed that the errors in producing the fan blade did not exceed 10 ⁱⁿ/_{feet} to 20 ⁱⁿ/_{feet} for the blade angle, and 0.5 to 1 millimeter for the blade width.

3. Special Features of the Procedure

There is no need to dwell in detail on the procedure of typical fan tests since it has been fully explained in a special paper (reference 4). We shall only note certain features in testing and working up the results. Instead of the usual procedure of testing the fan in a short pipe with sharp edges the fans were enclosed in a streamlined casing. In this way the axial direction required by the theory of the lines of flow at the fan inlet was assured.

Great attention was paid to the measurement of the size of the clearance between the wheel and casing. Corrections in the computed characteristics of the fan were made as functions of this magnitude. The necessity for such corrections is dictated by the fact that our method is based on the assumption that the fan operates at a vanishingly small clearance. For this reason, in order to be able to compare the computed with the test characteristics obtained at some definite clearance, we first introduce a correction for the effect of the clearance. We have already pointed out that the effect of the clearance is particularly strong on the value of the pressure. The effect on the power is somewhat less marked. Evidently the effect on the power is particularly strong for operating conditions near the maximum air discharge. For this reason we consider it possible to introduce a correction for clearance only in constructing the curves of computed pressure. This correction is made with the aid of figure 19 making use of the obvious relation

$$H_s = H_{s=0} \left(\frac{H_s}{100} \right) \quad (116)$$

where H_s is the required pressure at a given clearance ratio, $H_{s=0}$ the pressure at a vanishingly small clearance,

and H_g the percent pressure at the given clearance. From figure 19 it is seen that the pressure falls very sharply as a function of the clearance. In view of this fact it is clear that the mean value of the clearance must be determined with considerable accuracy. The required accuracy was obtained by measuring the clearance with a special measuring apparatus at 8 to 10 places of the casing.

Finally, we wish to point out that the dynamic pressure head of the fan was computed for all operating conditions from the mean velocity of flow at the fan outlet $c_{am} = Q/F$. The effect of the expected axial velocity distribution on the value of the dynamic pressure head of the fan was not taken into account since there was no opportunity to conduct tests on the velocity field behind the fan.

4. General Observations on the Agreement between the Computed and Test Results

On figures 39 to 65* comparison curves are given of the computed and test characteristics of all the fans considered.** For each of these fans there are also given curves of axial velocity distribution for various operating conditions and the complete test characteristics with the test points. The importance of taking into account the axial velocity distribution is seen in figure 66 which gives the characteristics of fan 2 drawn to take into account the axial distribution and the characteristics drawn on the assumption of constant axial velocity.

We shall first consider, from a general point of view, the agreement of the pressure and power curves and then proceed to the question of the agreement of the computed with test results on rotating the blades about their axes or removing some of the blades. We shall make only one preliminary remark with regard to the limits of the computed interval, which as is seen from the comparison curves, is not very large. In the range of large volume discharges the computed characteristic extends beyond the limits of the test characteristic. This is explained by the fact that in this range the test characteristic is discontinued where the static fan pressure becomes zero (see figs. 41, 44, etc.); whereas the computed characteristic is drawn also for

*All curves were drawn for normal conditions, that is referred to $\gamma_{air} = 1.2 \text{ kg/m}^3$, 760 mm Hg, 20° C and 50 percent humidity.

**In the value of the computed power no account was taken of the power expended by the rotation of the fan hub since this power is very small as seen in table II.

negative static pressures since we may assume small values for the rotational flow velocity c_u for which the corresponding total pressure and power are near zero. The limit of the computed characteristic in the region of small volume discharge is determined by the start of flow separation (cavitation) from the blade. The impossibility of computing the characteristic when separation occurs is due to the fact that on account of the discontinuation of any further increase in the pressure at the blade elements it is not possible to obtain the pressure distribution required by the law $rc_u = \text{constant}$.

From an examination of the computed and test characteristics the following general conclusion may be drawn. The agreement between the characteristics for the fans with small relative circulations may be considered as fully satisfactory as regards the pressures; the agreement of the power curves is somewhat less favorable. With regard to the trend of the latter curves the following fact may be pointed out. It is known that the power of an axial fan may be considered approximately constant. In this connection a point of view has been widely held that the deflection in the power curve appearing in the test characteristics is explained by the inaccuracy of the experiment. Our computed power curves show that this is not so and that the deflection in the power curve conforms with the facts.

On figures 66 and 67 are given the characteristics of the fan with rotatable blades for three different blade angles. It is seen from the curves that the computed characteristics agree sufficiently well with the test characteristics for this case.* This confirms the fact that there is no fundamental difference in the performance of axial fans when operating at different blade angles. A more detailed examination of the comparison curves shows

1. That the deviation between the computed and test characteristics increases somewhat with increase in volume discharge

2. That the drop in the fan characteristics occurs somewhat earlier than is expected from the computation.

The explanation of the first fact is that no account was taken of the change in the dynamic pressure resulting from the redistribution of the axial velocities. The second fact,

*There is again observed an entirely satisfactory agreement in the pressure curves and a somewhat less favorable agreement in the power curves.

as far as may be judged, is due to the interference effect and the conditions of operation of the cascade in a rotational flow. We have already pointed out that this effect is not taken into account either in the usual computation of the axial fan or in our method. The question of taking this effect into account is closely associated with the possibility of applying the fundamental aerodynamic profile characteristics as obtained for the isolated wing to the computation of the axial fan. It is clear that the application of the characteristics without introducing any correction coefficients to the computation of a cascade will result in a divergence between the computed and test results. In other words it may be foreseen that the aerodynamic characteristics of an airfoil operating as a fan blade differs from the characteristics of the airfoil as an isolated wing. Consideration of the comparison curves gives a basis for the supposition that this difference increases as the rotation of the flow increases. To the smaller volume flows there correspond, in fact, larger values of the rotational velocity c_u and hence also of the circulation. At the smaller discharges, near the deflection in the fan characteristic as we have already pointed out, there is observed a greater deviation between the computed and test characteristics than in the remaining parts.

Figures 68 and 69 show computed and test characteristics illustrating the performance of the axial fan with some of its blades removed. The twelve blade fan which was used as an example in section IV was taken as a basis for the computation. Besides the tests at the full number of blades tests were also conducted for the case of the removal of six and nine blades, that is, with six and three blades. A comparison of the computed and test curves clearly brings out the effect of blade interference. Figure 70 shows computed and test curves of the percent total pressure developed by one blade as a function of the number of blades. The strong interference effect is clearly brought out.

It is clear therefore that the introduction into the computation of correction coefficients that take into account the blade interference effect is absolutely necessary. A detailed consideration of the problem of blade interference exceeds, however, the limits of our present investigation and the theory at present is far from perfected. In section 6 we shall, very briefly, present one of the methods of taking this factor into account.

5. Construction of Preliminary Characteristics

We have already pointed out that in a number of engineering computations, for example, in selecting a fan or making a first rough approximation of its performance, it is desirable to know not only its rated performance but also, at least roughly, the general shape of its characteristics.

Let us note the most important points that determine the shape of the preliminary characteristic. These, in addition to the point of computed performance, are

1. The point of maximum pressure corresponding to zero discharge

2. The point at which there is a straight drop in the characteristic with no further rise in pressure

3. The point at which there is again a rise in pressure. It is evidently also necessary to know the slope of the characteristic at the point where it may be considered a straight line. As regards the first of the above-mentioned points statistical computations on the basis of test data show that the maximum pressure may be considered approximately twice the rated pressure. The second point at which there is a straight drop in the fan characteristic, may be found from the blade tip element in the same manner as in constructing the fully computed characteristic. The difference being that in constructing the latter we correct the value of the discharge at which there is no further increase in the pressure; whereas, in the case of the preliminary characteristic the value of the discharge at which there is a straight drop in the pressure is determined by the slope of the characteristic, about which more will be said later.

Setting down the formulas

$$H = \eta_{pr} \rho c_u \left(u - \frac{c_u}{2} \right)$$

$$H = K_{ka} c_{as} K_a \rho \frac{\left(u - \frac{c_u}{2} \right)}{\cos \beta} \frac{b_i}{2\pi r}$$

and choosing values of c_u and β at the maximum value of K_a until the values of M become equal we find the required value of H . Since for preliminary computations it is advantageous to underestimate the value of the pressure we recommend introducing in the formula a correction coefficient $K_{k_a \text{ cas}}$ that takes into account the blade interference effect.*

This coefficient is a factor by which it is necessary to multiply the pressure coefficient K_a for the isolated blade in order to obtain the value of the pressure coefficient for a given cascade and value of flow rotation. The coefficient may be selected with the aid of figure 74. To obtain the third of the above-mentioned points; namely, the point at which the pressure again starts to rise, is a little more difficult. An examination of the experimental data at our disposal shows that the value of the pressure for this point is equal to or somewhat exceeds (by 10 to 20 percent) the value of the pressure for the point of start of straight pressure drop. We are unable, at the present time, to give an accurate criterion as to when the pressure curve is horizontal and when it rises somewhat in the interval under consideration. For this reason the preliminary characteristic at the deflection region may be taken arbitrarily within the limits considered.

A consideration of the experimental data shows furthermore that the part of the characteristic from point 3 to the point of maximum pressure may be considered parallel to the portion of the characteristic on which the point of rated performance lies. The determination of the slope of this part will be considered. Taking this into account we give the following simple method of determining the end points of the deflection interval of the preliminary characteristic (fig. 72). Through the point of zero discharge we draw a line of the same slope as the initial part of the curve. We mark on this curve a the value of the pressure 20 percent higher than the value of the pressure found for the point 2. The point thus found determines the second boundary of this interval of the fan characteristic.

We consider, finally, how to determine the slope of the preliminary characteristic at the portion where it may be considered straight. The slope is known if we have the value of the maximum discharge or more accurately, the discharge for zero total pressure. This discharge may be deter-

*For the method by which this coefficient is obtained see sec. 6.

mined from the curve shown in figure 73* where the ratio $\varphi_c / (\overline{Q}_{\max} - \overline{Q}_c)$ is laid off as a function of the circulation. All the magnitudes entering this ratio are nondimensional: $\varphi = H/\rho u^2$ and \overline{Q}_{\max} and \overline{Q}_c are the discharges obtained by dividing the actual discharges Q_{\max} and Q_c by $\pi R^2 u_k$. It is readily seen that the ratio $\varphi_c / (\overline{Q}_{\max} - \overline{Q}_c)$ actually gives the inclination of the nondimensional characteristic to the volume axis.

We now resume the order of the steps in constructing the characteristics. There is first laid off the rated point. Then from the relative computed circulation $\frac{\Gamma}{\Gamma_1}$ there is determined the value of the ratio $\varphi_c / \overline{Q}_{\max} - \overline{Q}_c$ from figure 73; we find Q_{\max} from the known φ_c and Q_c , plot the point of maximum discharge and draw straight line connecting with the rated point. The straight line is prolonged a certain distance beyond the rated point in order to find point 2. We find by the method given above the value of the pressure at point 3 and mark this point on the straight line. We mark the point of pressure at zero discharge and then by the above method we draw the deflection interval in the fan characteristic and prolong the latter until it meets the Q axis.

Having plotted the total pressure characteristic, we obtain in the case where it is required the curve of static pressures by deducting the dynamic pressure. The latter, as is known, may be determined by the formula

$$H_{\text{dyn}} = \rho \frac{c_{a_m}^2}{2} \quad (117)$$

where the velocity $c_{a_m} = Q_{\text{sec}}/F$ is equal to the given discharge divided by the swept area.

We shall now make some observations with regard to the shape of the power curve. In constructing the preliminary characteristic it is convenient to take the rated computed power as unity. Then

1. At the point at which the static pressure is zero the power $N = 0.8 N_c - 0.95 N_c$

*The curve given on this figure was constructed on the basis of an analysis of the test characteristic slopes of five fans.

2. At the point corresponding to half the rated discharge the power attains a value equal to $0.85 N_c - 0.95 N_c$.

3. Finally at the point of zero discharge the power is somewhat larger than the rated, being of the order $1.15 N_c - 1.30 N_c$.

We may note that large fluctuations in the power correspond evidently to high pressure fans.

The pressure and power curves determine the efficiency curve. We remark only that the efficiency curve is generally level without any deflections.

We conclude our remarks on the construction of the preliminary characteristics and proceed to the problem of mutual blade interference. Again we point out that the preliminary characteristic can be used only for very approximate orienting computations. The error in using these characteristics may, in certain cases, amount to 20 to 30 percent so that the regularly computed characteristics must be used where greater accuracy is required.

6. Blade Interference Effect

We have pointed out that the aerodynamic characteristics of an airfoil operating as a fan blade element differs from the characteristics of the same airfoil when operating as an isolated airfoil. The problem thus arises of determining the airfoil characteristics from the fan characteristics. If it were possible to do this, then by computing the other fans by the new characteristics we would obtain considerably better agreement with experiment.

The problem of obtaining the profile characteristics from the fan characteristics may be approached in the following manner. We divide, as previously, the fan into a number of elements. It is possible to determine the aerodynamic characteristics of the profile section for such an element if we know the pressure developed by the element and the power required. The fundamental difficulty in finding these magnitudes is that we do not know the axial velocity distribution along the radius and hence also the magnitude and direction of the relative velocity without which the power and pressure cannot be found. This fundamental difficulty may, however, be resolved in the following manner. It may be assumed that the character of the

axial velocity distribution will actually be the same for the corresponding values of the rotational velocity c_u as in constructing the computed characteristics. Thus the actual distribution of the axial velocities at various operating conditions may be found if the corresponding value of c_u is known. Since we assume that the law $rc_u = \text{constant}$ holds true also in these computations the value of c_u may be found from the experimental power with the aid of the relation

$$N = \rho Q c_u u \quad (118)$$

whence

$$c_u = \frac{N}{\rho Q u} \quad (119)$$

or

$$c_u = \frac{.75 \times 3600 \times N}{\rho Q_{hr} u} \quad (120)$$

where N is in horsepower and Q_{hr} in cubic meters per hour.

From the discharge Q corresponding to a given c_u the mean axial velocity may be determined

$$c_{a_m} = \frac{Q}{F} \quad (121)$$

Assuming that the mean velocity c_{a_m} will actually be for a certain mean fan radius r_m as in the computed curve of axial velocity distribution we may find the value of the axial velocity at other radii, assuming, as we have already pointed out, that the relation between the axial velocities at the given radius and at the mean radius is the same as for the computed characteristic at a given c_u .

Thus before proceeding to determine the individual points of the profile characteristics we construct on the

basis of the above considerations the curve of axial velocity distribution. With the axial velocity known and taking into account the law $rc_u = \text{constant}$ and the value of the rotational velocity c_u for any element the angle β of an element is determined and since the blade angle is known the angle of attack can also be found.

The pressure head H which for the given operating conditions can be determined from the test characteristics gives also, as we have already seen, the pressure of the blade tip element. The pressure for the other elements may be found from the relation

$$H_{el} = H_{tip\ el} + \rho \frac{c_u R}{2} - \rho \frac{c_u^2}{2} \quad (122)$$

on the basis of considerations analogous to those previously adduced in constructing the curve of pressure along the fan blade.

If the pressure is known, the relation

$$H = K_a \rho \frac{\left(u - \frac{c_u}{2}\right)^2}{\cos^2 \beta} \frac{bi}{2\pi r} \quad (123)$$

enables us to obtain K_a , that is, we thus obtain a point of the required profile characteristic from the fan characteristics.

In a similar manner there may be obtained from the fan characteristics the value of the coefficient K_u . It is, here, necessary to remember that if the swept area is divided into ring elements of equal area unequal air volumes flow through these areas on account of the inequality of the axial velocities. For this reason the power expended in rotating these elements will not be the same but is distributed in proportion to the volume flow. Since the latter may be found for each ring from the curve of axial velocity distribution there is no difficulty in determining the power expended by each element.

Knowing the power N_{el} required by each element the formula

$$N_{el} = K_u \rho \frac{\left(u - \frac{c_u}{2}\right)^2}{\cos^2 \beta} b \Delta r u \quad (124)$$

enables us to find the value of K_u .

The ratios $K_{a, char}/K_{a, prof}$ and $K_{u, char}/K_{u, prof}$ define correction coefficients by which it is necessary to multiply the values K_a and K_u taken from the characteristics of the isolated airfoil in order to obtain the values of the corresponding coefficients for the blades of the cascade.

We have already pointed out that the aerodynamic characteristics of the airfoil operating as a blade element, the coefficients K_a and K_u depend on two factors; namely, on the blades spacing and the degree of rotation of the flow through the cascade. The blade spacing is defined by the ratio of the blade width at a given element to the distance between the blades:

$$\gamma = \frac{b}{2\pi r} = \frac{bi}{2\pi r} \quad (125)$$

The degree of flow rotation is naturally characterized by the relative circulation

$$\bar{\Gamma} = \frac{c_{uR}}{2u_R}$$

Figure 74 shows the curves of correction coefficient $K_{k_a, cas}$ to the pressure coefficients which were obtained from the

preliminary computations for two fans. ~~We consider it possible for these preliminary computations for two fans.~~ We considered it possible for these preliminary computations to assume these correction coefficients independent of the angle β and angle of attack. It is evident that this is possible only as a first approximation as is also indicated by the considerable scatter of the points. The thin continuous curves on the figure were obtained by interpolation between the round values of Γ .

It should be noted that the results obtained require considerably greater accuracy. We consider, however, that introduction of these correction coefficients into the computation approaches more nearly the true conditions than taking account of the interference effect by computing the fan for a higher pressure.

On figure 75 are shown our preliminary results with regard to the effect of the cascade spacing and degree of flow rotation on the profile efficiency. This effect, as shown by the curve, is very small.

The correction coefficient K_{kac} is introduced into the formula for the determination of the blade width b . Since, however, the coefficient depends on an initially unknown value of b it is necessary to have recourse to the method of successive approximations. For speeding the work it is recommended to assume outright a value of K_{kac} at a somewhat higher value of b than given by the approximation.

CONCLUSION

Although the method developed by us for the computation of an axial fan is approximate it nevertheless provides results of definite practical value. The method permits constructing the computed characteristics for the operating blade angle and number of blades as well as the different blade angle and with some blades removed. The volume of air delivered by the fan is determined from the characteristics with an accuracy sufficient for nearly all fans. The only exceptions are fans with relatively large circulation. In this case too, however, the method can be made more accurate by making use of the correction coefficient K_{kac} discussed in section VI,

section VI, 6. The use of this coefficient for drawing the computed characteristics only slightly complicates these computations. Since the magnitude $b_i/2\pi r$ is already computed it is merely necessary to add three additional columns for $\bar{\Gamma}$, $K_{k a \cos}$ and $.K_{\eta \text{ prof}}$ in the computation sheet. The rest of the computation procedure remains the same.

We consider briefly, in concluding, three problems whose solution is of immediate practical importance in the aerodynamic computation of an axial fan. These are, first of all, the problem of the blade interference effect and the closely associated problem of the effect of the degree of rotation of the flow. Both of these problems should be solved by the two complementary methods; namely, by analysis of the performance of the fan by the blade element theory and by direct experimental investigation of the performance of the blade cascade in a flow with rotation. The latter method is rendered difficult by the necessity of constructing special complicated apparatus. As regards the first, further success is possible only with a further perfecting of the theory.

One of the fundamental problems awaiting solution is that of constructing the computed fan characteristics for operation of the fan under various entry conditions. All the conclusions of our present paper refer to a fan provided with a smooth collector assuring axial entry of the flow as required by the theoretical considerations. Preliminary investigations conducted by CAHI show that the effect of the entry conditions is very marked. There is a sharp drop in the efficiency on account of the fall in pressure head although there is a relatively small change in volume flow (of the order of 5 to 10 percent).

Further investigations are also required on the problem of the effect of the clearance. The correction coefficient, with the aid of which we took account of the effect of clearance, is a mean value obtained on the basis of a large number of tests. The scatter of the curves shown in figure 18, from which this mean value was obtained, is relatively large, however, and for clearances of 1 to 2 percent attains the values of 5 to 7 percent. In connection with this it may be stated that a more detailed study of the effect of clearance as a function of a number of factors, primarily, the circulation about the blades, would considerably reduce the possible error in the construction of the computed characteristics. What was said refers especially to the value of the

computed power since in the value of the latter we introduced no correction coefficients that take the clearance into account. Tests have shown, however, particularly for high-pressure fans, that the power does not remain constant but drops with increase in the clearance.

In the present paper the method of constructing the computed characteristics is given only for a small range of the latter representing operation of the blade elements at normal angles of attack. The development of a computation method for operating conditions outside this range is of great theoretical as well as practical value. An understanding of the mechanism of the fan performance for these conditions will make it possible to find new ways for improving the performance of the fan as a whole and permit solving the problem of the relation between axial and centrifugal fans and the possibility of passing continuously from the first type to the second. The latter possibility promises very important practical applications. The above-mentioned theoretical and applied investigations should be confirmed by investigations of the flow structure, primarily, by surveying the velocity and pressure field ahead of and behind the fan. Further investigations along the lines mentioned will be undertaken by CAHI.

Translation by S. Reiss,
National Advisory Committee
for Aeronautics.

APPENDIX

The appendix gives the original aerodynamic airfoil characteristics (C_x and C_y curves for infinite span) the curves of the pressure and power coefficients, the fan blade efficiency K_p/K_u airfoil efficiency for the three fundamental fan airfoils:

1. English propeller section with various modifications, differing in the relative thickness
2. Metal fan blade 1
3. Symmetric profile section.

REFERENCES

1. Ushakov, K.: Axial (Propeller) Fan Design. CAHI Rep. No. 277, 1936.
2. Bushel, A. R., and Surnov, W. V.: Handbook of Fan Construction. CAHI Rep. No. 157, 1935.
3. Sichev, A: The Power Expended in the Rotation of the Axial Fan Hub. CAHI T.N. No. 120, 1936.
4. Ushakov, K.: Handbook of Fans and Deflectors. CAHI Rep. No. 172, 1934.

TABLE I

						Tip element		
Fan	D_M	d_M	ξ	b_{hub} (mm)	i	Θ	b (mm)	$\bar{\delta}$
1	0.6	0.18	0.3	60	3	16°	38	0.1
2	.7	.35	.5	70	8	$14^\circ 30'$	92	.1
3	.66	.364	.55	52	8	$19^\circ 20'$	45	.09
4	.595	.25	.42	80	8	20°	49	.08
5	.6	.3	.5	105	12	21°	71	.09

Computed										Test
Fan	n rpm	u	Q m ³ /hr	H	N_{hp}	η	n imp	$\phi = \frac{H}{\rho u^2}$	$\bar{\Gamma} = \frac{cuR}{2uR}$	$\phi = \frac{H}{\rho u^2}$
1	1785	56	7,400	7.8	0.3	0.71	7100	0.0203	0.013	0.0224
2	1450	53	-----	-----	-----	-----	-----	-----	-----	-----
3	1200	41.4	-----	-----	-----	-----	-----	-----	-----	-----
4	1800	56	10,300	31	1.63	0.725	3100	0.0308	0.046	0.0729
5	1200	37.7	5,610	30.8	.79	.81	1600	.177	.121	.1163

TABLE II

Fan	d_{hub} (mm)	b_{hub} (mm)	n rpm	Re	β_N	N_{hub} hp
1	180	60	1785	209.10^5	105.10^{-6}	0.00365
2	350	70	1450	644.10^5	29.10^{-6}	.00643
3	364	52	1200	577.10^5	30.10^{-6}	.00719
4	250	80	1800	408.10^5	41.10^{-6}	.00734

$$Re = \frac{ud}{1446.10^{-6}} \tag{109a}$$

$$N_{hub} = \beta_N \rho \omega^3 d^5 \left(1 + \frac{3.9 b_{hub}}{d} \right) \tag{109}$$

Division I CAHI	Object	Fan computation with and of pressure coefficient K_a			
		<table border="1" style="width: 100%;"> <tr> <td style="text-align: center;">Model scale</td> <td style="text-align: center;">Center of area</td> <td style="text-align: center;">Area</td> </tr> </table>	Model scale	Center of area	Area
Model scale	Center of area	Area			

$n = 2800 \text{ rpm}$; $Q = 13100 \text{ m}^3/\text{hr}$; $H = 168 \text{ mm H}_2\text{O}$. $D = 0.6 \text{ m}$; $\xi = 0.5$; $\bar{s} = 1\%$;

$R = 0.3 \text{ m}$; $r_{BR} = 0.175 \text{ m}$, $F_o = 0.212 \text{ m}^2$

Impeller no.	r in ring	δ	u	c_a	$\frac{u}{c_a}$	c_u	$\frac{c_u}{2}$	$u - \frac{c_u}{2}$	$\frac{c_a}{u - \frac{c_u}{2}}$
Top element	0,300	0,08	87,8	17,15	5,11	21,3	10,65	77,15	0,222
I	0,285	0,1	83,6	17,15	4,87	22,4	11,2	72,4	0,237
II	0,254	0,12	74,5	17,15	4,34	25,2	12,6	61,9	0,278
III	0,218	0,14	64	17,15	3,73	29,4	14,7	49,3	0,35
IV	0,176	0,16	51,7	17,15	3,01	36,4	18,2	33,5	0,512

$$H_{comp} = HK_{cl} = 168 \cdot 1,13 = 189,5 \text{ mm H}_2\text{O} \quad (71)$$

$$K_{cl} = 1,13 \text{ (Fig 18)}$$

$$r = R r_{ring} \text{ (Fig 24)}$$

δ is assumed

$$u = r\omega = r \frac{\pi n}{30} \text{ (74)}$$

$$c_a = \frac{Q}{3600 F}$$

$$c_{uR} = u_R - \sqrt{u_R^2 - \frac{2H_{comp}}{\rho}} = 87,8 - \sqrt{87,8^2 - \frac{2 \cdot 189,5}{0,1223}} = 20 \text{ (78)}$$

To compute c_u choose $\eta_{prof. max}$ from fig. 82 for β' , determined by

$$\operatorname{tg} \beta' = \frac{c_a}{u - \frac{c_{uR}}{2}} = \frac{17,0}{87,8 - 10} = 0,22; \beta' = 12^\circ 24'$$

$$c_{uR} = u_R - \sqrt{u_R^2 - \frac{2H_{comp}}{\rho \eta_{prof.}}} = 87,8 - \sqrt{87,8^2 - \frac{2 \cdot 189,5}{0,1223 \cdot 0,94}} = 21,3 \text{ (77)}$$

		Model			
		Project No.			
P _____ mm t° _____ °C Humidity _____ % Δ = _____	Corrections		Apparatus _____	" _____ 193	
	Before	After			

β	Cos β	η _{prof}	α	θ	K _a	b		
12°25'	0,976	0,925	7°30	19°55'	0,52	0,0736		
13°20'	0,973	0,925	8°	21°20'	0,56	0,0721		
15°29'	0,964	0,935	9°	24°29'	0,64	0,0734		
19°11'	0,944	0,935	10°	29°11'	0,685	0,0826		
27°07'	0,89	0,935	11°	38°07'	0,68	0,109		

$$c_u = \frac{c_{uR} R}{r} \quad (80)$$

Angle β found from relation

$$\operatorname{tg} \beta = \frac{c_a}{u - \frac{c_u}{2}} \quad (75)$$

α Assumed (in range of η_{prof} near maximum) θ = α + β (82)

i - Assumed

$$b = \frac{2 \pi r c_u \cos^2 \beta}{K_a \left(u - \frac{c_u}{2} \right) i} \quad (85)$$

$$N = \frac{\rho Q c_u u}{75 \cdot 3600} = \frac{0,1223 \cdot 13100 \cdot 21,3 \cdot 87,8}{75 \cdot 3600} = 11,1 \text{ s. c.}$$

$$\eta = \frac{Q H}{75 \cdot 3600 N} = \frac{13100 \cdot 168}{270000 \cdot 11,1} = 0,73$$

Division I CAHI	Object	
Object: Obtain computed characteristics of fan no 4.		Model scale
		Center of area
		Area
$D = 0.595 \quad R = 0.2975 \quad i = 8$ $b_{hub} = 0.25 \quad r_{hub} = 0.125 \quad F_0 = 0.228$		
} Figs. 31 & 32		

Regime no.	r	δ	θ	u	c _u	η _{prof}	- $\frac{c_u}{2}$	u - $\frac{c_u}{2}$	H	β
I	0,2975	0,08	19°45'	56	3	0,927	1,5	54,5	18,55	18°15'
II	0,2975	0,08	19°45'	56	4	0,935	2,0	54	24,7	16°45'
III	0,2975	0,08	19°45'	56	5	0,940	2,5	53,5	30,8	14°45'
VI	0,2975	0,08	19°45'	56	6	0,930	3,0	53	36,2	12°15'

Regime no.	r	δ	θ	u	c	η _{prof}	- $\frac{c_u}{2}$	u - $\frac{c_u}{2}$	H	β
I	0,252	0,09	21°	47,5	3,54	0,92	1,77	45,73	18,25	20°
II	0,252	0,09	21°	47,5	4,72	0,942	2,36	45,14	24,6	18°10'
III	0,252	0,09	21°	47,5	5,9	0,941	2,95	44,55	30,3	16°30'
IV	0,252	0,09	21°	47,5	7,1	0,94	3,55	43,95	35,8	14°45'

Regime no.	r	δ	θ	u	c _u	η _{prof}	- $\frac{c_u}{2}$	u - $\frac{c_u}{2}$	H	β
I	0,164	0,12	30°	30,9	5,44	0,963	2,72	28,18	17,4	30°15'
II	0,164	0,12	30°	30,9	7,25	0,967	3,62	27,28	23,5	28°
III	0,164	0,12	30°	30,9	9,07	0,969	4,54	26,36	28,3	25°45'
IV	0,164	0,12	30°	30,9	10,9	0,951	5,45	25,45	32,4	22°45'

r, δ, θ, b — taken from charts (Fig 21)

$$u = \frac{\pi D n}{60} \quad (\text{cp. c 74}) \quad c_a = \left(u - \frac{c_u}{2}\right) \operatorname{tg} \beta \quad (97)$$

$$c_{uR} \text{ — assumed} \quad H = \eta_{prof} \rho c_u \left(u - \frac{c_u}{2}\right) \quad (93)$$

$$c_{u_r} = \frac{c_{uR} R}{r} \quad (80)$$

$$\eta_{prof} \text{ — from charts for English fan profiles; } H_{K_a} = K_a \rho \left(\frac{u - \frac{c_u}{2}}{\cos \beta}\right)^2 \frac{bl}{2\pi r} \quad (94)$$

$$\beta = \theta - \alpha \quad (95)$$

		Corrections		Apparatus _____		" " " " 193 _____	
		Before	After				
P _____ mm							
t° _____ °C							
Humidity _____ %							
Δ = _____							

α	K_a	$\cos \beta$	$\left(\frac{u - c_u}{2}\right) / \cos \beta$	$\left(\frac{u - c_u}{2}\right)^2 / \cos \beta$	b	$\frac{bi}{2\pi r}$	H_{K_a}	$\text{tg } \beta$	c_a
1°30'	0,22	0,95	57,4	3290	0,0495	0,212	18,75	0,329	17,9
3°00'	0,292	0,957	56,5	3190	0,0495	0,212	24,2	0,30	16,2
5°00'	0,397	0,97	55	3030	0,0495	0,212	31,2	0,263	14,1
6°30'	0,47	0,977	54,2	2940	0,0495	0,212	35,8	0,217	11,5

α	K_a	$\cos \beta$	$\left(\frac{u - c_u}{2}\right) / \cos \beta$	$\left(\frac{u - c_u}{2}\right)^2 / \cos \beta$	b	$\frac{bi}{2\pi r}$	H_{K_a}	$\text{tg } \beta$	c_a
1°0'	0,214	0,393	48,7	2370	0,0595	0,301	18,7	0,363	16,6
2°50'	0,292	0,95	47,6	2260	0,0595	0,301	24,3	0,327	14,8
4°30'	0,382	0,958	46,6	2170	0,0595	0,301	30,6	0,296	13,2
6°15'	0,462	0,967	45,4	2060	0,0595	0,301	35,6	0,263	11,52

α	K_a	$\cos \beta$	$\left(\frac{u - c_u}{2}\right) / \cos \beta$	$\left(\frac{u - c_u}{2}\right)^2 / \cos \beta$	b	$\frac{bi}{2\pi r}$	H_{K_a}	$\text{tg } \beta$	c_a
0°15'	0,205	0,862	32,6	1060	0,086	0,666	17,7	0,583	16,4
2°00'	0,305	0,882	30,9	960	0,086	0,666	23,9	0,531	14,5
4°15'	0,41	0,900	29,25	855	0,086	0,666	28,6	0,482	12,7
7°15'	0,52	0,922	27,6	762	0,086	-0,666	32,2	0,419	10,69

α — assumed, $R - r_{\text{hub}} = 172,5 \text{ mm}$

K_a — from curves

$S = 2,0 \text{ mm}$

$$S = \frac{S \cdot 100}{R - r_{\text{hub}}} = 1,16\% \text{ (71)}$$

$$\overline{H}_{S=1,16\%} = H_{K_a} \cdot 0,89 \text{ (Fig 18)}$$

Division I CAHI		Object						
Object. Obtain computed characteristics of fan no 4					Model scale	Center of area	Area	
Computation of discharge, pressure, power and efficiency.								
1								
Points nos.	Regime no.	r	c_a Fig 55	P	$c_a P$	Regime no.	r.	c_a Fig 55
1		0,140	10,2	0,0286	0,292	II	0,140	12,2
2	I	0,170	10,7	0,0286	0,306	II	0,170	12,6
3	I	0,195	11,0	0,0286	0,315	II	0,195	12,8
4	I	0,217	11,2	0,0286	0,32	II	0,217	12,9
5	I	0,238	11,3	0,0286	0,323	II	0,238	13,1
6	I	0,256	11,4	0,0286	0,326	II	0,256	13,3
7	I	0,276	11,5	0,0286	0,329	II	0,276	13,6
8	I	0,290	11,5	0,0286	<u>0,329</u> 2,54	II	0,290	14
Points nos.	Regime no.	r	c_a Fig 55	P	$c_a P$			Regime no.
1	IV	0,140	16,39	0,0286	0,469			I
2	IV	0,170	16,4	0,0286	0,47			II
3	V	0,195	16,4	0,0286	0,47			III
4	IV	0,217	16,4	0,0286	0,47			IV
5	IV	0,238	16,5	0,0286	0,471			
6	IV	0,256	16,7	0,0286	0,477			
7	IV	0,276	17,2	0,0286	0,492			
8	IV	0,290	17,6	0,0286	<u>0,504</u> 3,823			

				Model _____	
				Project No. _____	
P _____ mm	Corrections		Apparatus _____	" _____ 193 _____ R.	
t° _____ °C	Before	After			
Humidity _____ %					
Δ = _____					

F	c _a F	Regime no	r	F	c _a Fig 55	c _a F			
0,0286	0,349	III	0,140	0,0286	14,37	0,410			
0,0286	0,360	III	0,170	0,0286	14,5	0,415			
0,0286	0,366	III	0,195	0,0286	14,5	0,415			
0,0286	0,369	III	0,217	0,0286	14,5	0,415			
0,0286	0,375	III	0,238	0,0286	14,7	0,42			
0,0286	0,38	III	0,256	0,0286	14,9	0,426			
0,0286	0,39	III	0,276	0,0286	15,4	0,44			
0,0286	0,4	III	0,290	0,0286	16,0	0,458			
	2,989					3,399			

Q m ³ /sec	Q m ³ /hr	u	c _u	N	H	H _s = 1,16%	η		
2,54	9150	56	6	1,39	36,2	31,8	0,775		
2,989	10750	56	5	1,36	30,8	27,1	0,792		
3,399	12220	56	4	1,235	24,7	21,8	0,802		
3,823	13750	56	3	1,07	18,55	16,35	0,780		

$$N = \frac{\rho Q_{sec} u c_u}{\gamma \bar{v}} \quad (89)$$

$$\eta = \frac{Q_{hr} H_{s=1,16\%}}{N \cdot 270000}$$

$$Q = \sum_{r=hub}^R Q_{ring} \quad (104)$$

Division I CAHI	Object				
Object: Computation of characteristics of fan no 5b.		<table border="1" style="width: 100%;"> <tr> <td style="width: 33%;">Model Scale</td> <td style="width: 33%;">Center of area</td> <td style="width: 33%;">Area</td> </tr> </table>	Model Scale	Center of area	Area
Model Scale	Center of area	Area			

$$\left. \begin{aligned}
 D &= 0.6 & R &= 0.3 \\
 d_{hub} &= 0.3 & b_{hub} &= 0.15 & F_0 &= 0.212
 \end{aligned} \right\} \text{Eqs. 33 \& 34}$$

Regime no	r	$\bar{\delta}$	θ	u	c_u	η_{Prof}	$\frac{c_u}{2}$	$u - \frac{c_u}{2}$	H	β
I	0,300	0,09	21°	37,7	5	0,925	2,5	35,2	19,9	12°20'
II	0,300	0,09	21°	37,7	4	0,946	2	35,7	16,55	15°30'
III	0,300	0,09	21°	37,7	3	0,934	1,5	36,2	12,4	18°
IV	0,300	0,09	21°	37,7	2	0,905	1	36,7	8,13	20°20'

Regime no.	r	$\bar{\delta}$	θ	u	c_u	η_{Prof}	$\frac{c_u}{2}$	$u - \frac{c_u}{2}$	H	β
I	0,234	0,13	27	29,2	6,4	0,946	3,2	26	19,35	17°30'
II	0,234	0,13	27	29,2	5,12	0,955	2,56	26,64	16	21°30'
III	0,234	0,13	27	29,2	3,85	0,937	1,93	27,27	12	25°
IV	0,234	0,13	27	29,2	2,565	0,912	1,28	27,92	8	27°30'

Regime no	r	$\bar{\delta}$	θ	u	c_u	η_{Prof}	$\frac{c_u}{2}$	$u - \frac{c_u}{2}$	H	β
I	0,176	0,16	37°30'	22,1	8,52	0,96	4,26	17,84	17,8	29°30'
II	0,176	0,16	37°30'	22,1	6,82	0,96	3,41	18,69	15	34°
III	0,176	0,16	37°30'	22,1	5,12	0,91	2,56	19,54	11,5	37°
IV	0,176	0,16	37°30'	22,1	3,41	0,885	1,71	20,39	7,5	40°

r, $\bar{\delta}$, θ , b — Taken from curves Fig 38

$$u = \frac{\pi D n}{60}$$

c_{uR} = assumed

$$c_u = \frac{c_{uR} \cdot R}{r} \quad (80)$$

η_{Prof} = From curves for English fan profiles

$$\beta = \theta - \alpha \quad (95)$$

α = given, R_α = from curves

		Model _____	
		Project No _____	
P _____ mm	Corrections		Apparatus _____
	Before	After	
t° _____ °C			" " _____ 193__
Humidity _____ %			
Δ = _____			

α	K_a	$\cos \beta$	$\frac{u - \frac{c_u}{2}}{\cos \beta}$	$\left(\frac{u - \frac{c_u}{2}}{\cos \beta}\right)^2$	b	$\frac{bi}{2\pi r}$	H_{K_a}	$\text{tg } \beta$	c_a
8°40'	0,557	0,977	35,9	1290	0,071	0,2265	19,9	0,218	7,67
5°30'	0,429	0,963	37,1	1375	0,071	0,2265	16,4	0,277	9,9
3°00'	0,307	0,951	38	1445	0,071	0,2265	12,2	0,324	11,72
0°40'	0,193	0,937	39,1	1530	0,071	0,2265	8,19	0,37	13,6

α	K_a	$\cos \beta$	$\frac{u - \frac{c_u}{2}}{\cos \beta}$	$\left(\frac{u - \frac{c_u}{2}}{\cos \beta}\right)^2$	b	$\frac{bi}{2\pi r}$	H_{K_a}	$\text{tg } \beta$	c_a
9°30'	0,663	0,954	27,3	745	0,078	0,3185	19,3	0,315	8,9
5°30'	0,505	0,93	28,65	820	0,078	0,3185	16,1	0,393	10,5
2°00'	0,34	0,906	30,05	902	0,078	0,3185	12	0,466	12,7
0°30'	0,21	0,887	31,45	990	0,078	0,3185	8,1	0,52	14,45

α	K_a	$\cos \beta$	$\frac{u - \frac{c_u}{2}}{\cos \beta}$	$\left(\frac{u - \frac{c_u}{2}}{\cos \beta}\right)^2$	b	$\frac{bi}{2\pi r}$	H_{K_a}	$\text{tg } \beta$	c_a
8°00'	0,59	0,87	20,5	421	0,107	0,58	17,7	0,566	10,1
3°30'	0,415	0,829	22,5	508	0,107	0,58	15	0,674	12,6
0°30'	0,275	0,798	24,5	600	0,107	0,58	11,7	0,753	14,7
-2°30'	0,15	0,766	26,6	705	0,107	0,58	7,5	0,839	17,09

$$c_a = \left(u - \frac{c_u}{2}\right) \text{tg } \beta \quad (79)$$

$$H = \eta_{rad} \rho c_u \left(w - \frac{c_u}{2}\right) \quad (93)$$

$$H_{K_a} = K_a \rho \frac{\left(u - \frac{c_u}{2}\right)^2}{\cos^2 \beta} \frac{bi}{2\pi r} \quad (94)$$

$$R_{hub} - r = 150 \text{ } \mu\text{m}$$

$$\frac{s}{\bar{s}} = \frac{s \cdot 100}{R - r_{hub}} = 2\% \quad (71)$$

$$H_{\bar{s}} = 2\% = H_{K_a} \cdot 0,81 \quad \text{Fig 18}$$

Division I CAHI		Object								
Object: Obtain computed characteristics of fan no. 5b.							Model scale	Center of area	Area	
Computation of discharge, pressure and efficiency.										
Points nos	Regime no	r_{cp} ring	c_a Fig 61	F	$c_a F$	Regime no.	r_{cp} ring	c_a Fig 61	F	$c_a F$
1	II	0,1635	12,9	0,0265	0,342	III	0,1635	15,3	0,0265	0,405
2	II	0,1875	12,1	0,0265	0,321	III	0,1875	14,2	0,0265	0,376
3	II	0,209	11,4	0,0265	0,302	III	0,209	13,5	0,0265	0,358
4	II	0,227	10,9	0,0265	0,289	III	0,227	12,9	0,0265	0,342
5	II	0,245	10,4	0,0265	0,276	III	0,245	12,5	0,0265	0,332
6	II	0,263	10	0,0265	0,265	III	0,263	12,2	0,0265	0,324
7	II	0,277	9,7	0,0265	0,257	III	0,277	12	0,0265	0,318
8	II	0,293	9,5	0,0265	0,252	III	0,293	11,8	0,0265	0,313
				2,304						2,768
Regime	Q m ³ /sec	Q m ³ /hr	u	c_u	N	H	$H_{s=2\%}$	η		
I	1,820	6 550	37,7	5	0,56	19,9	16,1	0,696		
II	2,304	8 300	37,7	4	0,566	16,4	13,3	0,721		
III	2,768	9 960	37,7	3	0,511	12,3	9,15	0,718		
IV	3,174	11 420	37,7	2	0,39	8,19	6,64	0,72		

				Model _____		
				Project No _____		
P _____ mm t° _____ °C Humidity _____ % Δ = _____	Corrections		Apparatus _____	" _____ 193 _____		
	Before	After				

Regime no.	r cp ring	c _a Fig 61	F	c _a F	Regime no.	r cp ring	c _a Fig 61	F	c _a F
IV	0,1635	17,7	0,0265	0,47	I	0,1635	10,5	0,0265	0,278
IV	0,1875	16,4	0,0265	0,435	I	0,1875	9,7	0,0265	0,257
IV	0,209	15,35	0,0265	0,406	I	0,209	9,0	0,0265	0,2385
IV	0,227	14,7	0,0265	0,39	I	0,227	8,5	0,0265	0,2255
IV	0,245	14,2	0,0265	0,376	I	0,245	8,1	0,0265	0,215
	0,263	14	0,0265	0,371	I	0,263	7,8	0,0265	0,207
IV	0,277	13,8	0,0265	0,366	I	0,277	7,6	0,0265	0,2015
IV	0,293	13,6	0,0265	0,360	I	0,293	7,5	0,0265	0,199
				3,174					1,820

$$N = \frac{\rho Q_{sec} u c_u}{75} \quad (89)$$

$$\eta = \frac{Q_{hr} H_{s=2\%}}{270000 N}$$

$$Q = \sum_{r_{em}}^R Q_{ring} \quad (104)$$

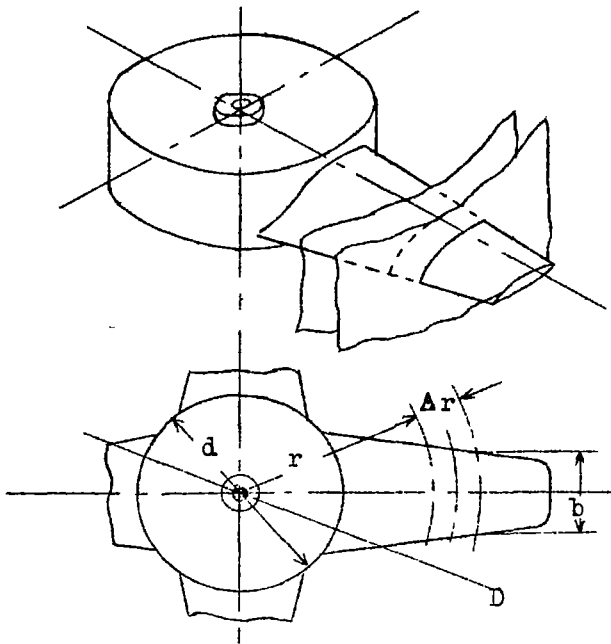


Figure 1.- Blade element.

Figure 3.- Approximate picture of lines of flow in blade cascade.

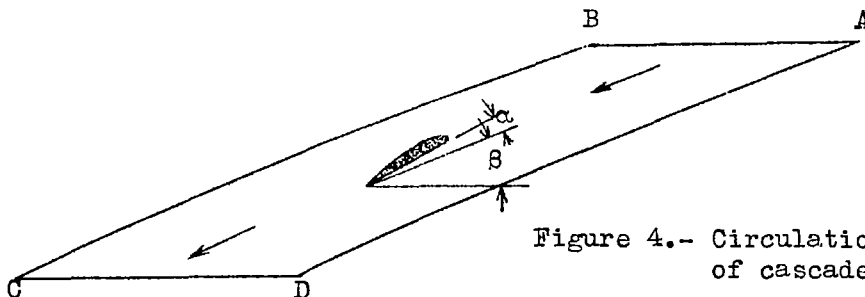
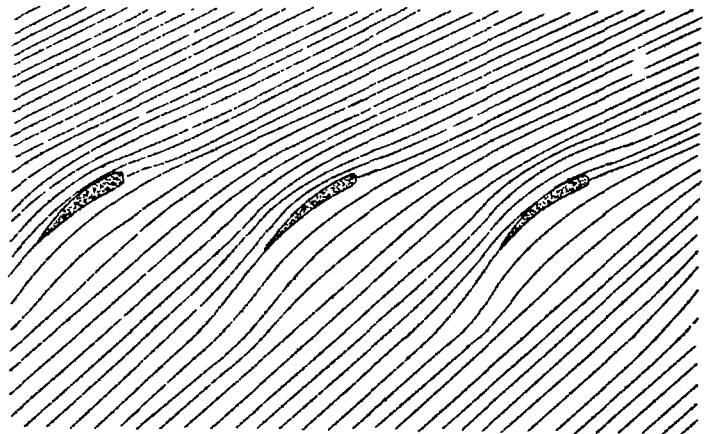


Figure 4.- Circulation about blade of cascade.

Fig. 2

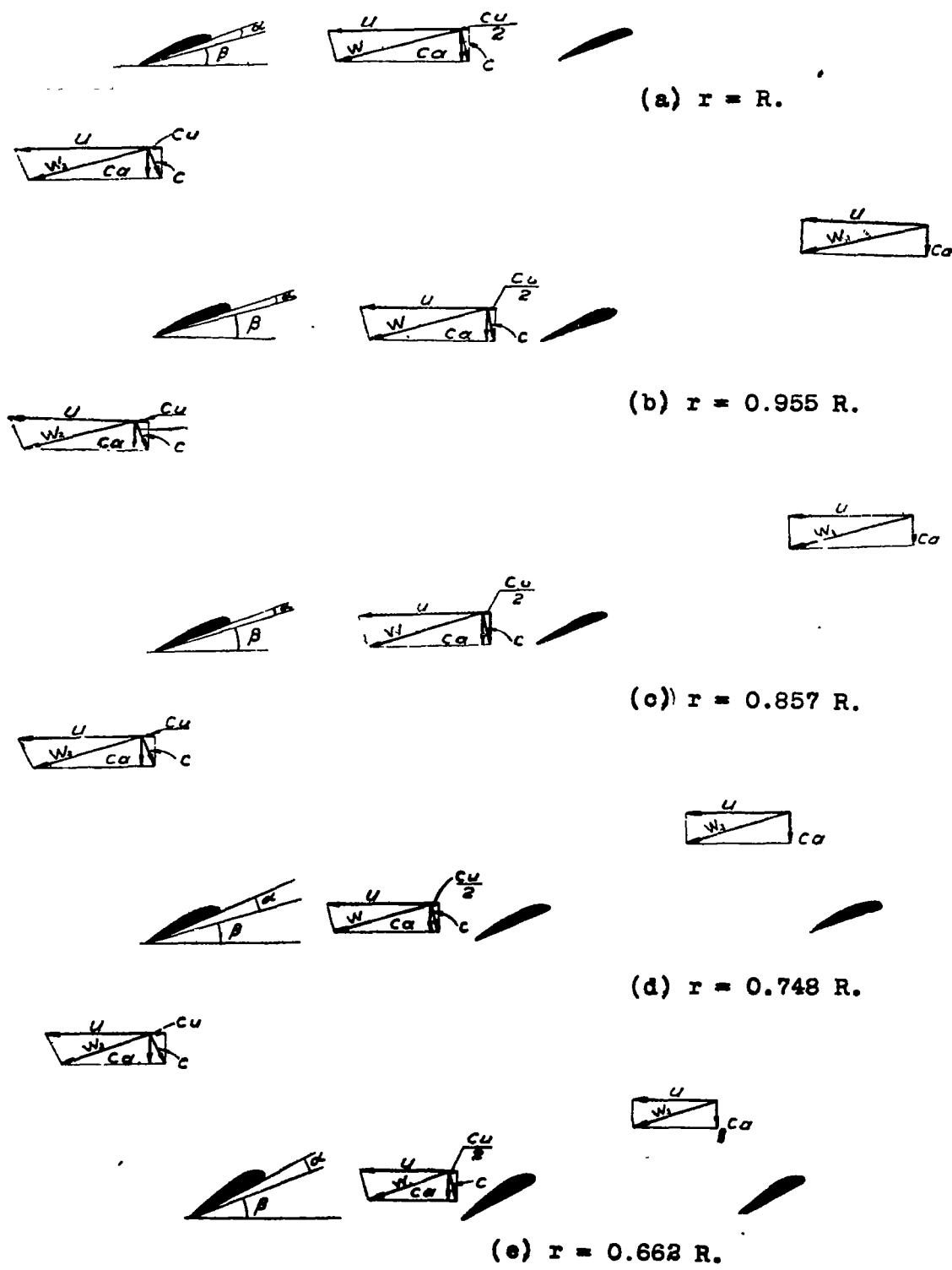


Figure 2.- Velocity vector diagram for blade cascade of axial fan.

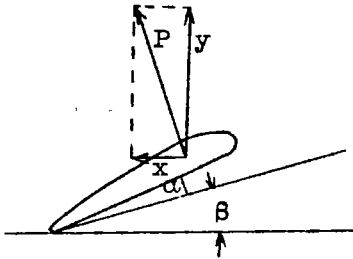


Figure 5.- Force components in peripheral and axial directions.

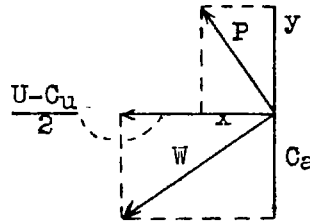


Figure 6.- Direction of lift of blade of cascade.

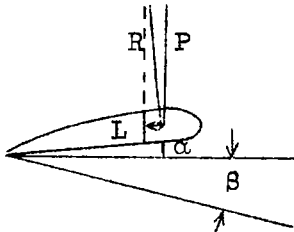


Figure 7.- Aerodynamic forces arising at blade element in presence of friction.

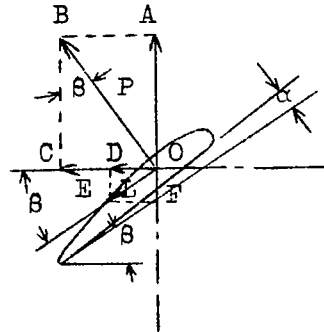


Figure 8.- Determination of pressure and power coefficients K_a and K_u .

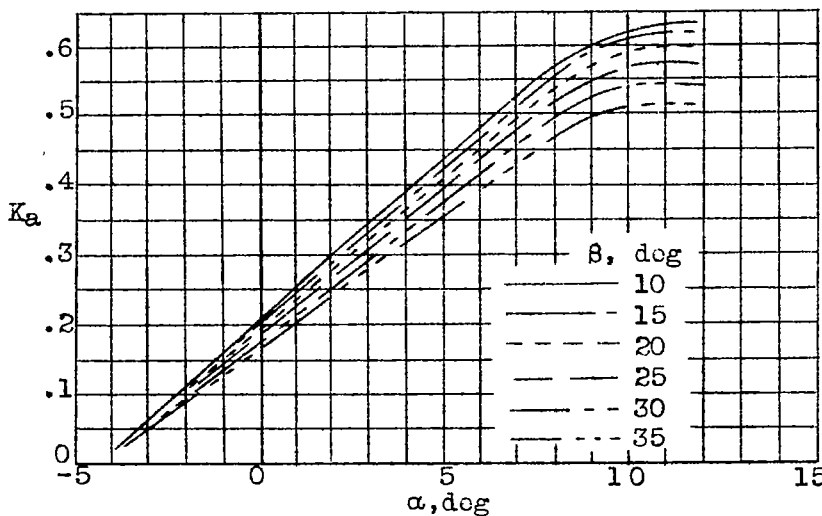


Figure 9.- Curves of pressure coefficients for English propeller section with relative thickness $\bar{\delta} = 0.1$.

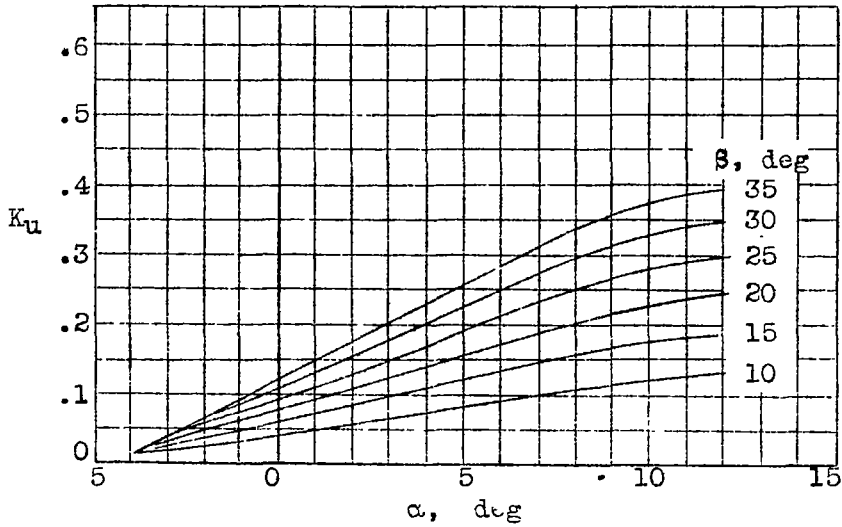


Figure 10.- Curves of power coefficients for English propeller section with relative thickness $\delta = 0.1$.

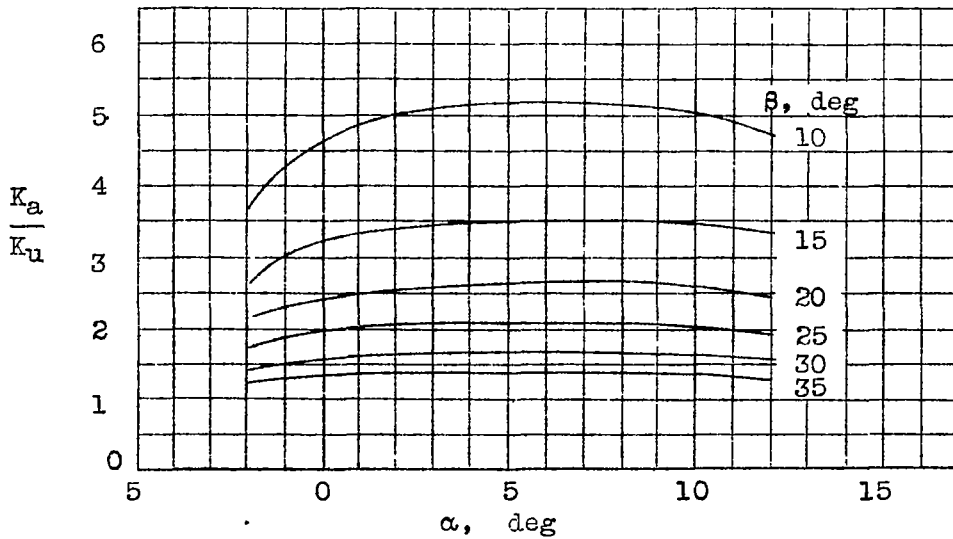


Figure 11.- Curves of ratio K_a/K_u for English propeller section with relative thickness $\delta = 0.1$.

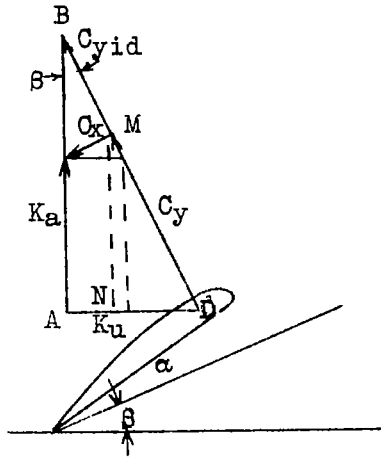


Figure 12.- Effect of friction on performance of blade element.

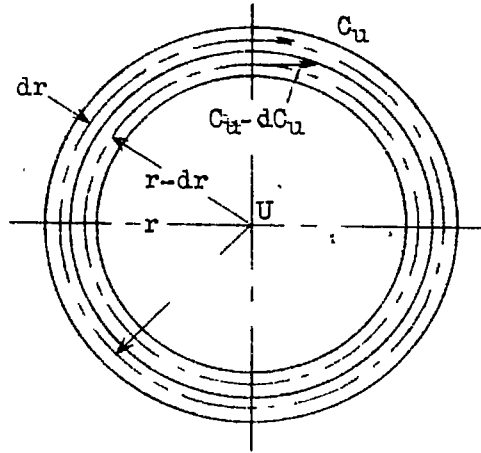


Figure 13.- Derivation of the law of velocity distribution of rotational flow behind the fan: $rc_u = \text{const.}$

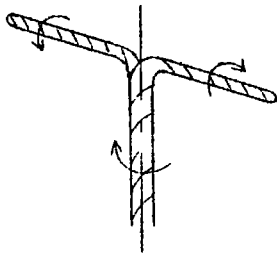


Figure 14.- Vortex system of axial fan.

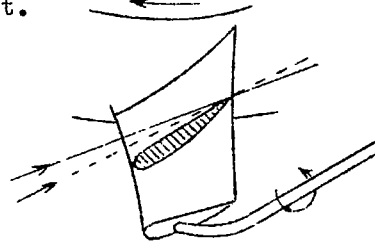


Figure 15.- Vortex line springing from the fan blade in presence of clearance.

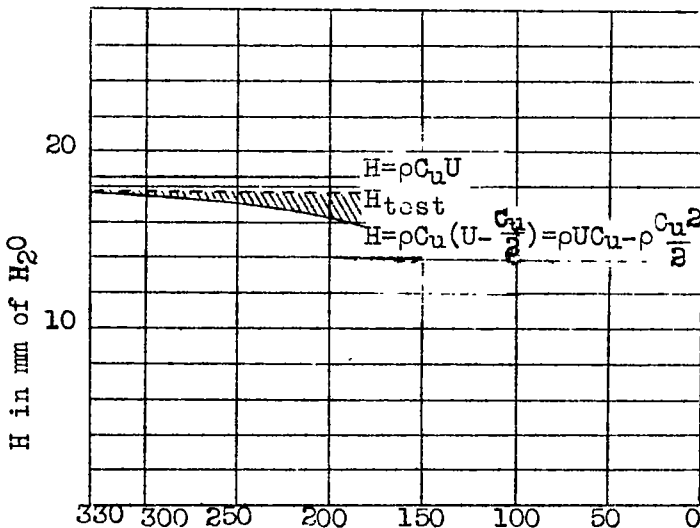


Figure 16.- Approximate picture of pressure distribution along the axial fan blade.

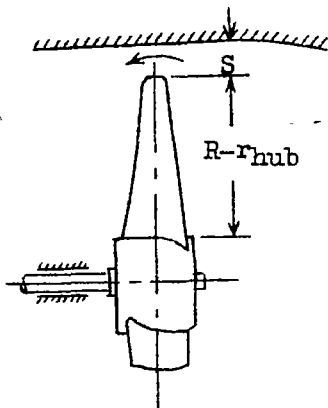


Figure 17.- Clearance between wheel and casing of axial fan.

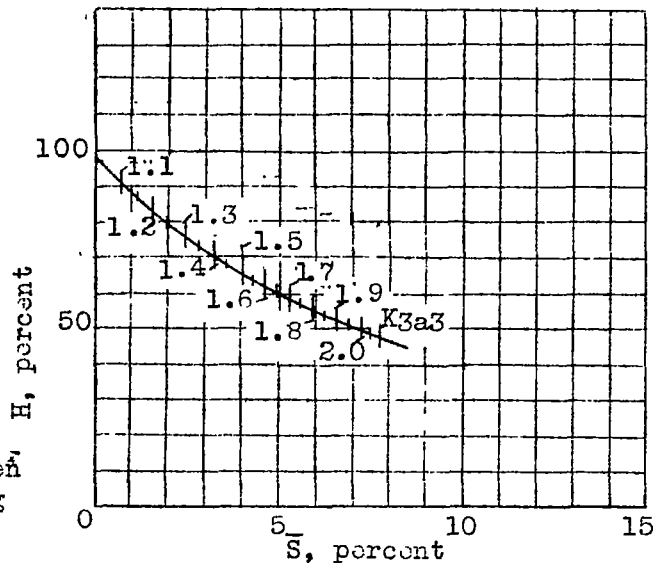


Figure 18.- Curve of pressure head against relative clearance in percent. The pressure is expressed in percent pressure $\bar{S} = 0$.

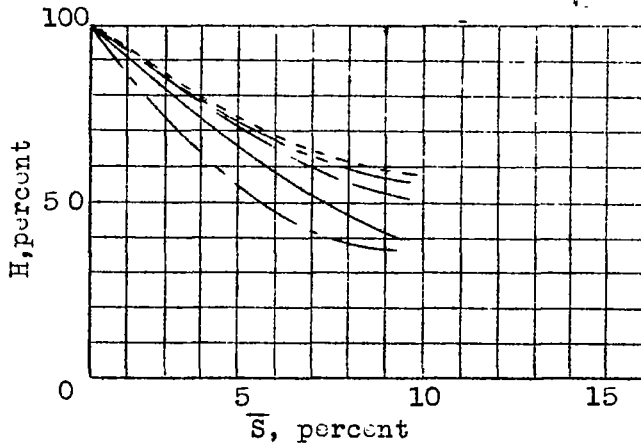
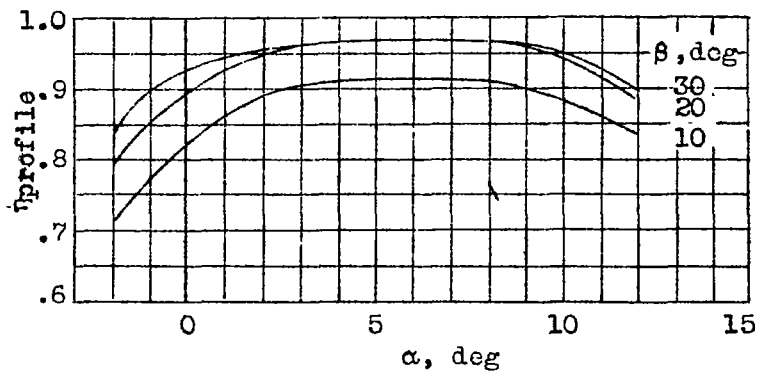


Figure 19.- Curves of pressure head against clearance for various fans.

Figure 20.- Curve of profile efficiency for English propeller section with relative thickness $\bar{\delta} = 0.1$.



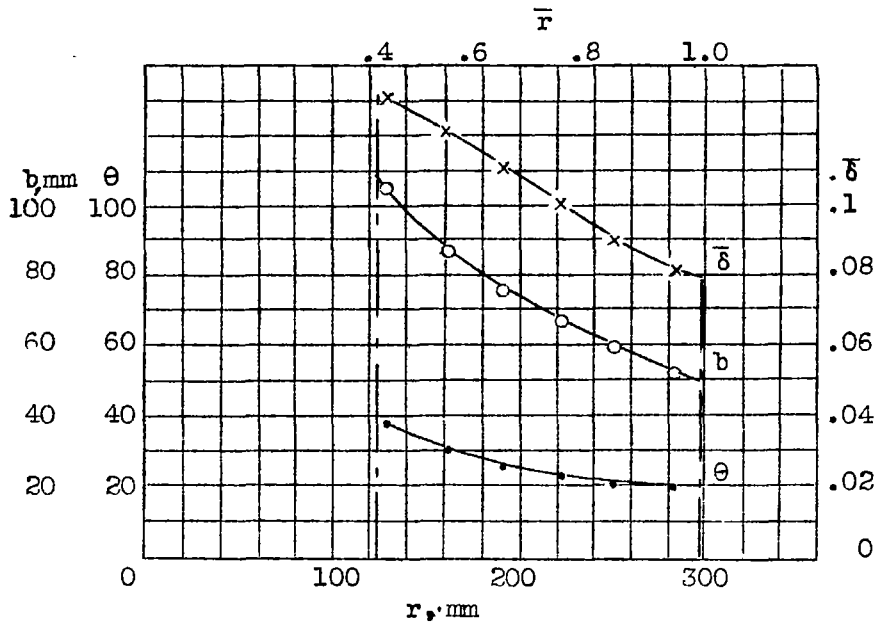


Figure 21.- Geometric parameters of fan No. 4; θ - blade angle, b - blade width; $\bar{\delta}$ - relative thickness.

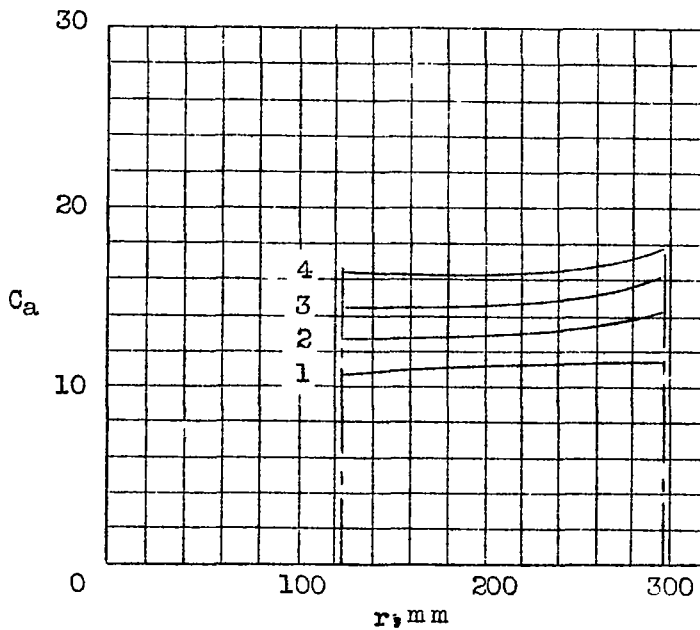


Figure 22.- Axial velocity distribution for fan No. 4.

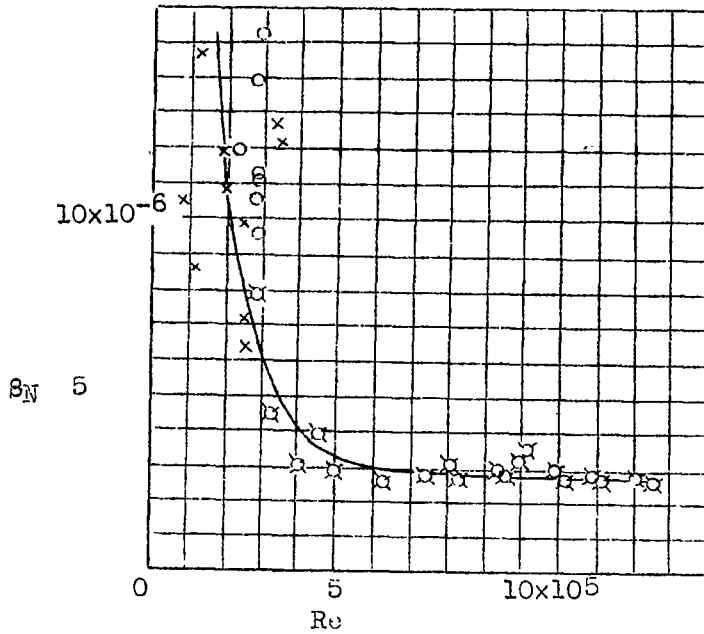


Figure 23.- Curve of coefficient S_N , determining the friction loss at the hub, against the Reynolds number Re .

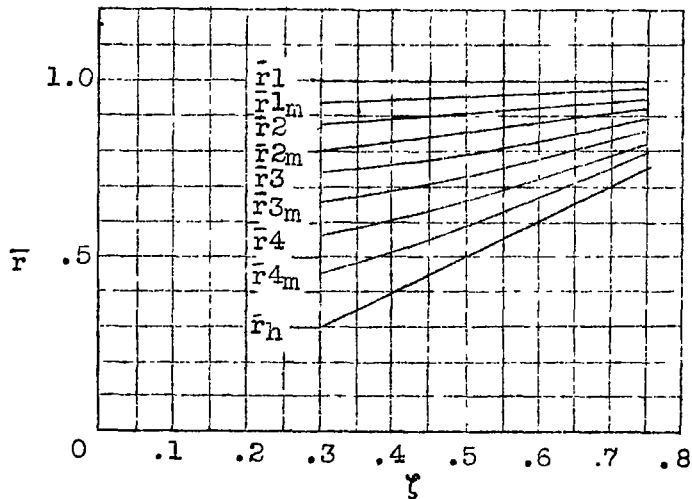
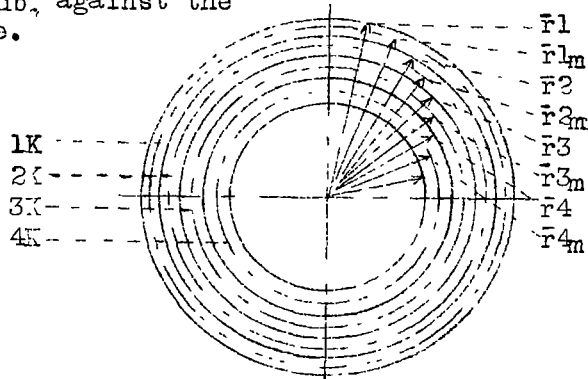


Figure 24.- Auxiliary curves for dividing swept disk area into equal area rings.

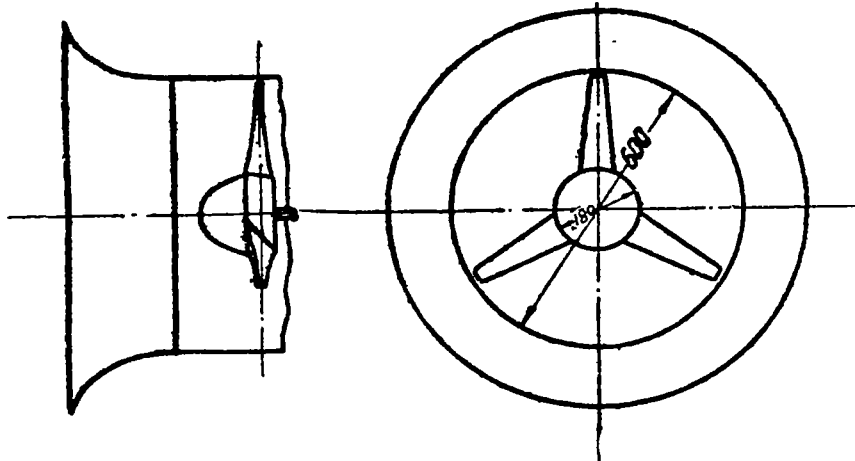


Figure 25.- Sketch of fan no. 1, $\bar{\alpha} = 1.3$ percent.

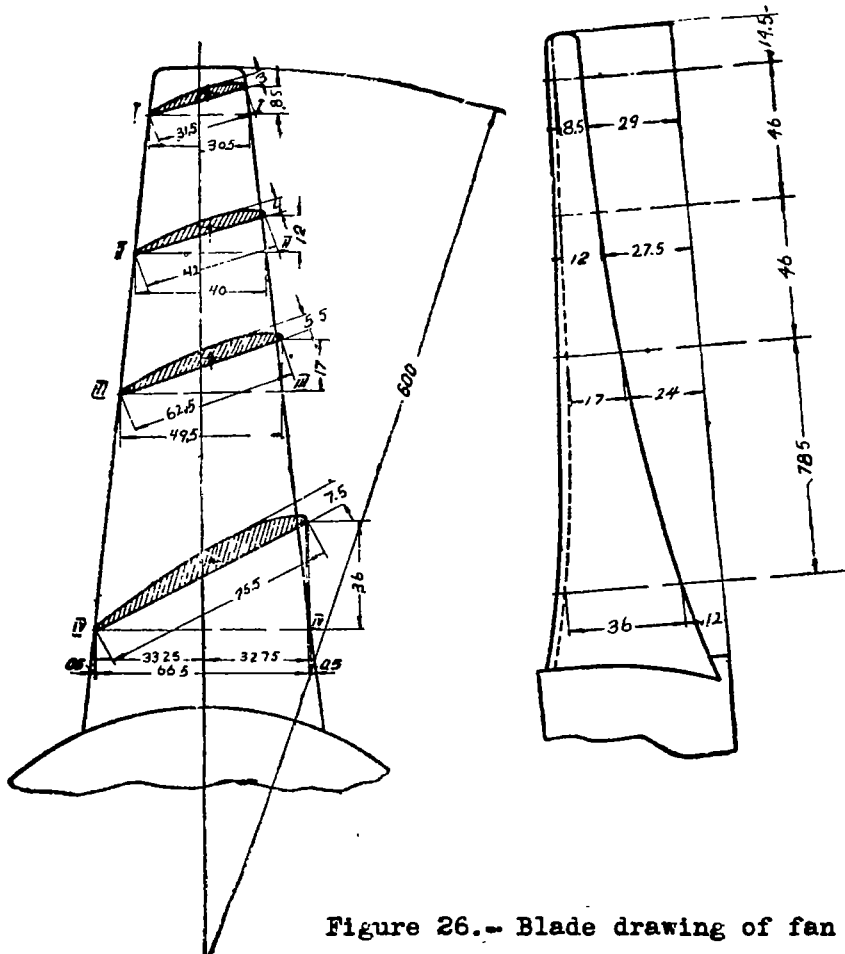


Figure 26.- Blade drawing of fan no. 1.

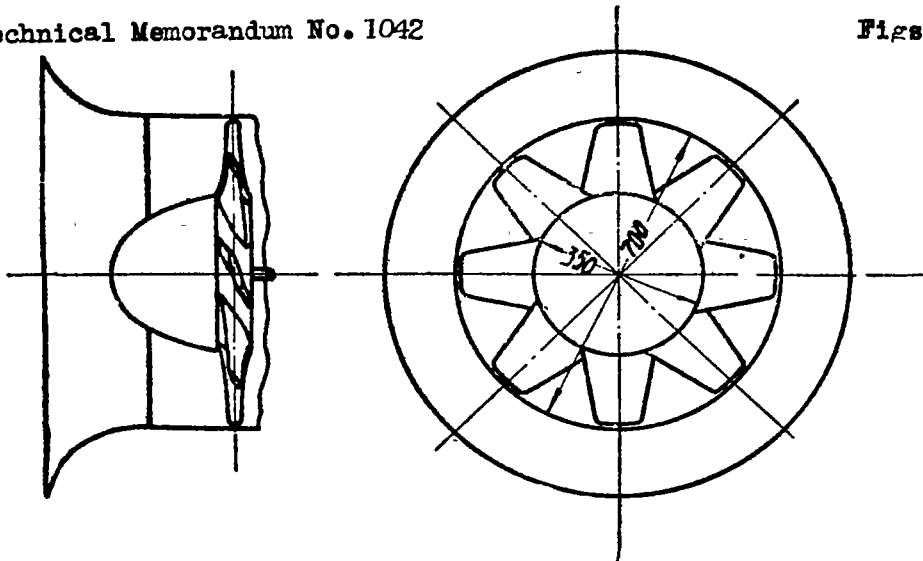


Figure 27.- Sketch of fan no. 2, $\bar{\alpha} = 1.5$ percent.

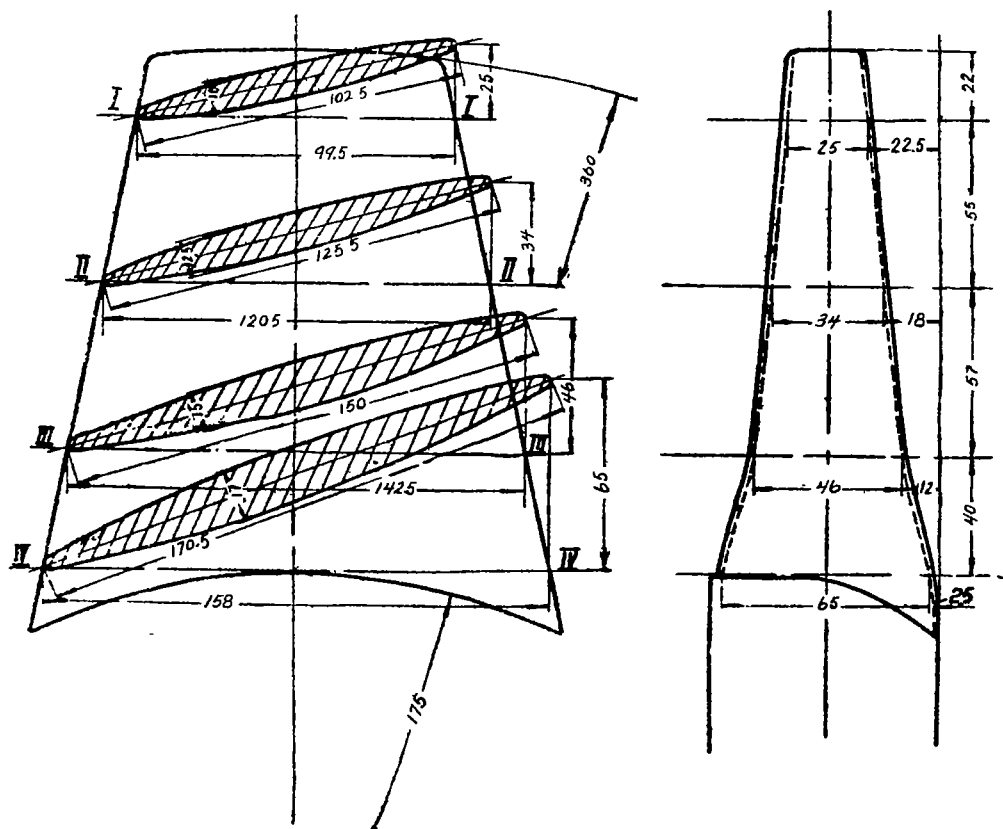


Figure 28.- Blade drawing of fan no. 2.

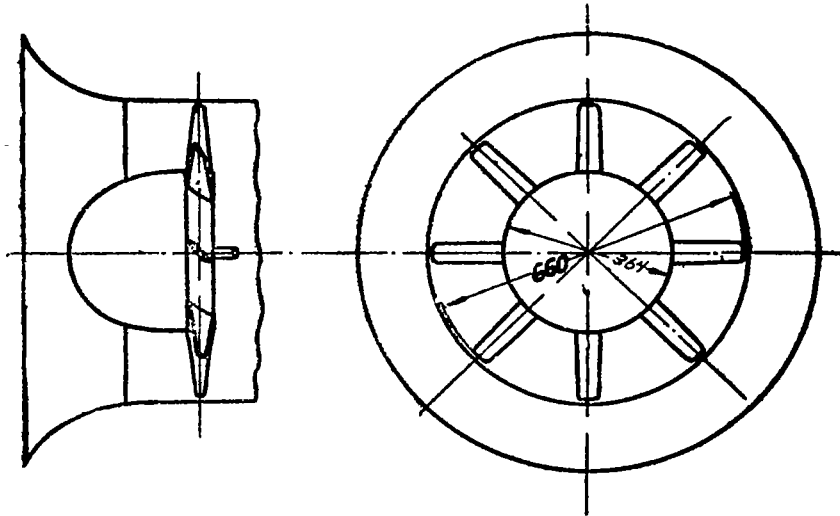


Figure 29.- Sketch of fan no. 3, $\bar{\alpha} = 1$ percent.

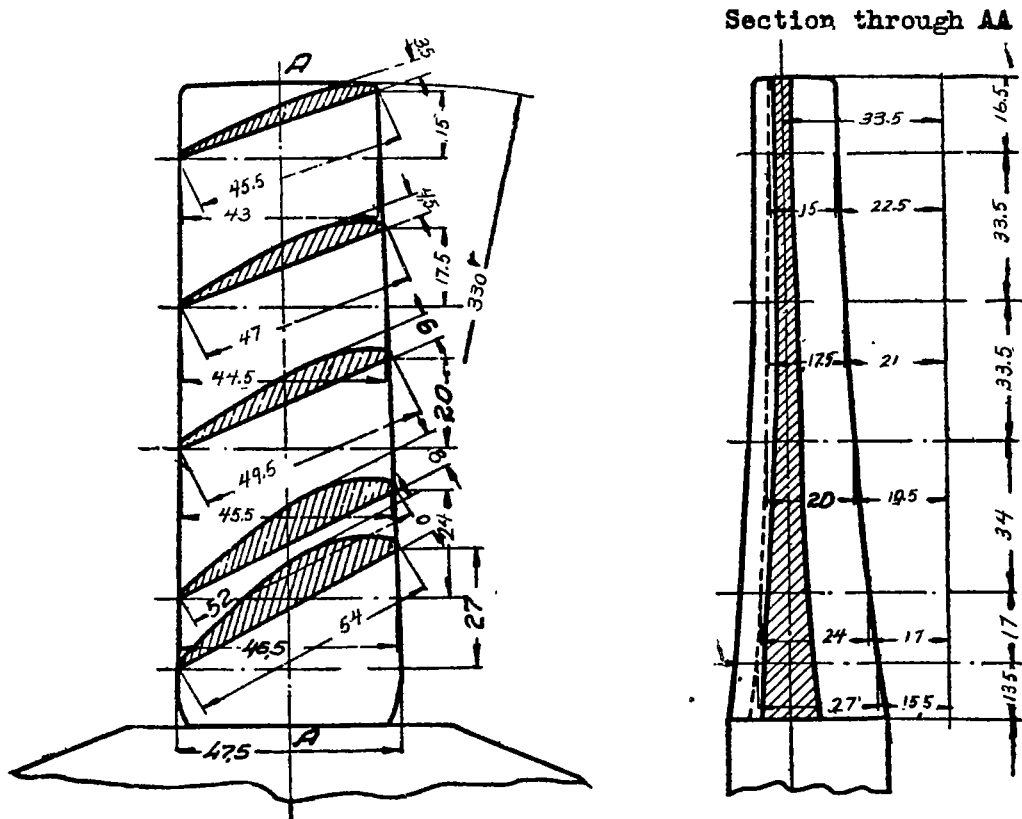


Figure 30.- Blade drawing of fan no. 3a.

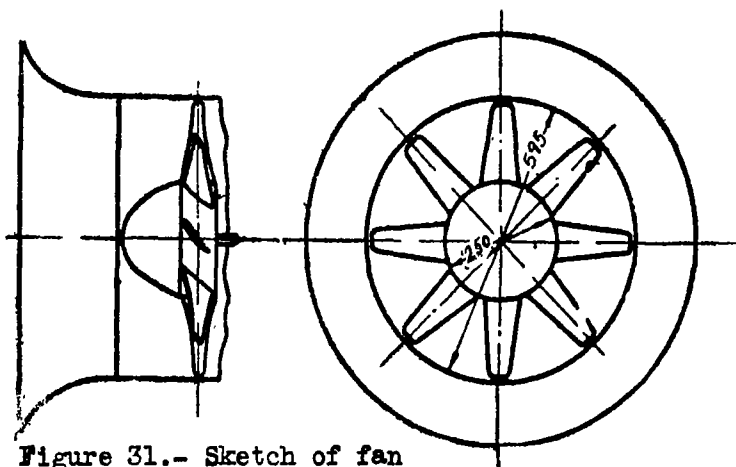


Figure 31.- Sketch of fan
no. 4, $\bar{\beta} = 1.16$ percent.

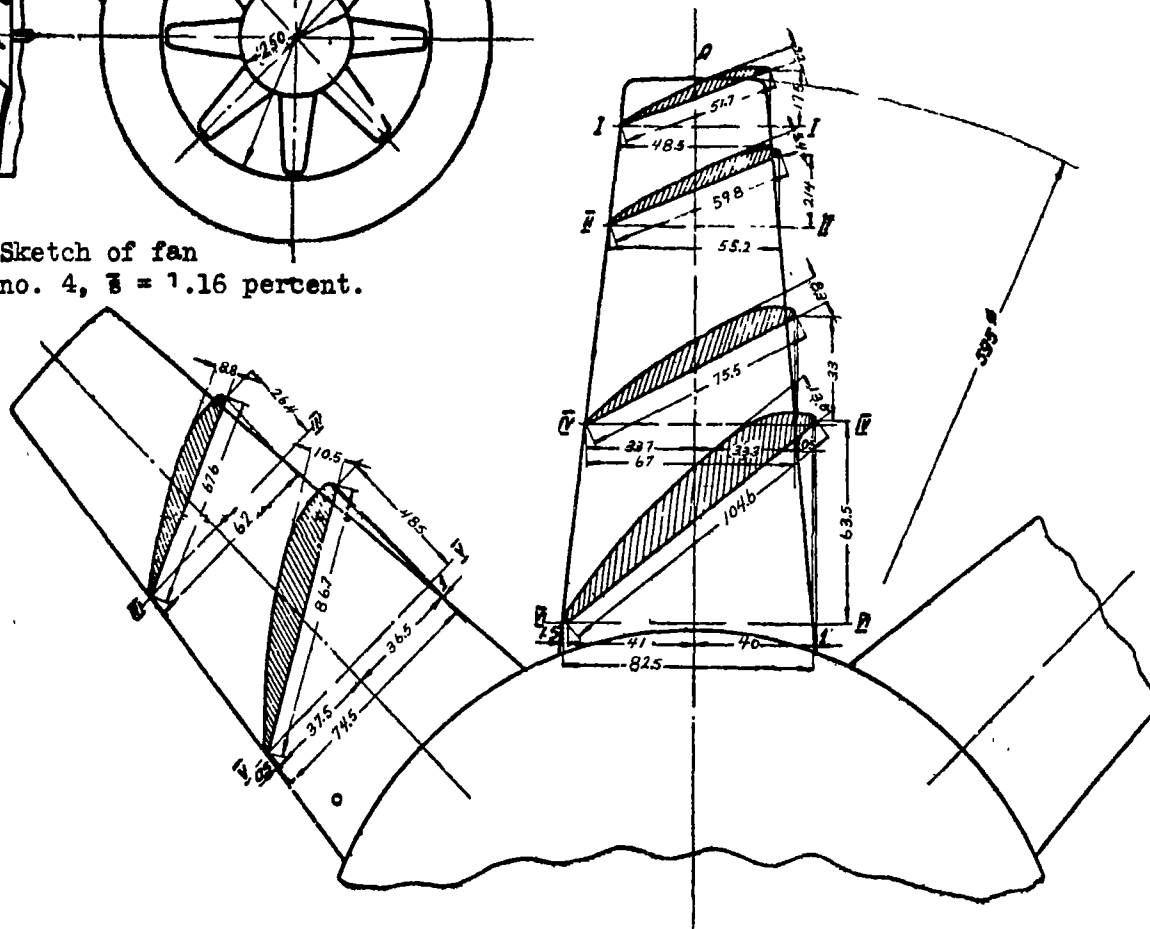
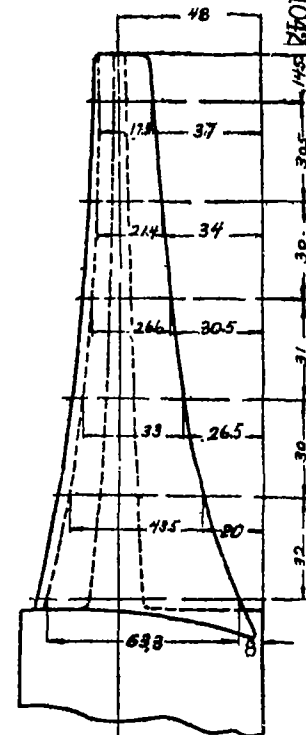


Figure 32.- Blade drawing of fan no. 4.



Figs. 31, 32

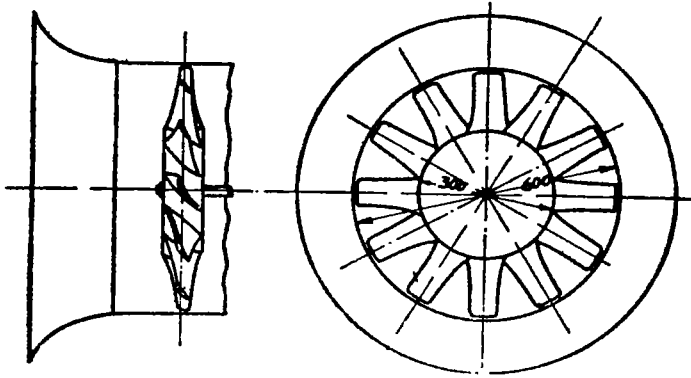


Figure 33.- Sketch of fan no. 5a, $\bar{\alpha} = 2$ percent.

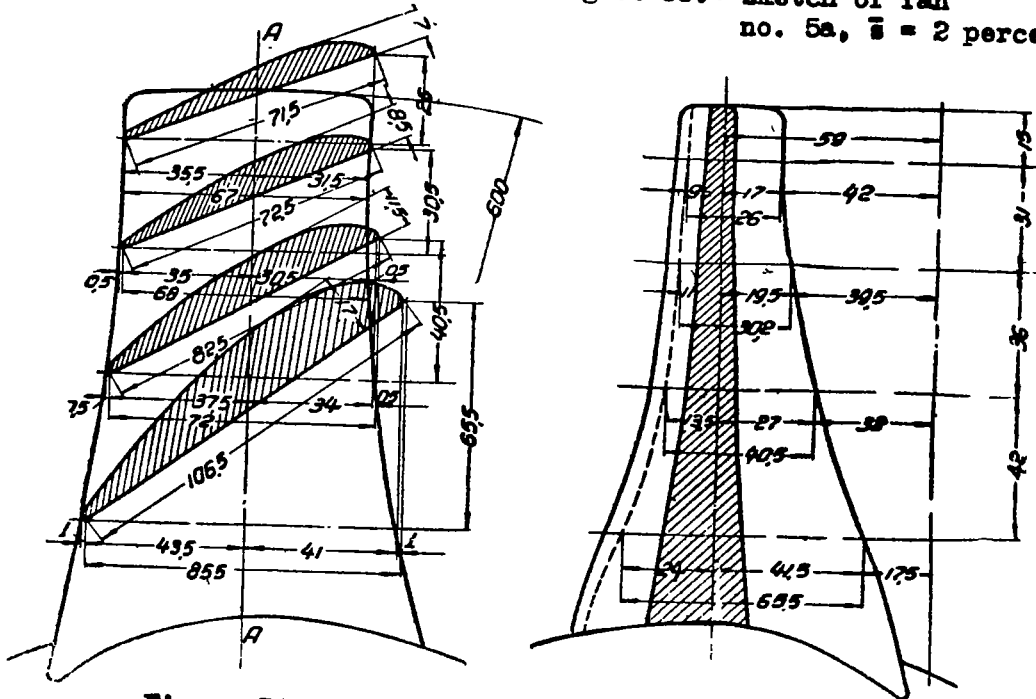


Figure 34.- Blade drawing of fan no. 5a.

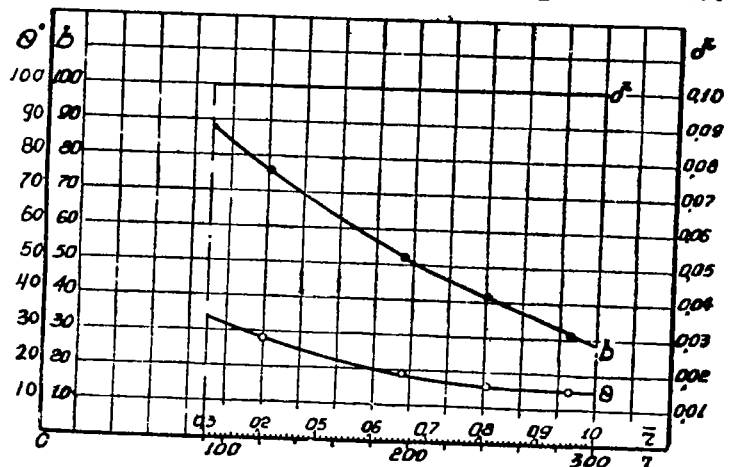


Figure 35.- Geometric parameters of fan no. 1. θ/n - blade angle, b - blade width, δ - blade thickness.

Figure 36.-
Geometric
parameters
of fan no. 2,

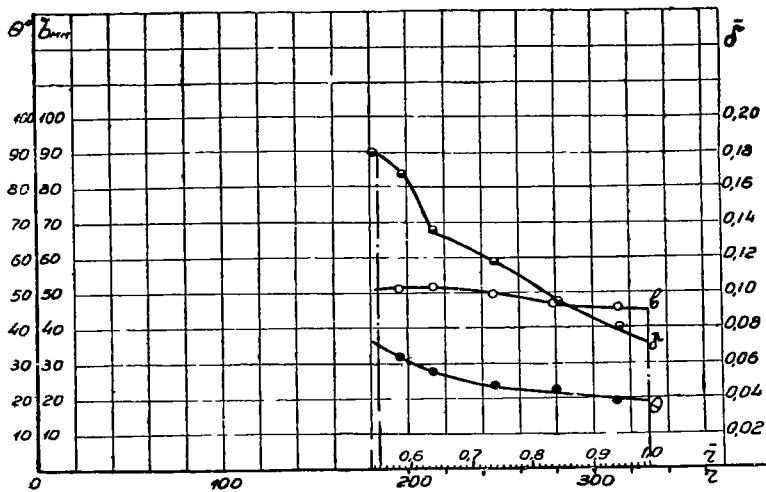
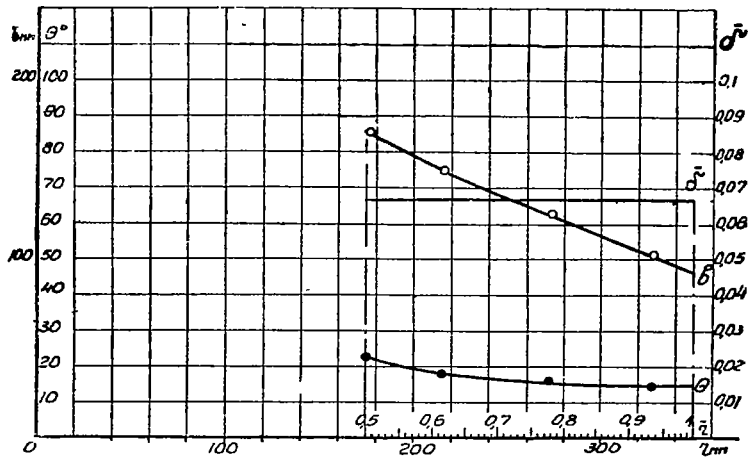
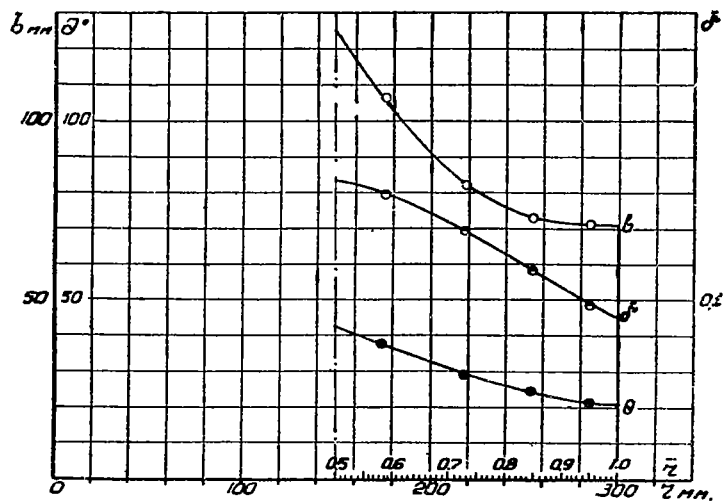


Figure 37.-
Geometric
parameters
of fan
no. 3a.

Figure 38.-
Geometric
parameters
of fan no. 5a.



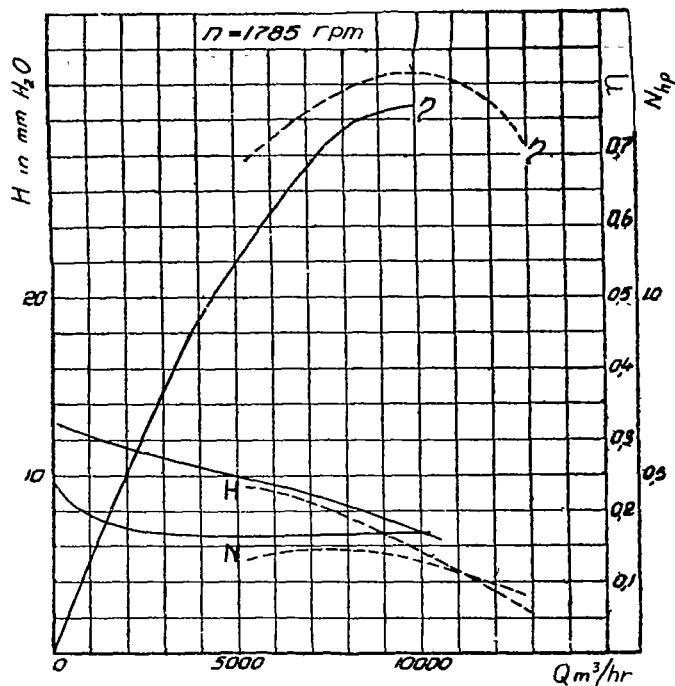


Figure 39.- Comparison of computed and test characteristics of fan no. 1, $\bar{s} = 1.3$ percent. test characteristics, -----computed characteristics.

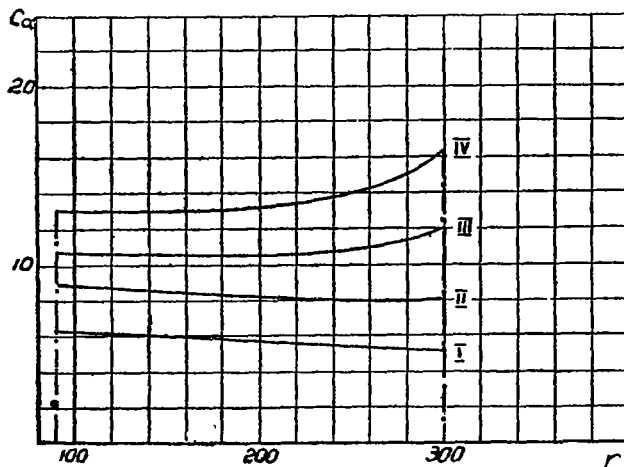


Figure 40.- Axial velocity distribution of fan no. 1.

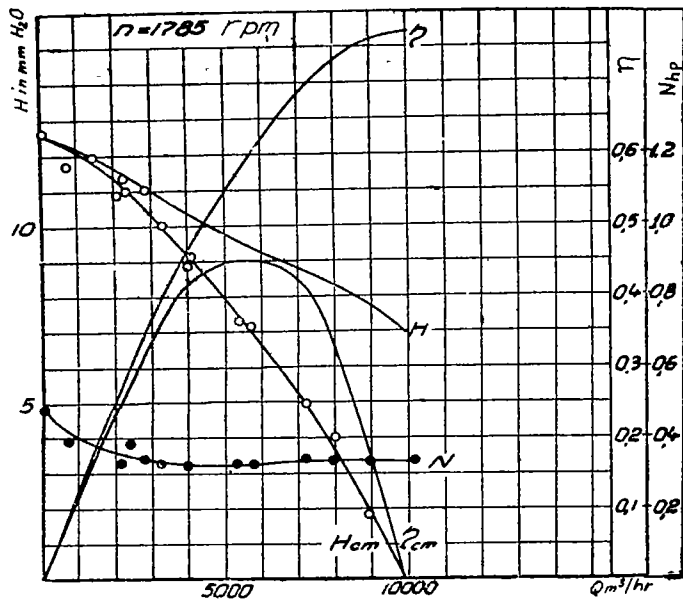


Figure 41.- Test characteristics of fan no. 1.

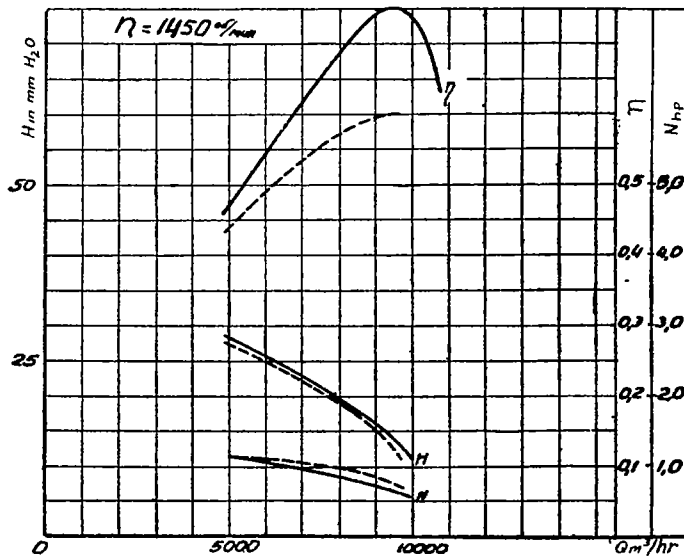


Figure 42.- Comparison of computed and test characteristics of fan no. 2, $\bar{\eta} = 1.5$ percent.
test characteristics,----- computed characteristics.

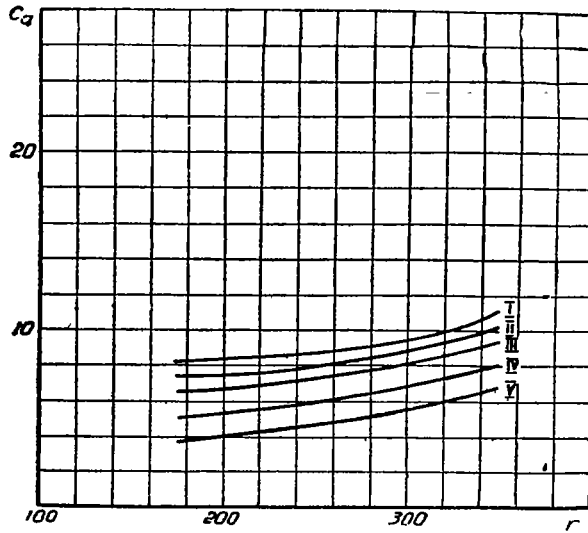


Figure 43.- Axial velocity distribution for fan no. 2.

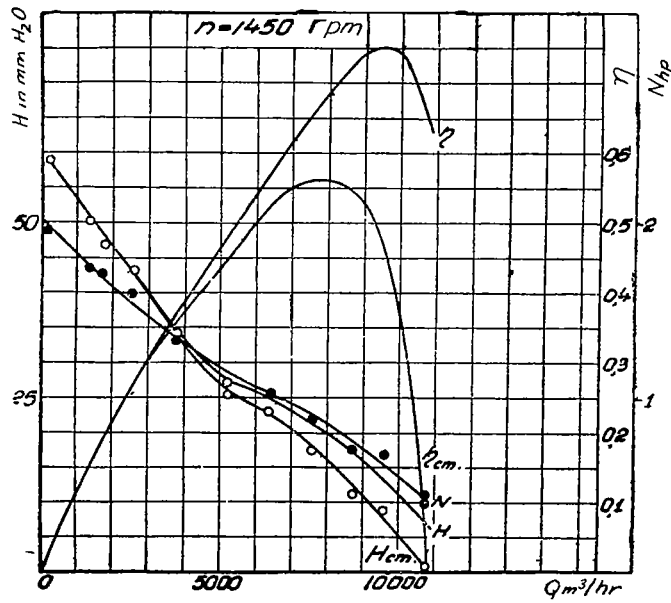


Figure 44.- Test characteristics of fan no. 2.

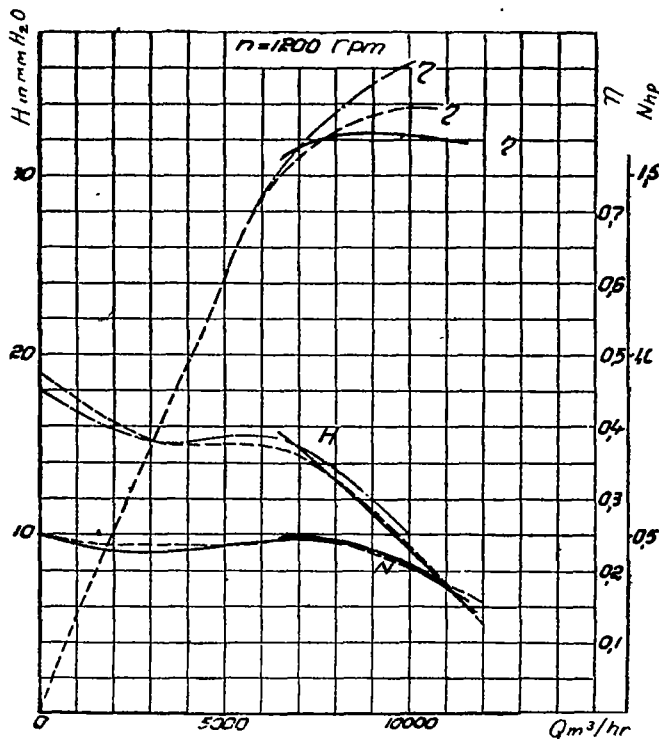


Figure 45.- Comparison of computed and test characteristics of fan no. 3a, $\theta = 19^\circ 20'$, $\bar{s} = 1$ percent.
 computed characteristics ——— test characteristics.

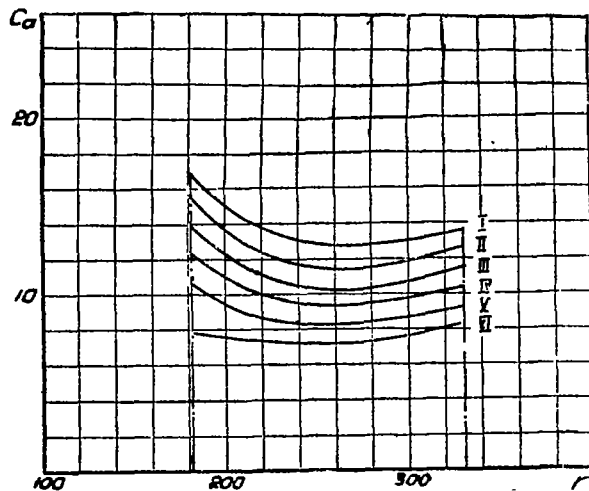


Figure 46.- Axial velocity distribution for fan no. 3a.

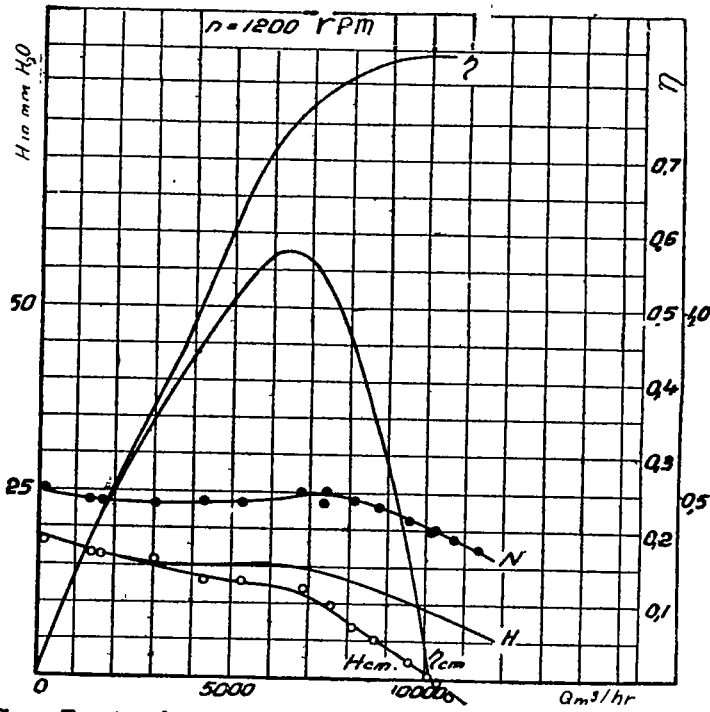


Figure 47.- Test characteristics of fan no. 3a, $\theta = 19^\circ 20'$.

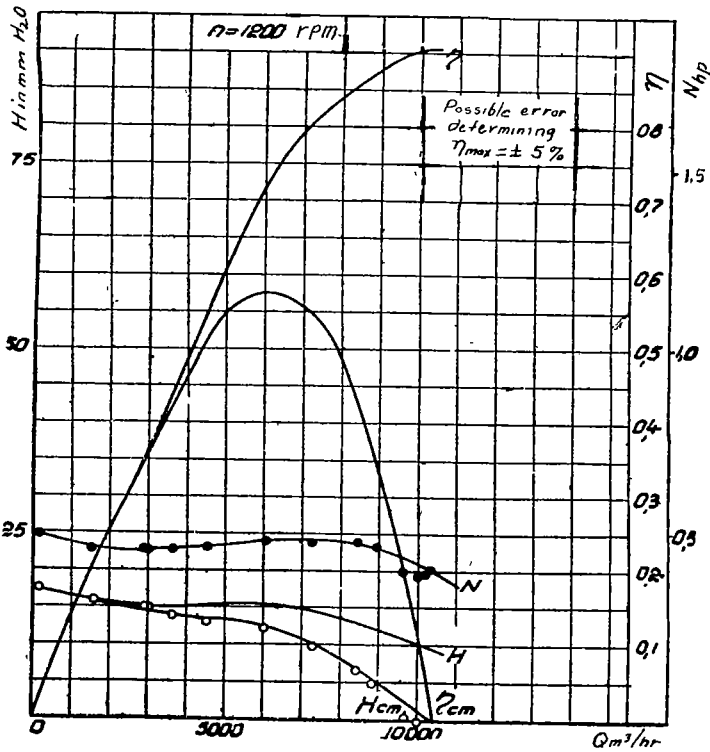


Figure 47a.- Test characteristics of fan no. 3a, $\theta = 19^\circ 20'$, check test.

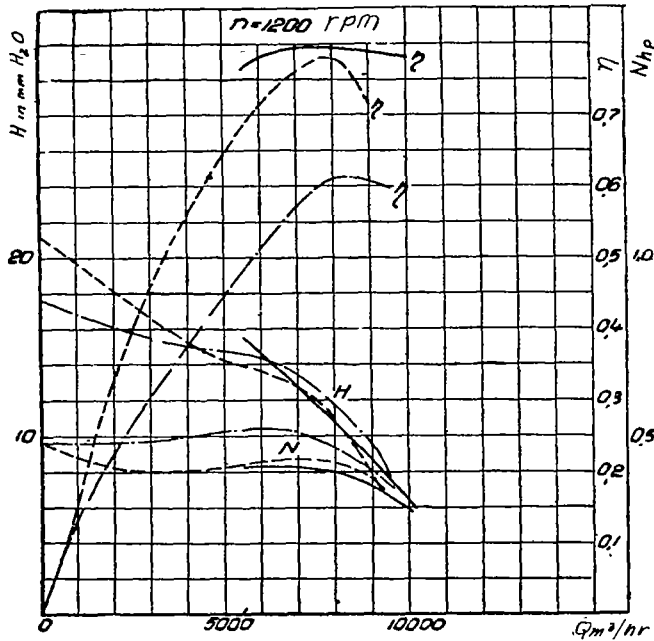


Figure 48.- Comparison of computed and test characteristics of fan no. 3b, $\theta = 16^\circ 59'$, $\bar{s} = 1$ percent. computed characteristics,-----test characteristics.

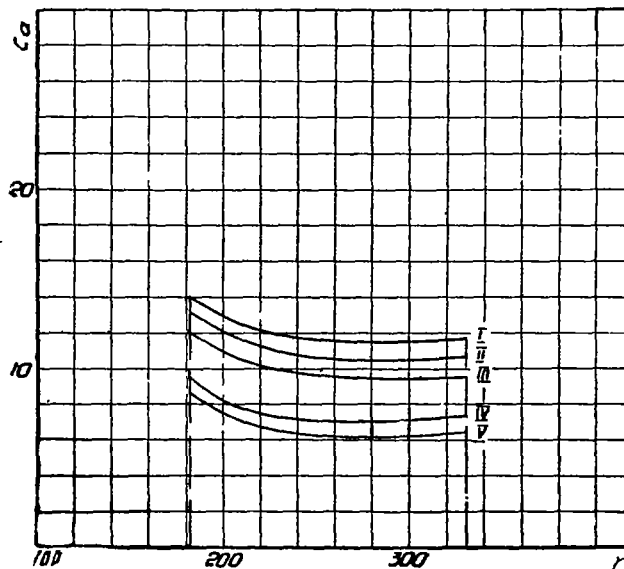


Figure 49.- Axial velocity distribution for fan no. 3b.

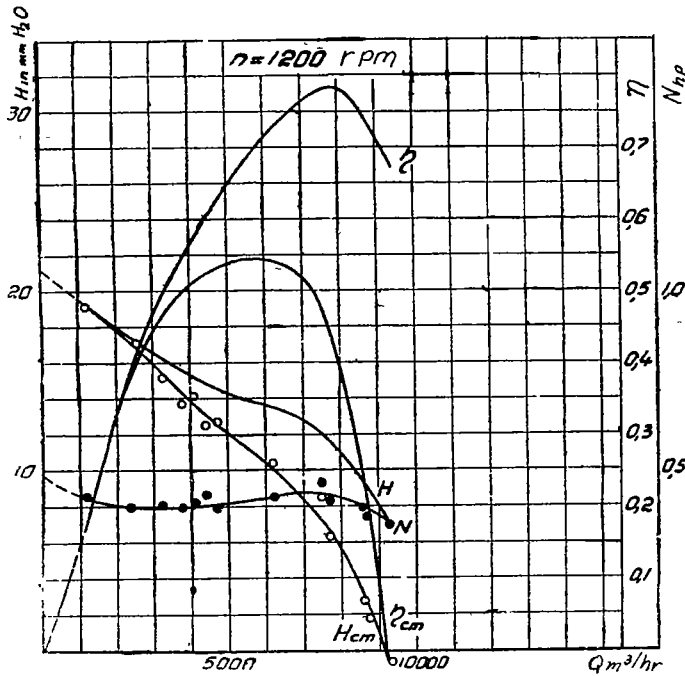


Figure 50.- Test characteristics of fan no. 3b, $\theta = 16^\circ 50'$

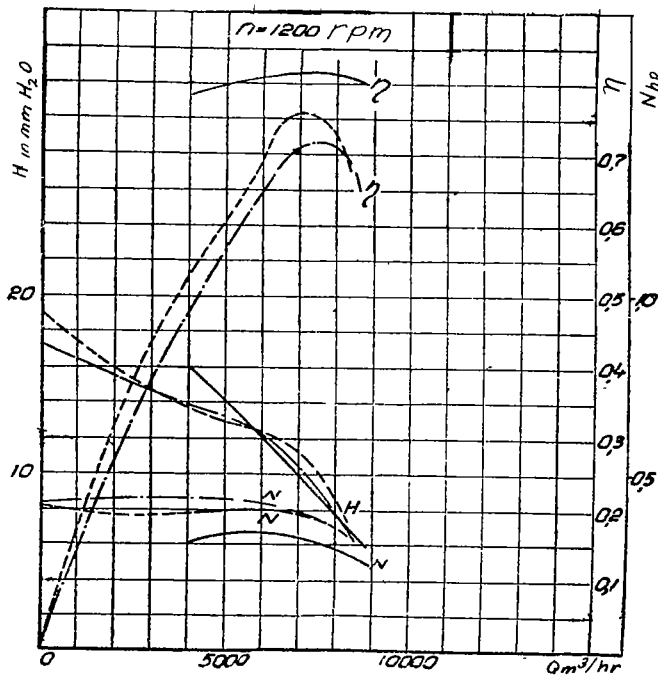


Figure 51.- Comparison of computed and test characteristics of fan no. 3c, $\theta = 14^\circ 05'$

— computed characteristics, - - - test characteristics.

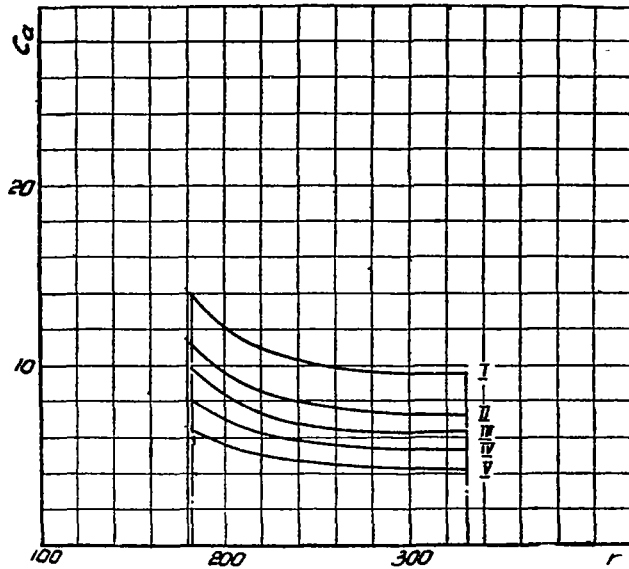


Figure 52.- Axial velocity distribution for fan no. 3c.

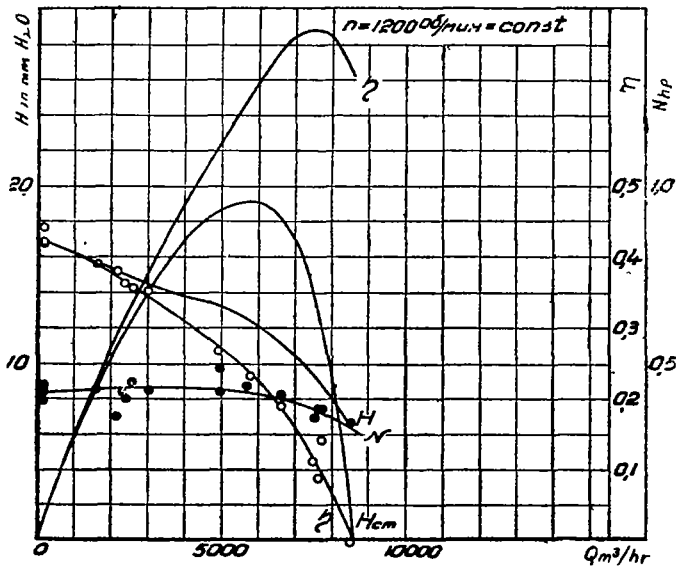


Figure 53.- Test characteristics of fan no. 3c, $\theta = 14^{\circ} 05'$

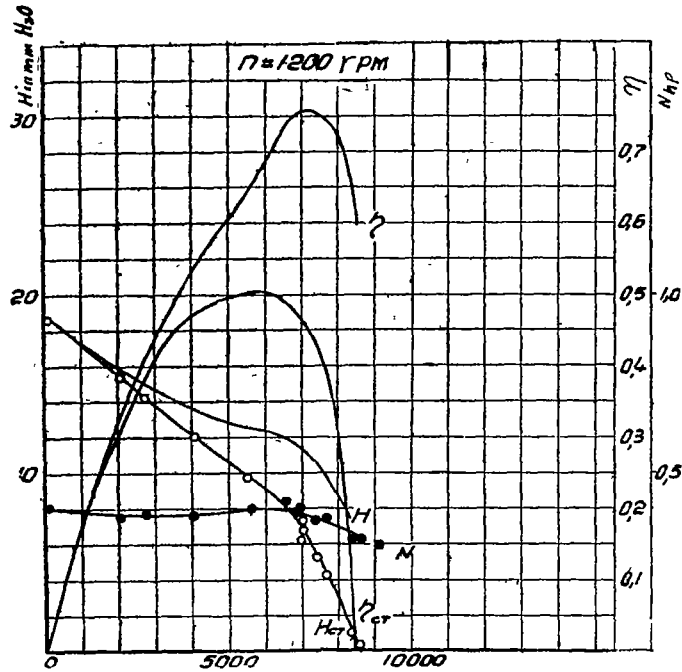


Figure 53a.- Test characteristics of fan no. 3c, $\theta = 14^\circ 05'$, check test.

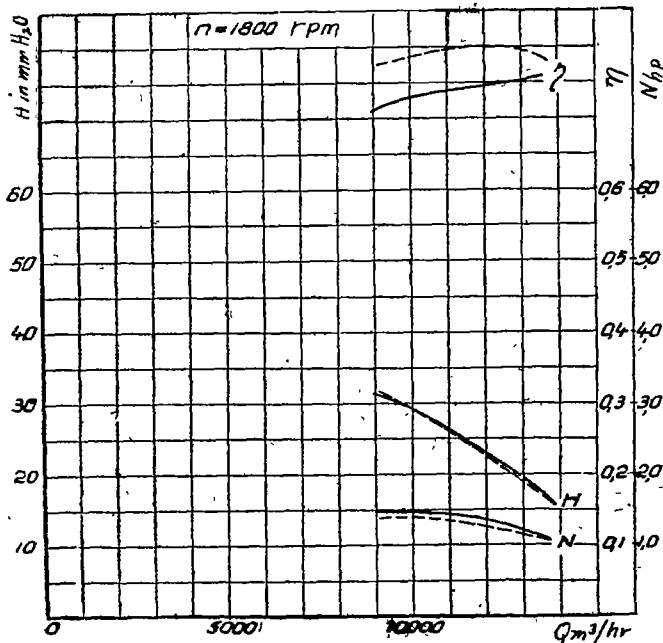


Figure 54.- Comparison of computed and test characteristics of fan no. 4, $\bar{s} = 1.16$ percent.
test characteristics,-----computed characteristics.

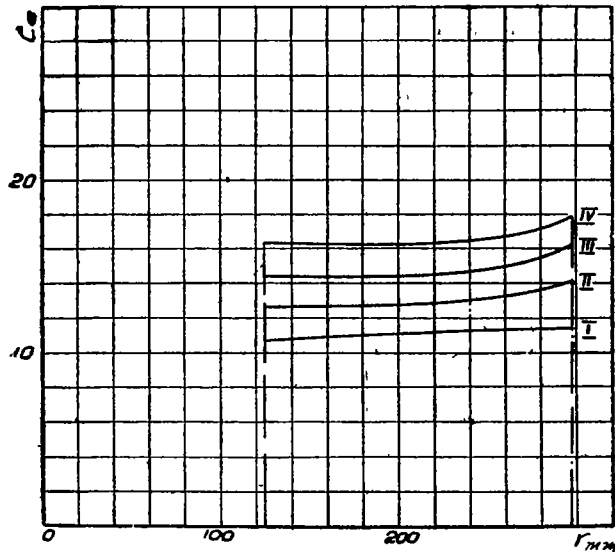


Figure 55.- Axial velocity distribution of fan no. 4.

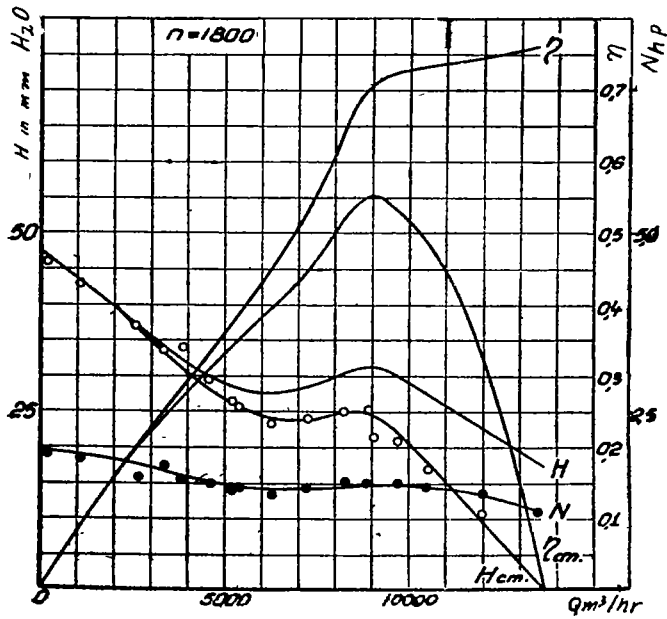


Figure 56.- Test characteristics of fan no. 4.

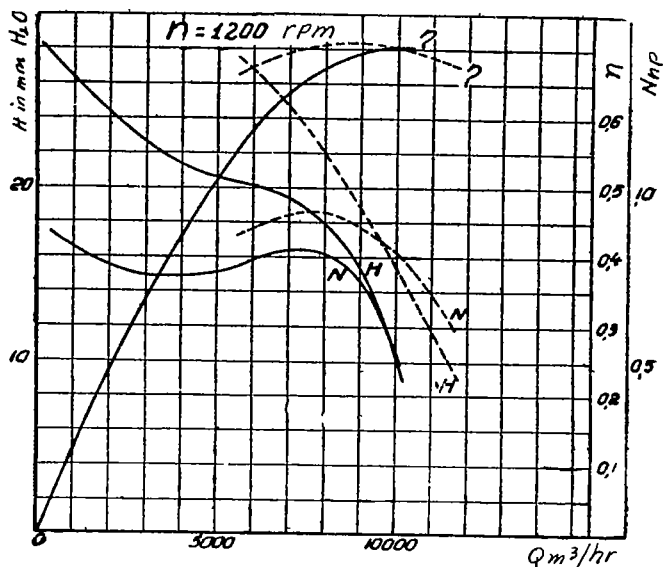


Figure 57.- Comparison of computed and test characteristics of fan no. 5a; $i = 12$, $\bar{s} = 2$ percent.
 ——— test characteristics, - - - - - computed characteristics.

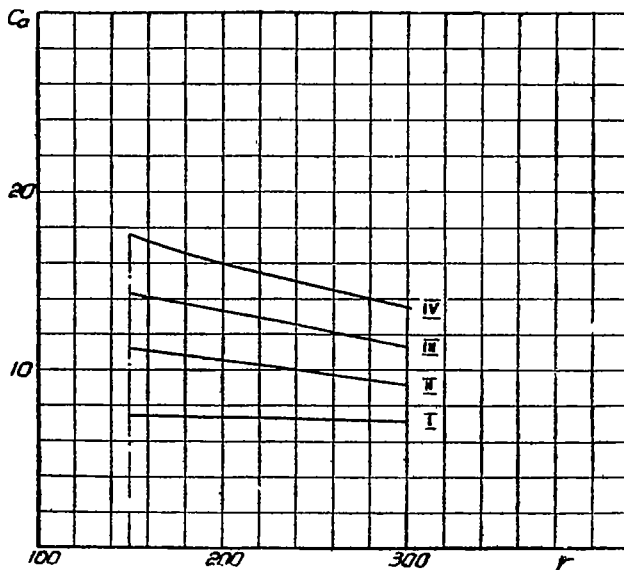


Figure 58.- Axial velocity distribution for fan no. 5a.

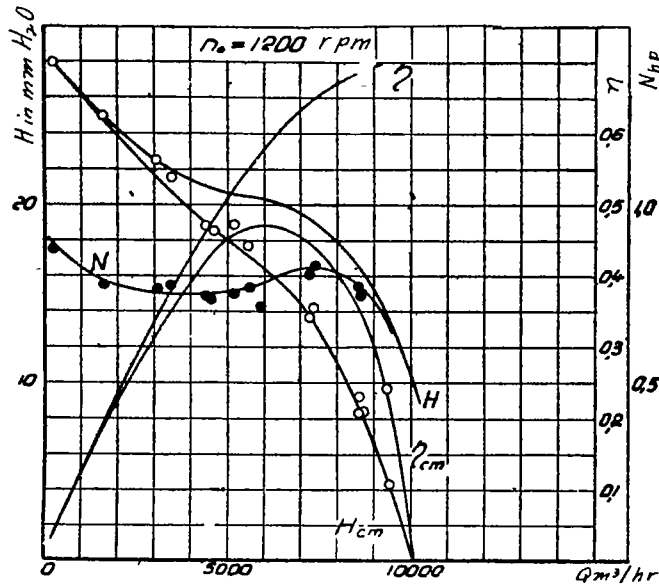


Figure 59.- Test characteristics of fan no. 5.

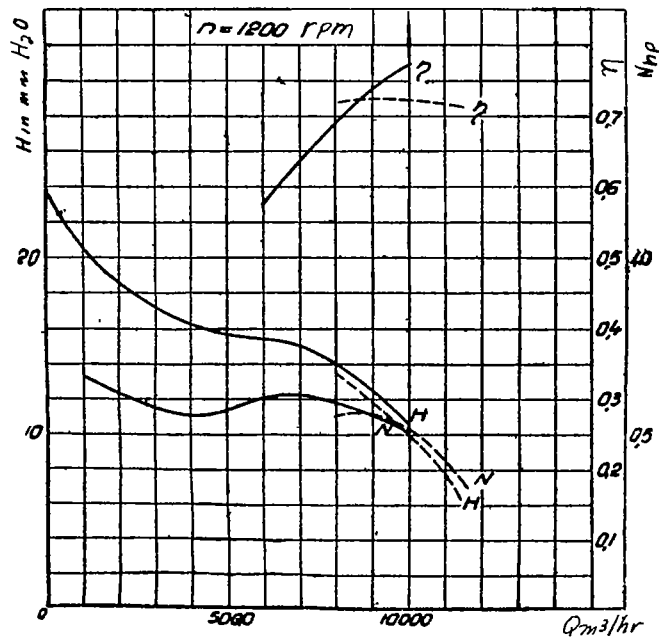


Figure 60.- Comparison of computed and test characteristics of fan no. 5b; $i = 6$, $\bar{s} = 2$ percent.
 ——— test characteristics, - - - - - computed characteristics.

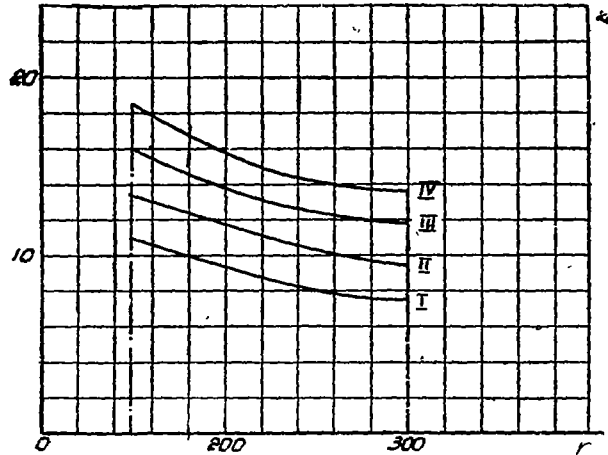


Figure 61.- Axial velocity distribution of fan no. 5b.

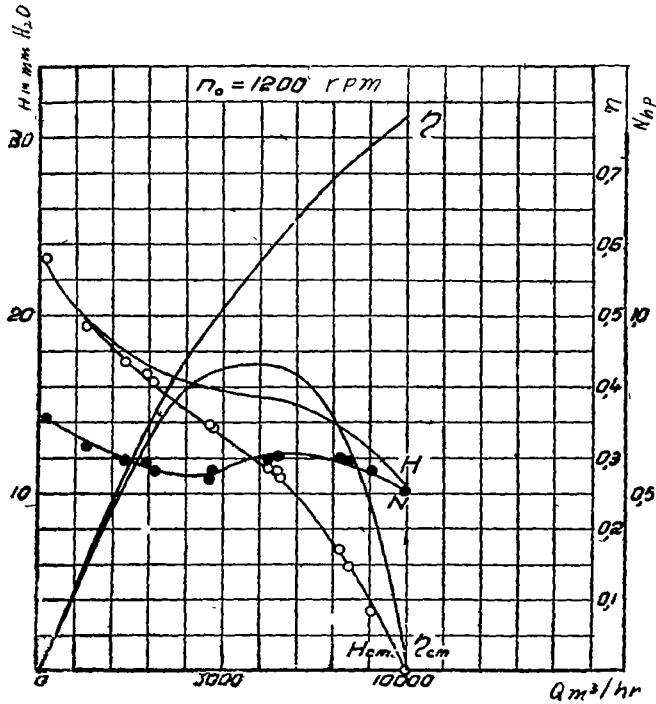


Figure 62.- Test characteristics of fan no. 5b, $i = 6$.

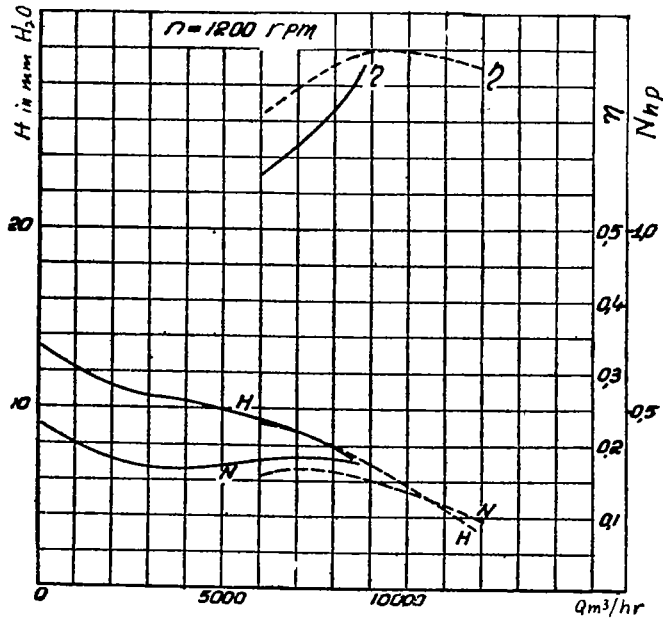


Figure 63.- Comparison of computed and test characteristics of fan no. 5c, $i = 3$, $\bar{s} = 2$ percent.
 ——— test characteristics, - - - - - computed characteristics.

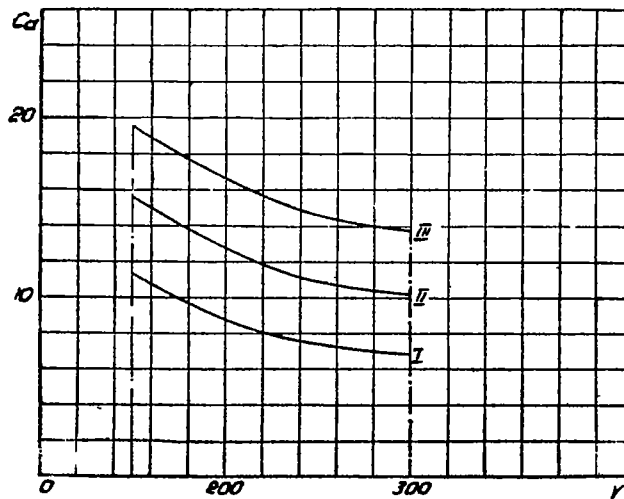


Figure 64.- Axial velocity distribution of fan no. 5c.

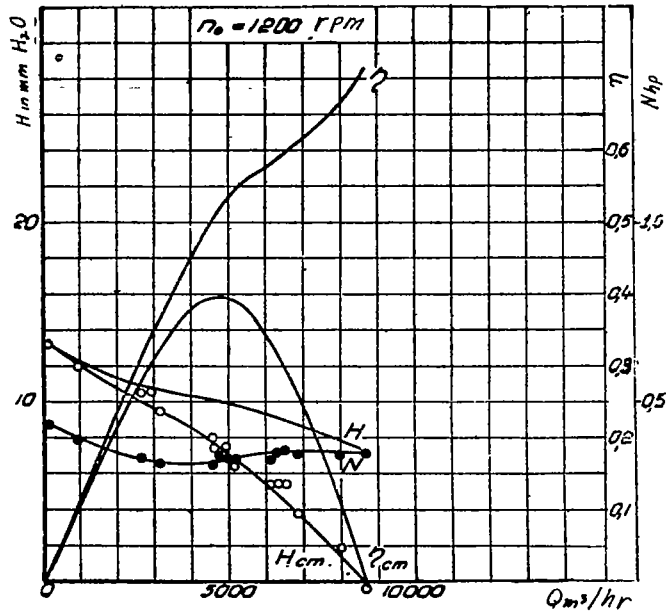


Figure 65.- Test characteristics of fan no.5c.

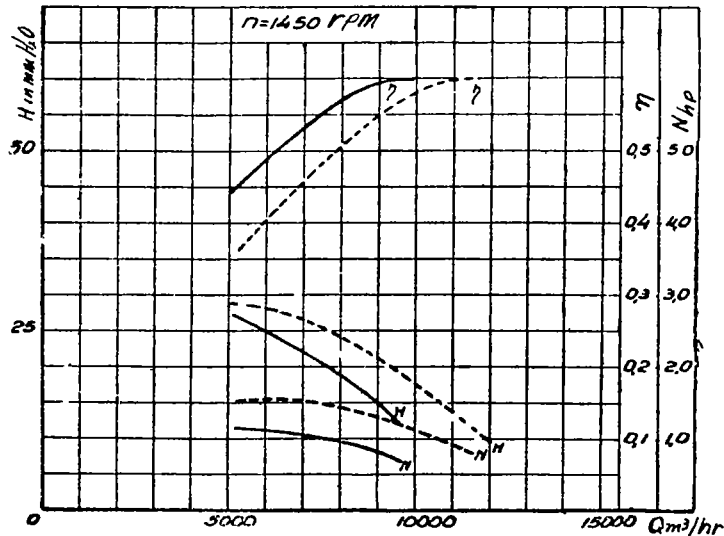


Figure 66.- Deviations of characteristics of fan no. 2 constructed: (1) with account taken of redistribution of axial velocities and (2) with axial velocities along radius assumed constant.

———— characteristics for first case
 - - - - - characteristics for second case

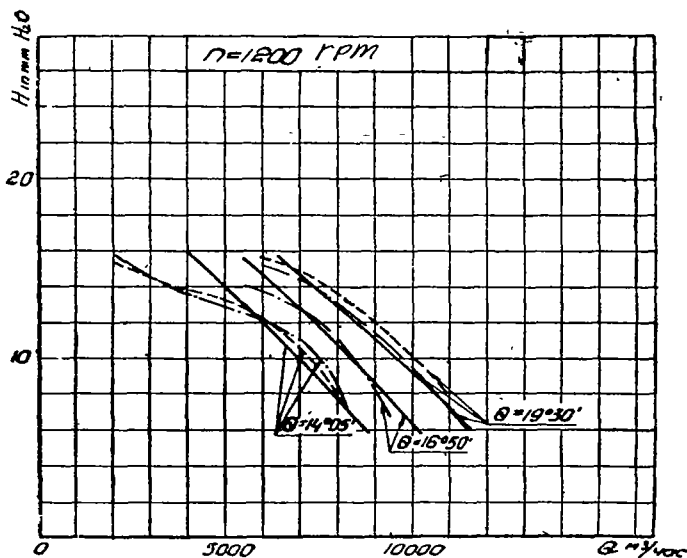


Figure 67.- Comparison of computed and test characteristics for rotation of blades of fan no. 3.

————— computed curve
 - - - - - experimental curve

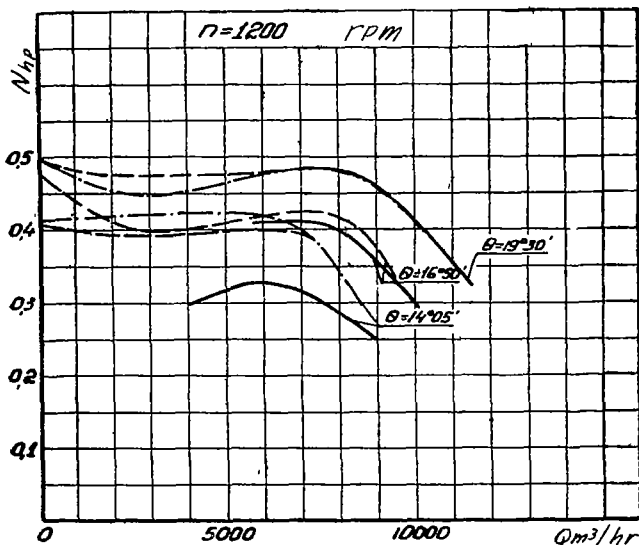


Figure 68.- Comparison of computed and experimental power curves of fan no. 3 for rotation of blades of fan no. 3.

————— computed curve
 - - - - - test curve

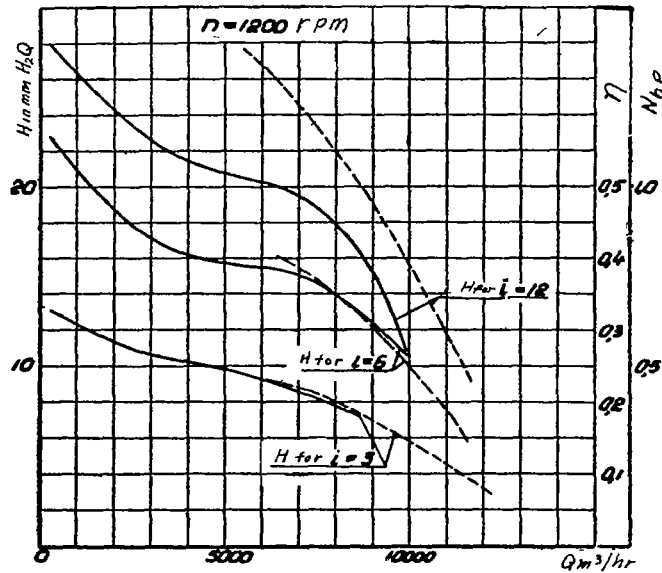


Figure 69.- Comparison of computed and experimental pressure curves of fan no. 5 for rated and smaller number of blades.

————— test curve, - - - - - computed curve.

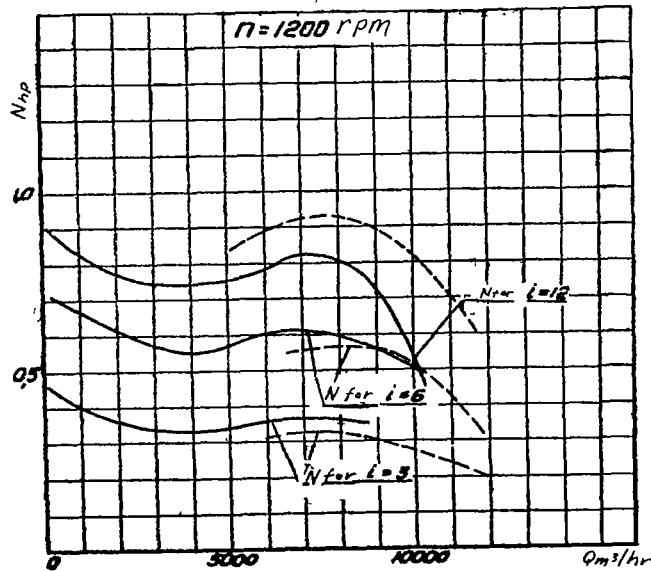


Figure 70.- Comparison of computed and experimental power curves of fan no. 5 for rated and smaller number of blades.

————— test curve, - - - - - computed curve.

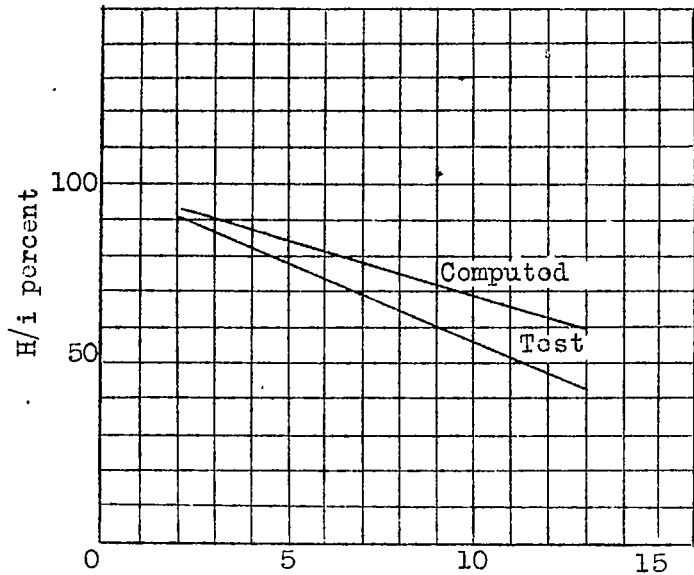


Figure 71.- Pressure developed per blade as a function of the number of blades.

Figure 72.- Method of construction of preliminary pressure characteristic.

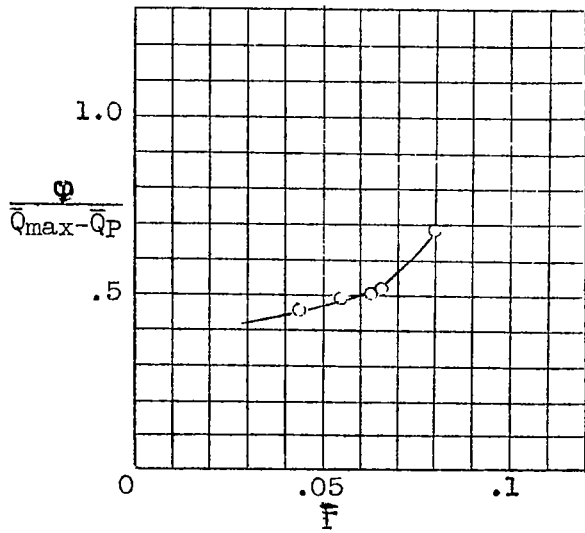
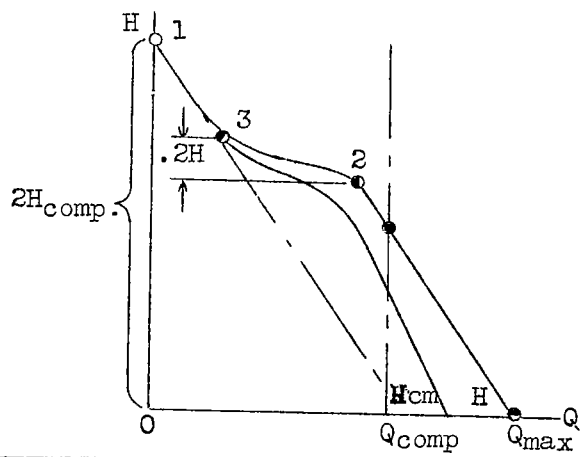


Figure 73.- Determination of the slope of the preliminary fan characteristic.

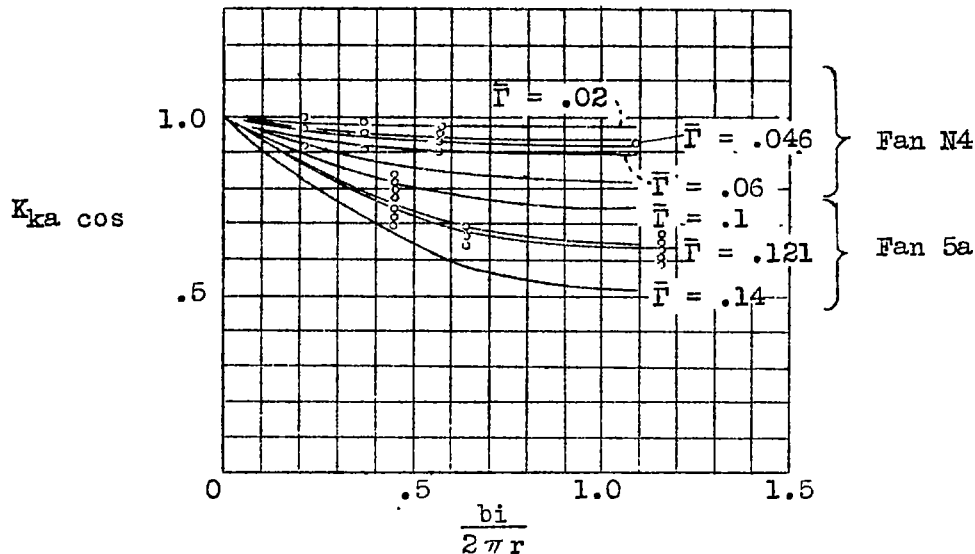


Figure 74.- Curve of correction K_{ka} taking into account the blade interference effect; $K_a \cos = K_a K_{ka}$.

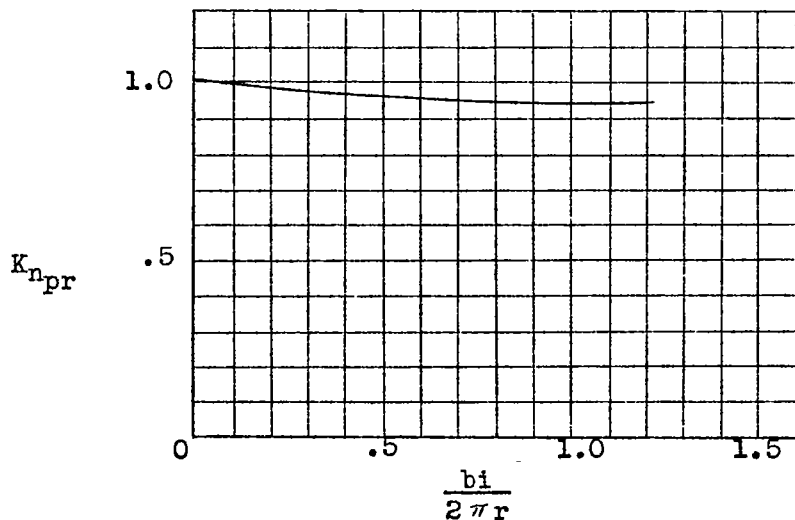


Figure 75.- Curve of correction coefficient that takes into account the change of the profile efficiency due to blade interference effect.

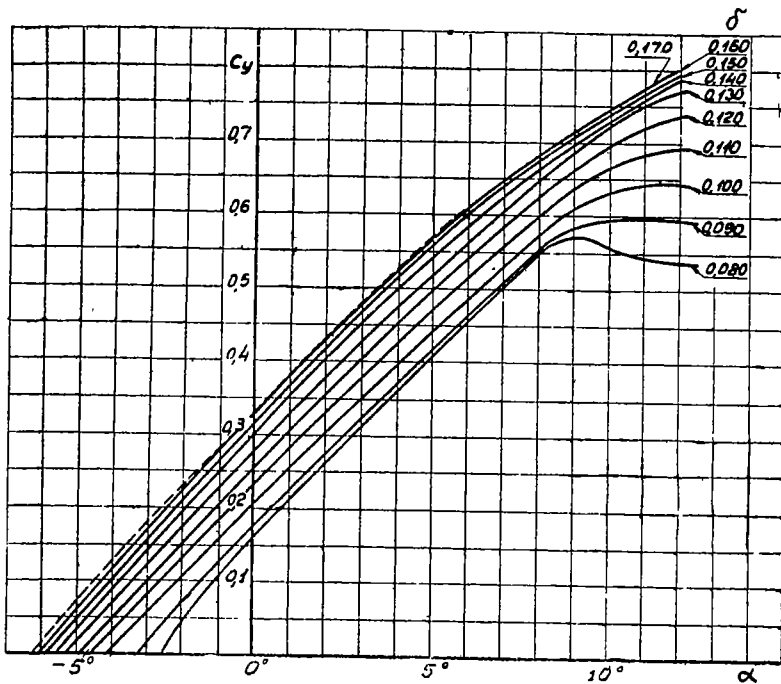
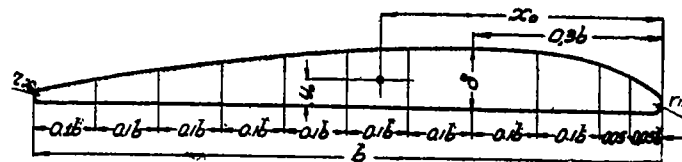


Figure 77.- Lift coefficient curves for English propeller sections with various relative thicknesses $\bar{\delta}$.



Distance from nose in Percent Chord	5	10	20	30	40	50	60	70	80	90	r_H	r_X
ordinate in Percent max thickness	52.2	72.6	96.1	100.0	99.1	95.1	87.9	74.7	57.2	36.9	14.0	2.0

Figure 76.- Data for the construction of the English propeller profile section.

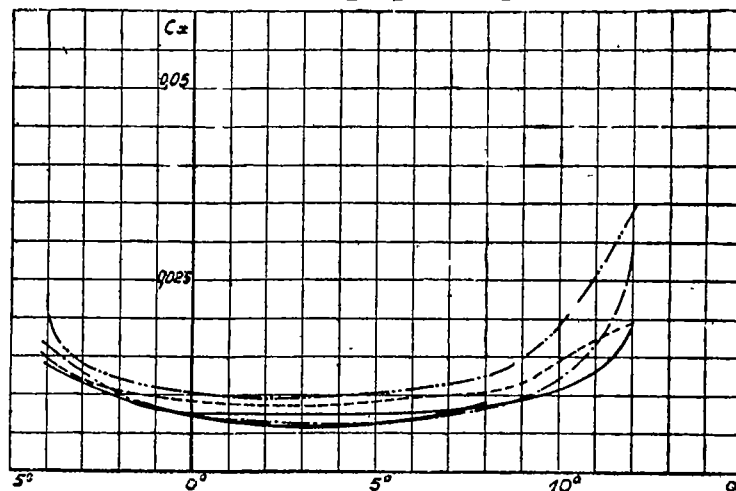


Figure 78.- Drag coefficient curves for English propeller sections with various relative thickness. $\bar{\delta} = 0.08$, $\bar{\delta} = 0.12$, $\bar{\delta} = 0.16$, $\bar{\delta} = 0.10$, $\bar{\delta} = 0.14$.

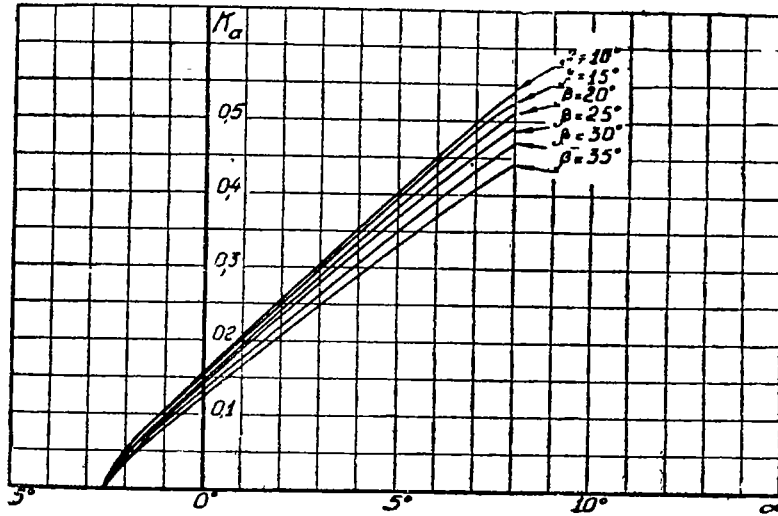


Figure 79.- Pressure coefficients for English propeller section with relative thickness $\bar{\delta} = 0.08$.

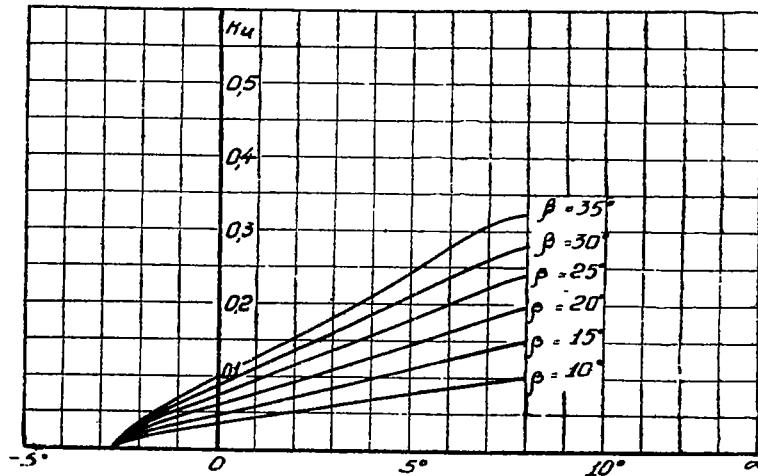


Figure 80.- Power coefficient curves for English propeller section with relative thickness $\bar{\delta} = 0.08$.

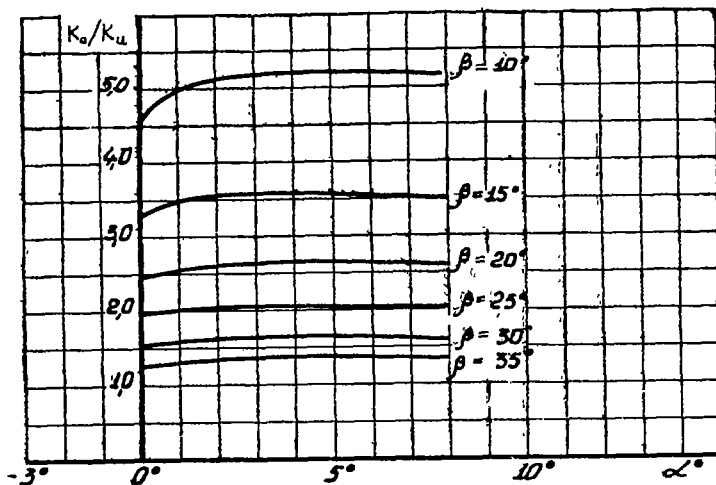


Figure 81.- Curves of K_a/K_u for English propeller section with relative thickness $\delta = 0.08$.

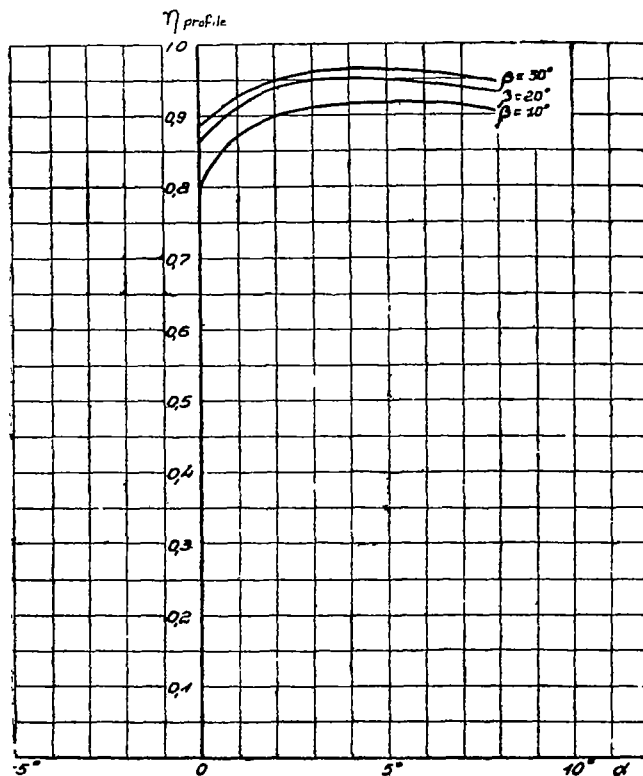


Figure 82.- Curves of profile efficiency for English propeller section with relative thickness $\delta = 0.08$.

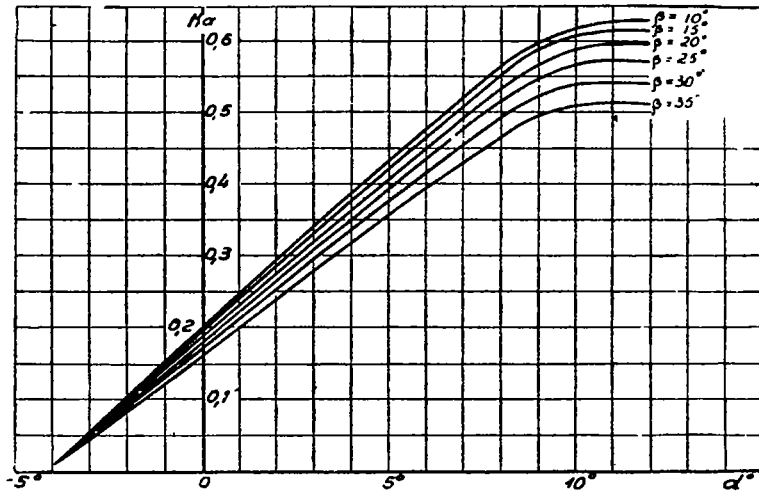


Figure 83.- Pressure coefficient curves for English propeller section with relative thickness $\delta = 0.01$.
0.1

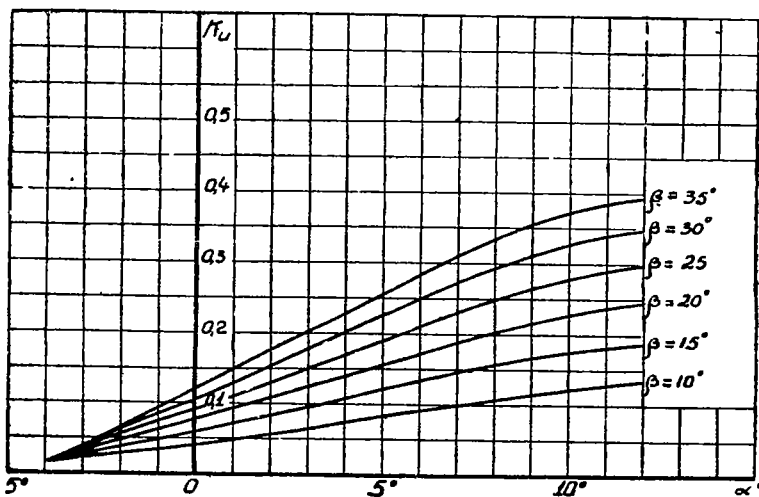


Figure 84.- Power coefficient curves for English propeller section with relative thickness $\delta = 0.1$.

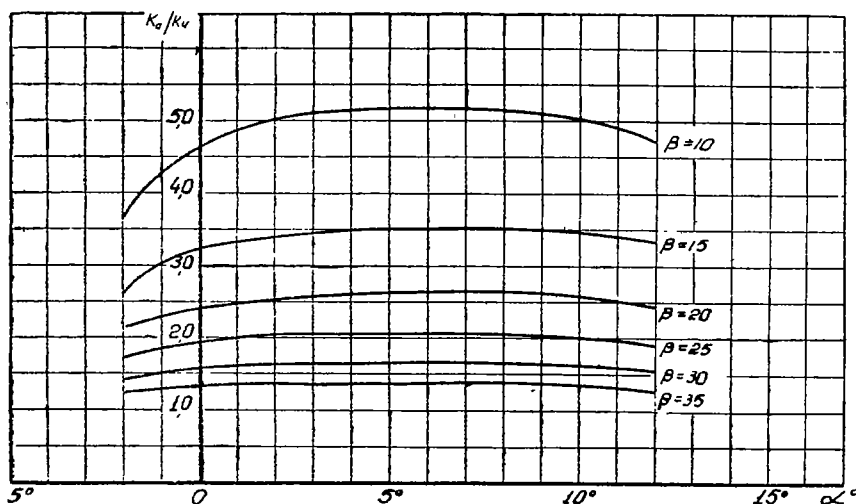


Figure 85.- Curves of K_a/K_u for English propeller section with relative thickness $\delta = 0.1$.

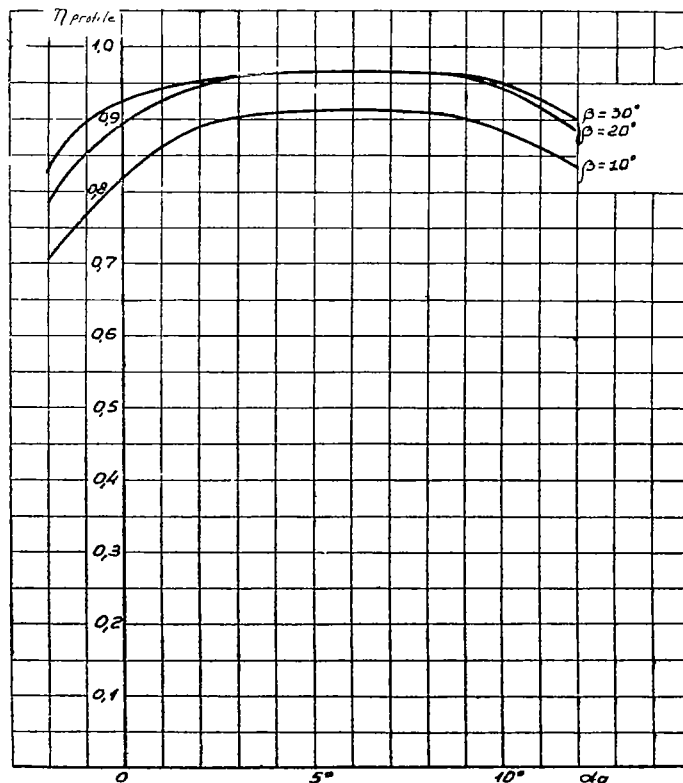


Figure 86.- Curves of profile efficiency for English propeller section with relative thickness $\delta = 0.1$.

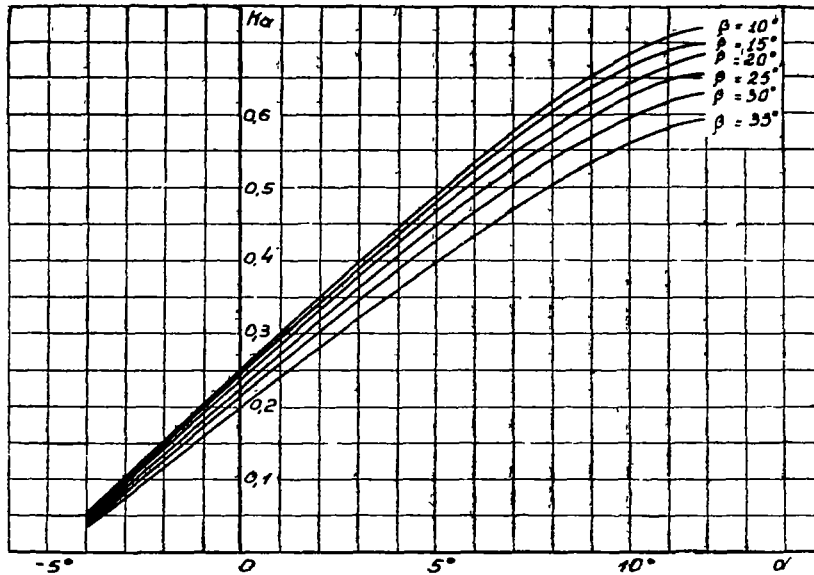


Figure 87.- Pressure coefficient curves for English propeller section with relative thickness $\bar{\delta} = 0.12$.

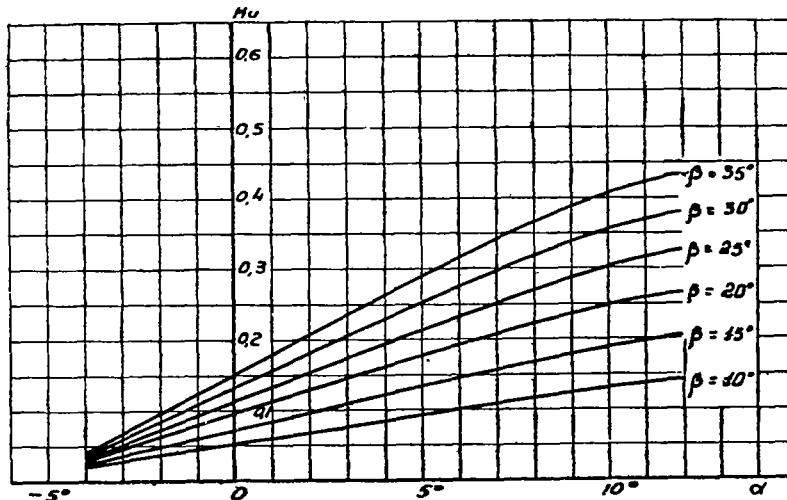


Figure 88.- Power coefficient curves for English propeller section with relative thickness $\bar{\delta} = 0.12$.

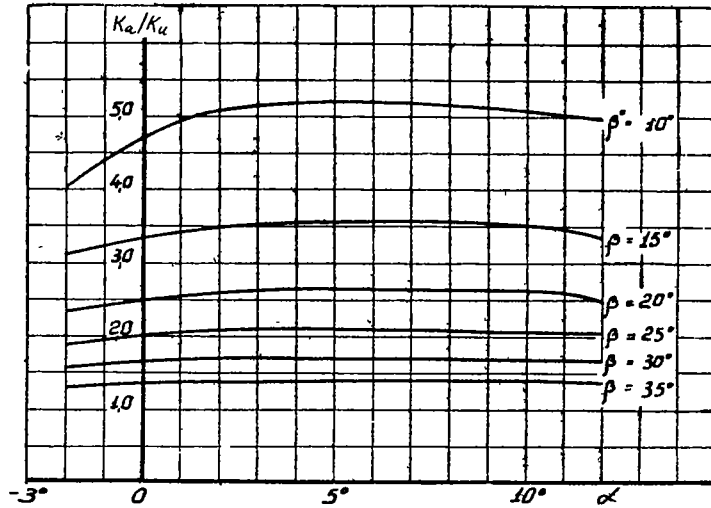


Figure 89.- Curves of K_a/K_u for English propeller section with relative thickness $\bar{\delta} = 0.12$.

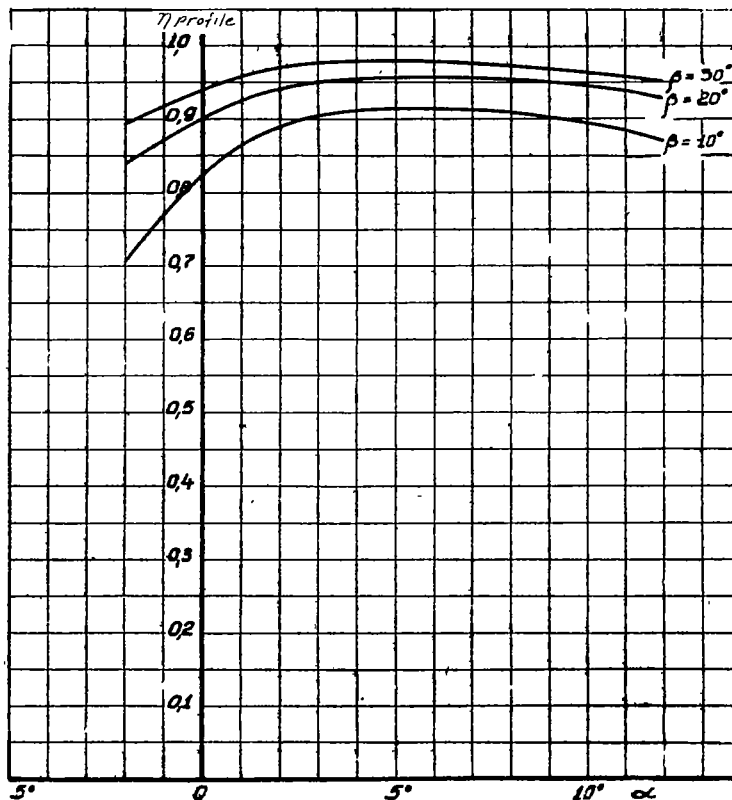


Figure 90.- Curves of profile efficiency for English propeller section with relative thickness $\bar{\delta} = 0.12$.

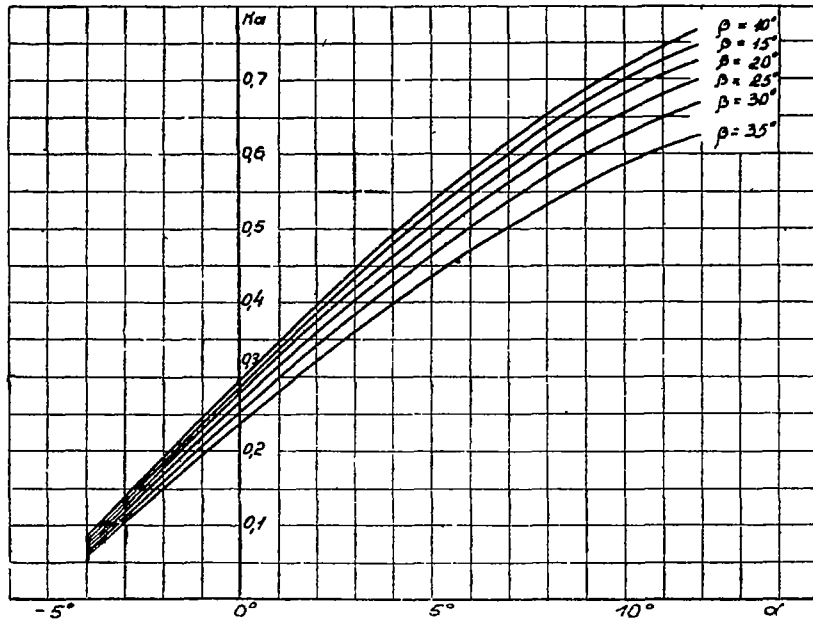


Figure 91.- Pressure coefficient curves for English propeller section with relative thickness $\delta = 0.14$.

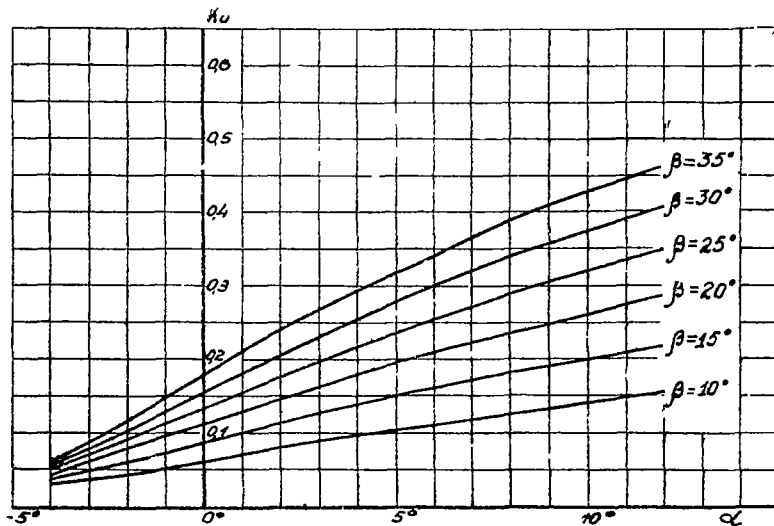


Figure 92.- Power coefficient curves for English propeller section with relative thickness $\delta = 0.14$.

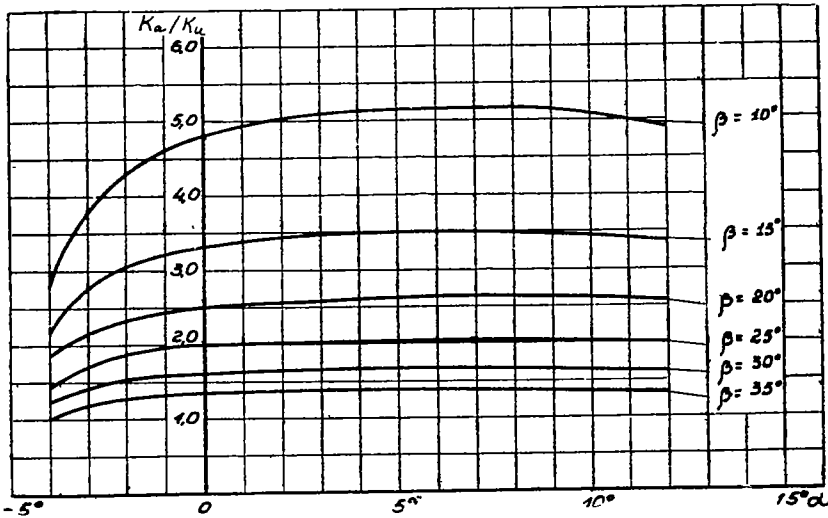


Figure 93.- Curves of K_a/K_u for English propeller section with relative thickness $\bar{\delta} = 0.14$.

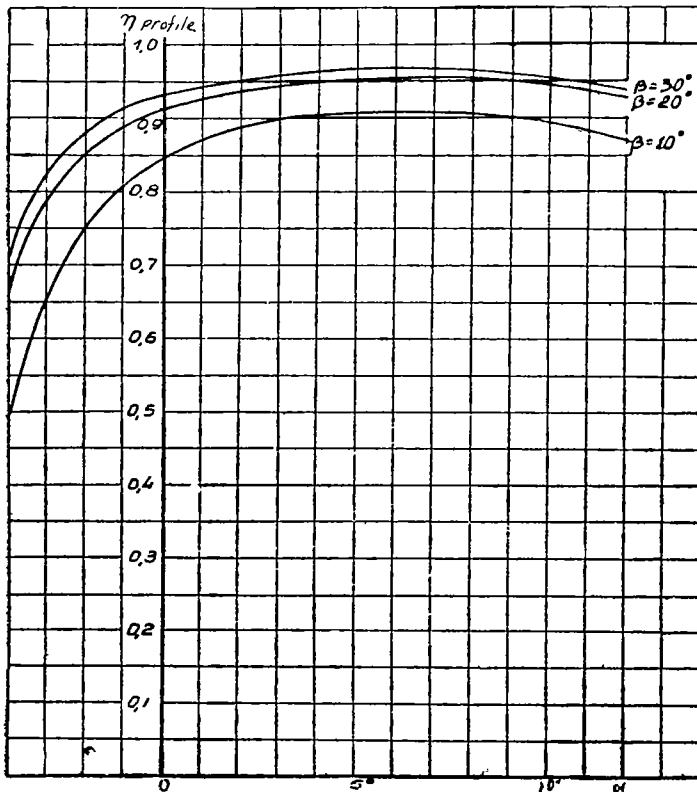


Figure 94.- Curves of profile efficiency for English propeller section with relative thickness $\bar{\delta} = 0.14$.

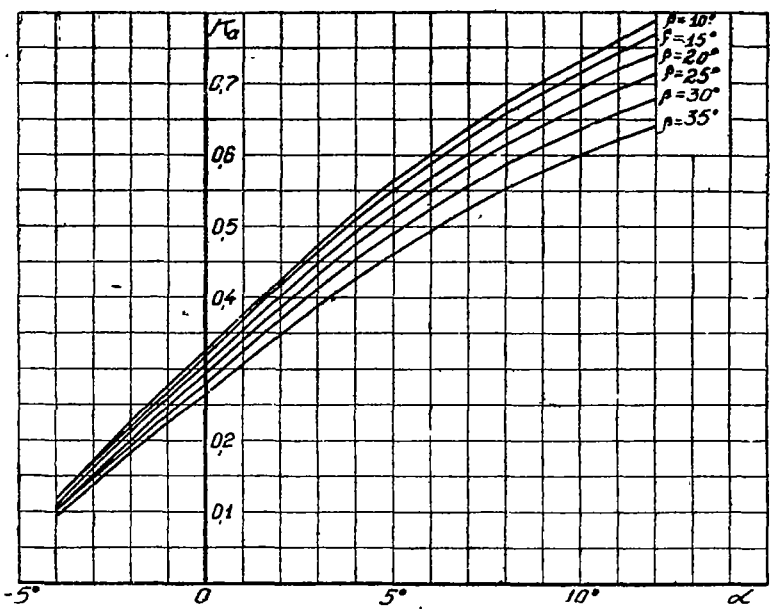


Figure 95.-- Pressure coefficient curves for English propeller section with relative thickness $\bar{\delta} = 0.16$.

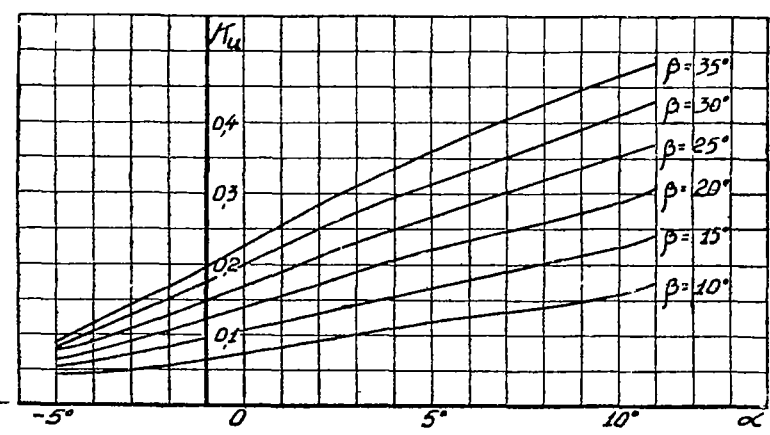


Figure 96.-- Power coefficient curves for English propeller section with relative thickness $\bar{\delta} = 0.16$.

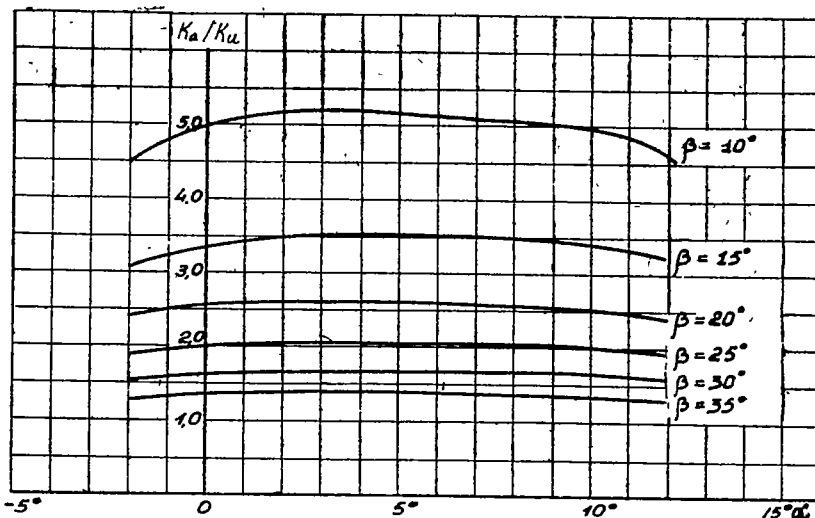


Figure 97.- Curves of K_a/K_u English propeller section with relative thickness $\bar{\delta} = 0.16$.

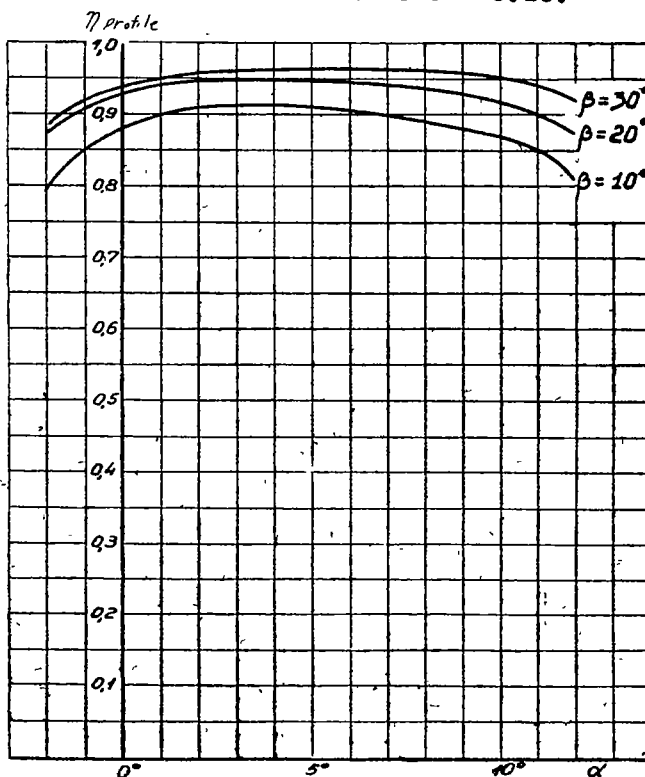


Figure 98.- Curves of profile efficiency for English propeller section with relative thickness $\bar{\delta} = 0.16$.

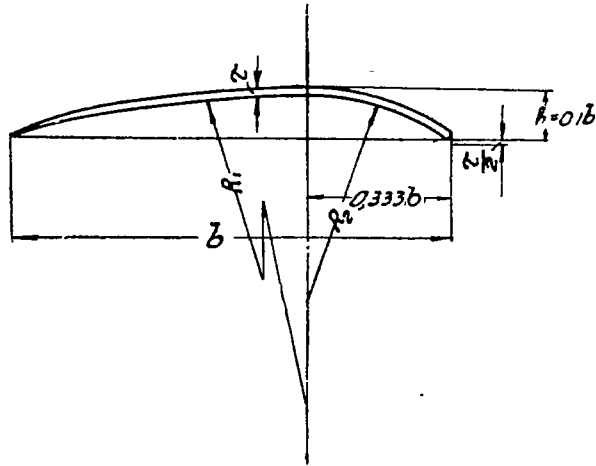


Figure 99.- Construction of curved metal blade no. 1.

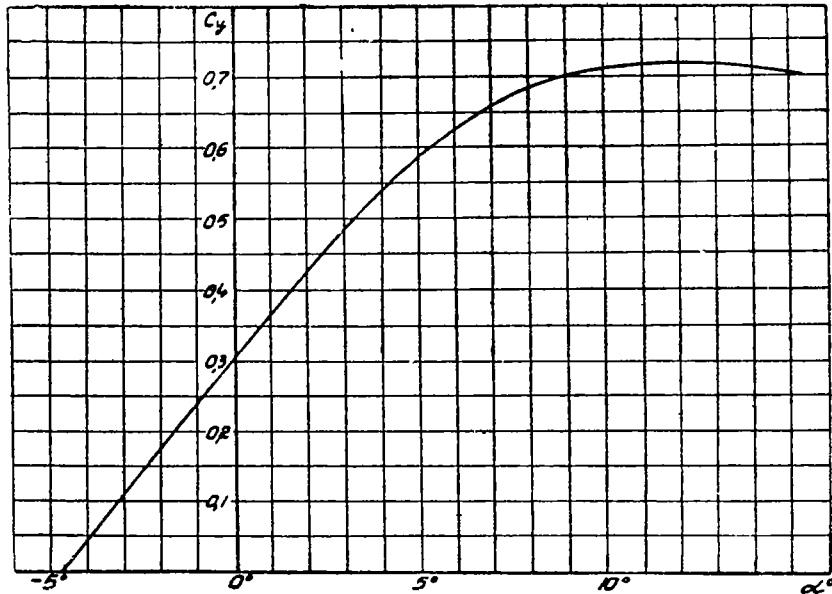


Figure 100.- Lift coefficient curve for curved metal fan blade.

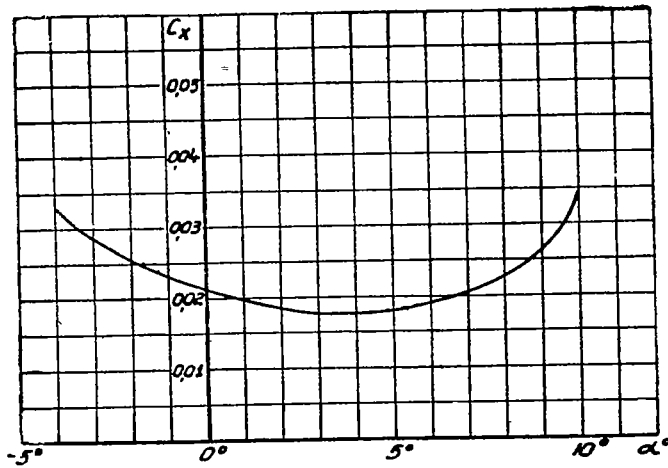


Figure 101.- Drag coefficient curve for curved metal fan blade.

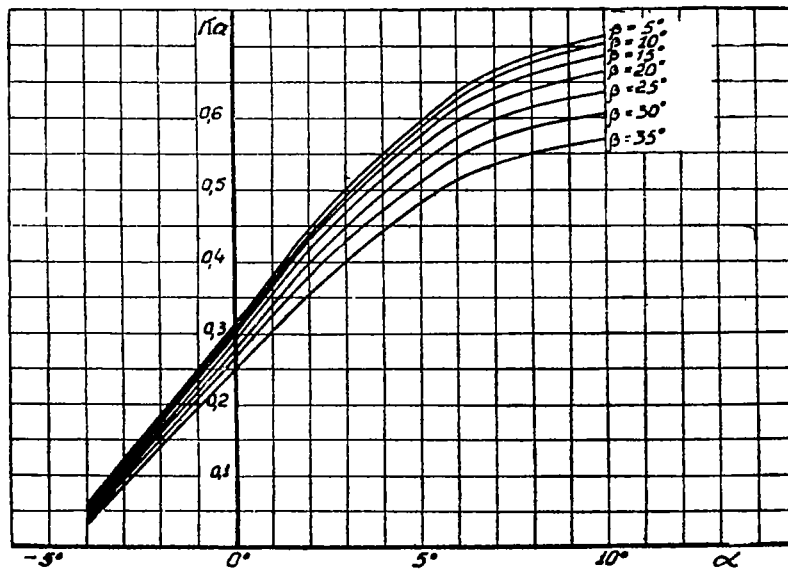


Figure 102.- Pressure coefficient curves for curved metal fan blade no. 1.

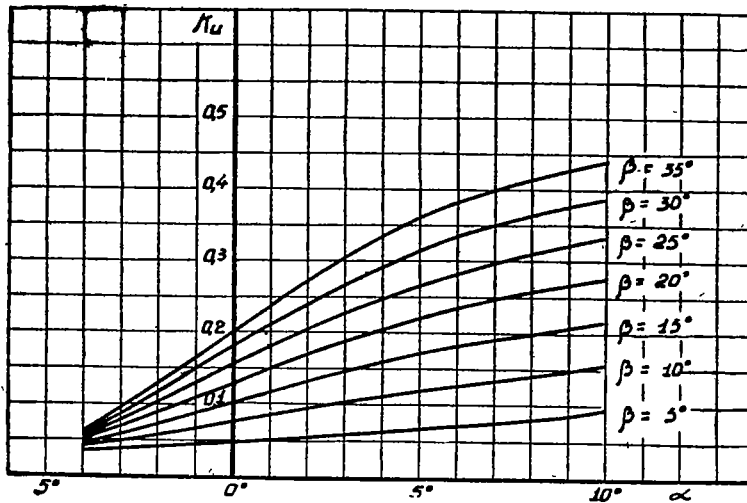


Figure 103.- Power coefficient curves for curved metal fan blade no. 1.

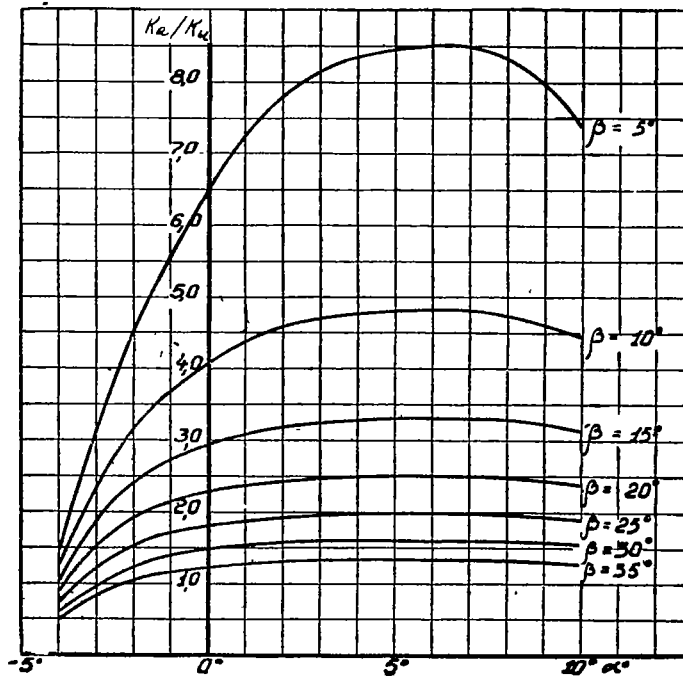


Figure 104.- Curves of K_a/K_u for metal blade no. 1.

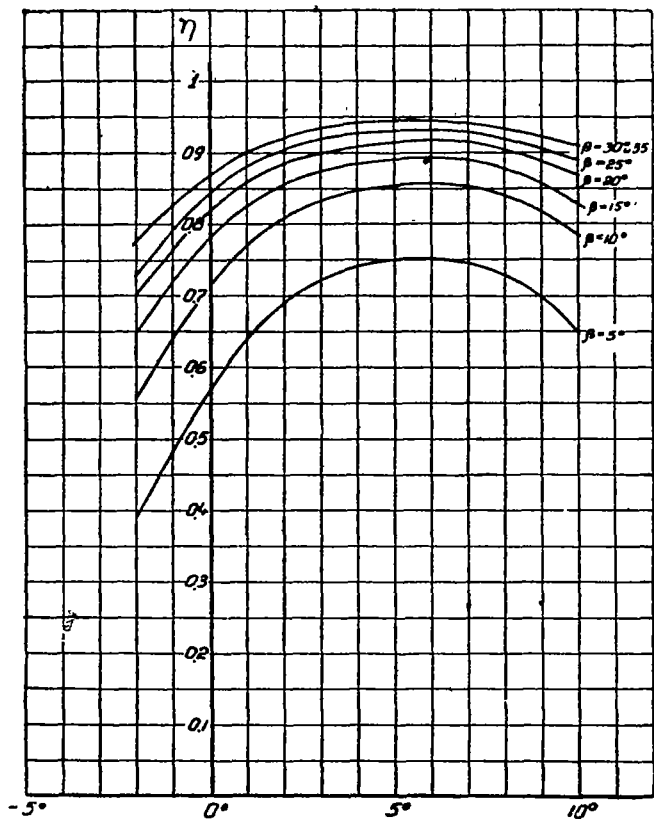


Figure 105.- Curves of profile efficiency for curved metal blade no. 1.

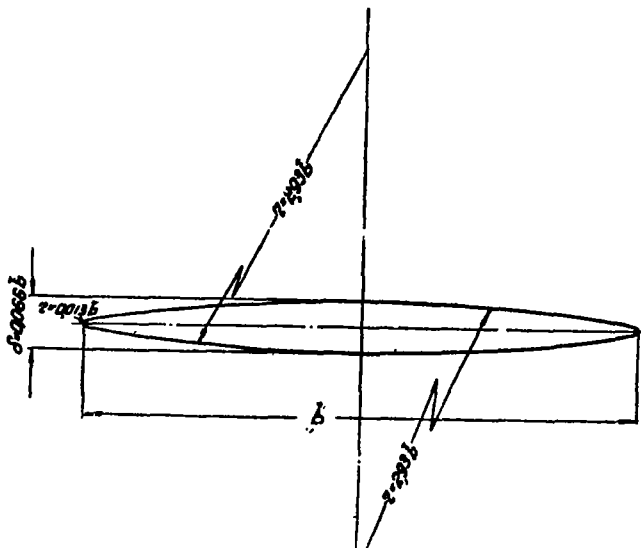


Figure 106.- Construction of symmetric profile.

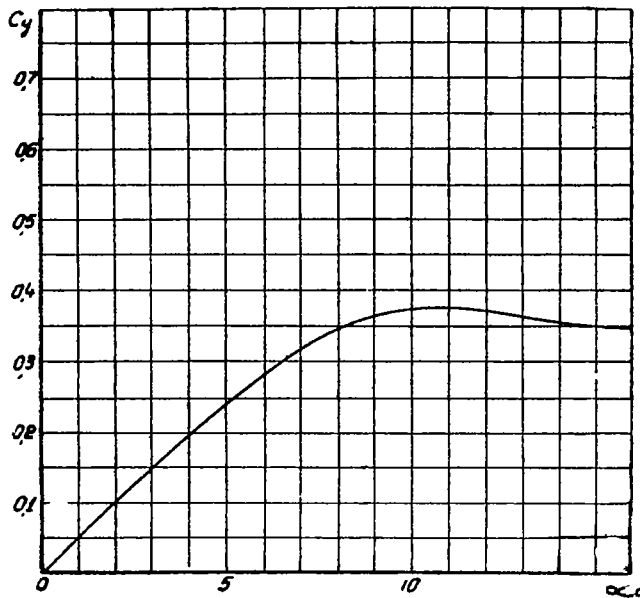


Figure 107.- Lift coefficient curve for symmetric profile.

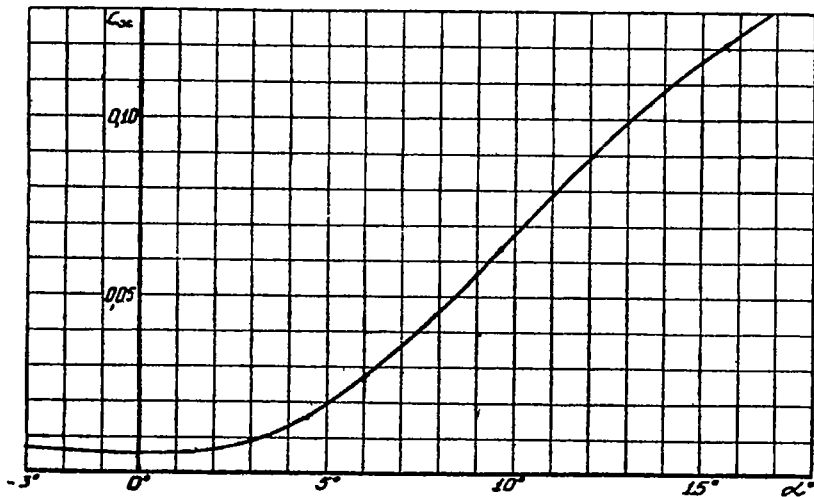


Figure 108.- Drag coefficient curve for symmetric profile.

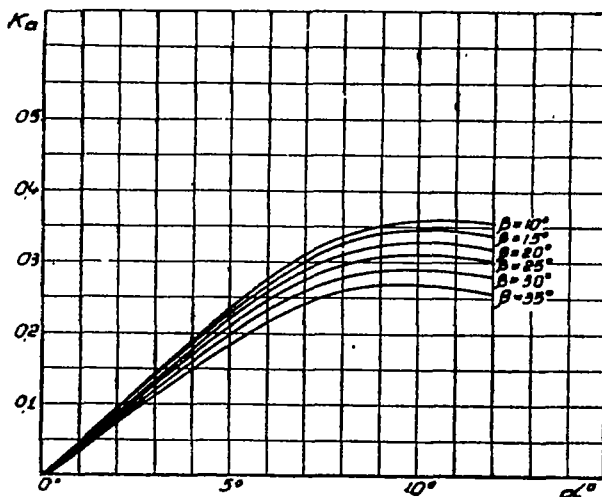


Figure 109.- Pressure coefficient curves for symmetric profile.

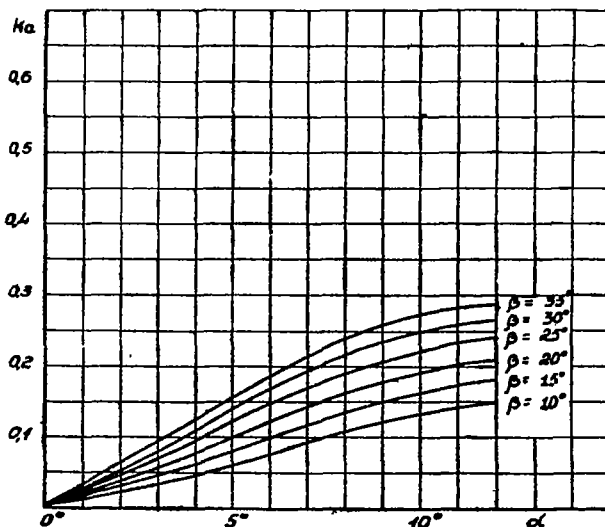


Figure 110.- Power coefficient curves for symmetric profile.

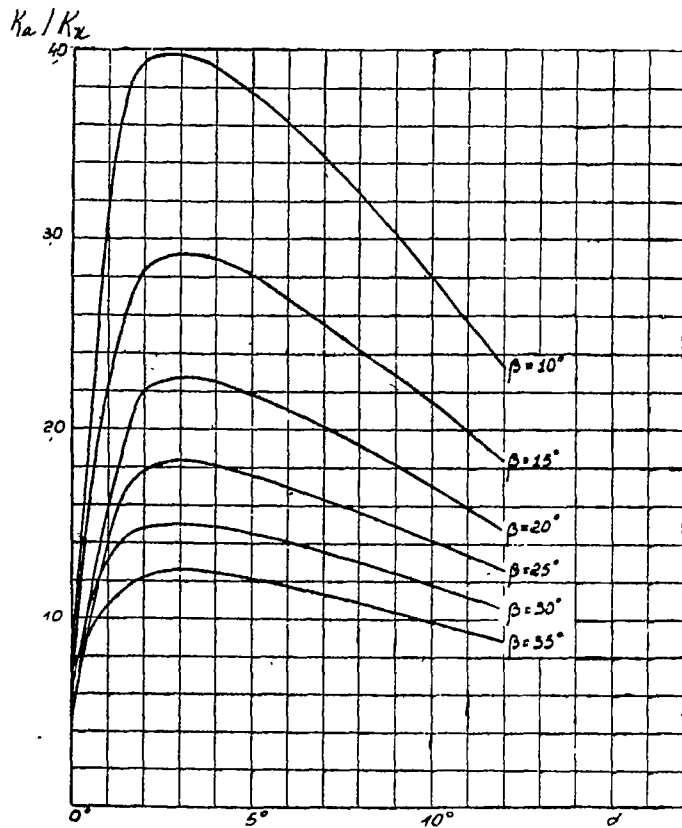


Figure 111.- Curves of K_a/K_x for symmetric profile.

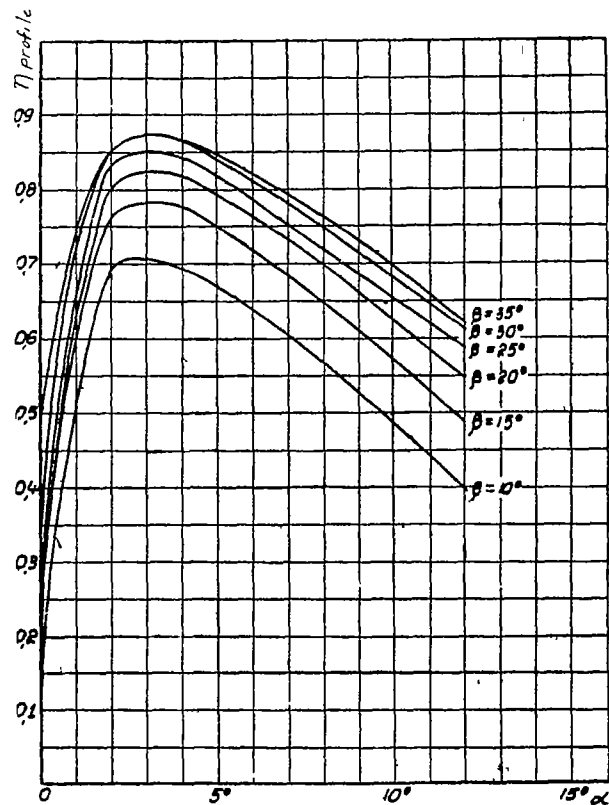


Figure 112.- Curves of profile efficiency of blade element for symmetric profile.

NASA Technical Library



3 1176 01441 5039